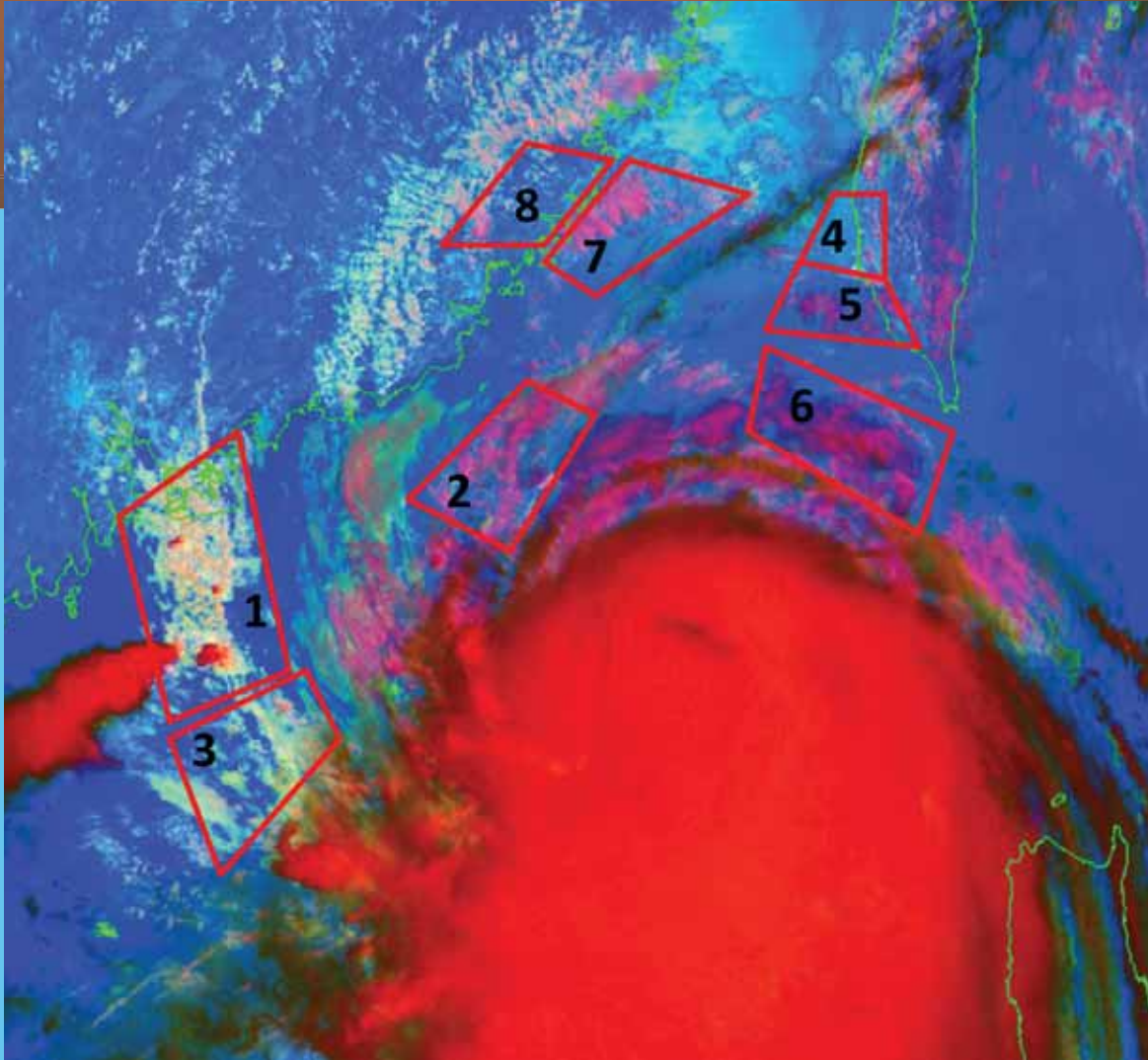


# Hurricane Aerosol and Microphysics Program (HAMP):

Improving Hurricane Forecasts by Evaluating the Effects of Aerosols on Hurricane Intensity

## FINAL REPORT

October 2010



**Submitted by: Dr. William L. Woodley, President  
Woodley Weather Consultants**

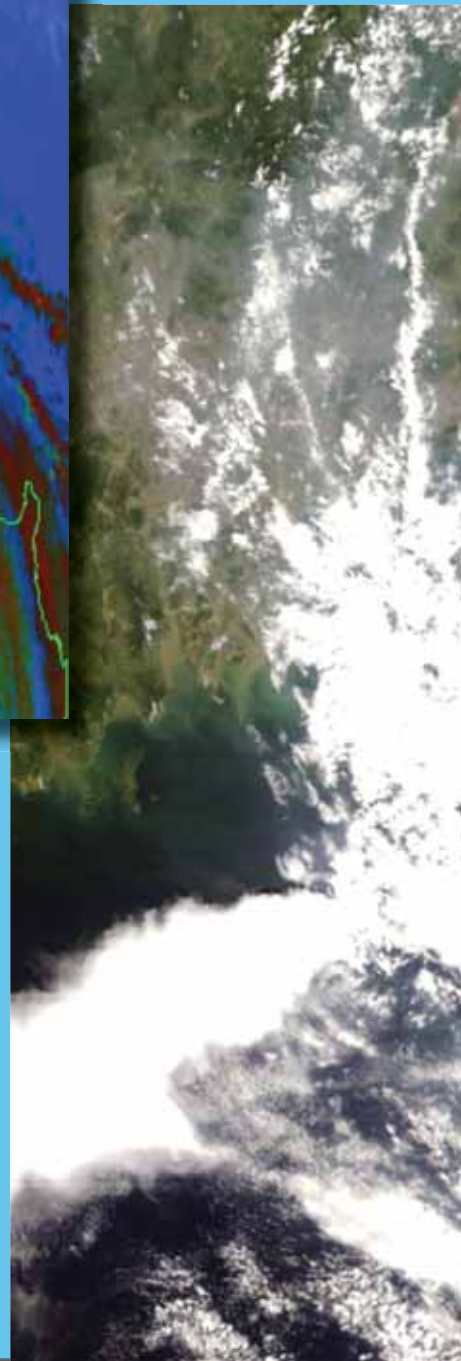
With major contributions from (in alphabetical order):

- Prof. Dr. William Cotton, Colorado State University, Colorado, USA
- Prof. Dr. Isaac Ginis, University of Rhode Island, Rhode Island, USA
- Dr. Joseph H. Golden, Golden Consulting Group, Colorado, USA
- Prof. Dr. Alexander Khain, Hebrew University of Jerusalem, Israel
- Prof. Dr. Daniel Rosenfeld, Hebrew University of Jerusalem, Israel

Prepared for the Department of Homeland Security, Science and Technology Directorate,  
Homeland Security Advanced Research Projects Agency/Infrastructure and Geophysical Division

Hurricane Aerosol and Microphysics Program (HAMP)

October 2010





# **Hurricane Aerosol and Microphysics Program (HAMP): Improving Hurricane Forecasts by Evaluating the Effects of Aerosols on Hurricane Intensity**

## FINAL REPORT

This report presents the research and analysis conducted under Contract Number: HSHQDC-09-C-00064. The findings presented in this final report do not necessarily reflect official DHS opinion or policy.

To the Department of Homeland Security  
Science and Technology (S&T) Directorate

Submitted by:  
Dr. William L. Woodley, President  
Woodley Weather Consultants  
Colorado, USA

With major contributions from (in alphabetical order):

Prof. Dr. William Cotton, Colorado State University, Colorado, USA  
Prof. Dr. Isaac Ginis, University of Rhode Island, Rhode Island, USA  
Dr. Joseph H. Golden, Golden Consulting Group, Colorado, USA  
Prof. Dr. Alexander Khain, Hebrew University of Jerusalem, Israel  
Prof. Dr. Daniel Rosenfeld, Hebrew University of Jerusalem, Israel

October 2010

# Contacts & Acknowledgements

For information about this publication contact:

William D. Laska  
Department of Homeland Security, Science and Technology  
245 Murray Drive, SW  
Washington DC 20373-5116  
Tel (202) 254-5337 • Fax (202) 254-6174  
william.d.laska@dhs.gov

Dr. William L. Woodley  
Woodley Weather consultants  
11 White Fir Court  
Littleton, Colorado 80127  
Tel (303) 979-7946  
Fax (303) 973-3446  
williamlwoodley@cs.com or bill@woodleyweather.com

## Cover illustrations:

Top: Figure 1.8 GOCART calculated AOTs for 5 aerosol species and the total AOT;

Center: clouds and Figure 1.4 Satellite microphysical analysis of Typhoon Nuri;

Bottom: Figure 1.2 Air pollution haze ingested into a spiral band of Typhoon Nuri

Prepared for the Department of Homeland Security, Science and Technology Directorate, Homeland Security Advanced Research Projects Agency/ Infrastructure and Geophysical Division

The impetus and support for the original HAMP workshop came from Rear Admiral (retired) Jay M. Cohen, Undersecretary of Homeland Security for Science and Technology of the United States Department of Homeland Security. His driving force was amplified by William D. Laska, Program Manager, of DHS's Advanced Research Projects Agency. The efforts of support specialists Robin Belen and David Ogden of DHS also helped make the HAMP research effort possible.

The research effort was significantly enhanced by the contributions of the following researchers list-

ed in alphabetical order: N. Benmoshe, Dr. Gustavo G. Carrió, Ms. Michal Clavner, Dr. Yalin Fan, Mr. Tal Halevi, Mr. Steve Herberner, H. Zvi Kruglyak, Dr. B. Lynn, L. Magaritz, Dr. M. Pinsky, Dr. A. Pokrovsky, J. Spund, Dr. Biju Thomas, Mr. Zhitao Yu.

This final report was edited, designed, and produced by PWT Communications, LLC, Boulder, Colorado.

# Abbreviations and Acronyms

AMS	American Meteorological Society
AOC	Aircraft Operation Center
AOD	aerosol optical depth
AOT	aerosol optical thickness
AP	aerosol particle
ASIM	air-sea interface module
BL	boundary layer
CCN	cloud condensation nuclei
CALIOP	cloud aerosol lidar with orthogonal polarization
COAMPS-TC	coupled ocean and atmosphere mesoscale prediction system for tropical cyclones
CWC	cloud water mass content
DHS	Department of Homeland Security
ESRL	Earth System Research Laboratory
GFDL	Geophysical Fluid Dynamics Laboratory
GOCART	Goddard Chemistry Aerosol Radiation and Transport
GRIP	Genesis and Rapid Intensification Processes
GSD	Global Systems Division
HAMP	Hurricane Aerosol and Microphysics Program
HFIP	Hurricane Forecast Improvement Project
HRD	Hurricane Research Division
HSARPA	Homeland Security Advanced Research Projects Agency
HUCM	Hebrew University Cloud Model
HUJI	Hebrew University Jerusalem, Israel
HBL	hurricane boundary layer
LPI	lightning potential index
MBL	marine boundary layer
MODIS	moderate resolution imaging spectroradiometer
NHC	National Hurricane Center
NOAA	National Oceanic and Atmospheric Administration
OFCM	Office of the Federal Coordinator for Meteorology
ONR	Office of Naval Research
PR	precipitation radar
RAMS	Regional Atmospheric Modeling System

SAR	synthetic aperture radar
SBM	spectral bin microphysics
SC	supercooled
SHIPS	model statistical hurricane intensity prediction scheme
SST	sea surface temperature
S&T	Science and Technology Directorate
TC	tropical cyclones
TD	tropical depression
TRMM	Tropical Rainfall Measuring Mission
TS	tropical storm
UAS	unmanned aircraft system
URI	University of Rhode Island
VIRS	Visible and Infra Red Scanner
WRF	Weather Research Forecasting model

Executive Summary .....	9
1. Satellite Observations of Pollution Aerosols Suppressing Warm Rain and Invigorating Spiral Cloud Bands of Tropical Cyclones .....	17
1.1 Introduction .....	17
1.2 Impact of Aerosols on the Dynamics and Electrification of Deep Tropical Convective Clouds .....	17
1.3 Possible Impact of Aerosols on the Dynamics of Tropical Cyclones .....	18
1.4 Quantitative Relations Between Aerosol Amounts and TC Intensity .....	19
1.5 Conceptual Model of the Ways by Which Aerosols Might be Affecting TCs .....	19
1.6 Observations of Aerosols Impacts on Cloud Bands in TCs .....	20
1.6.1 The Observational Methods .....	20
1.6.2 Typhoon Nuri on 21 August 2008 .....	20
1.6.3 Hurricane Gustav off the South Carolina Coast on 10 September 2002 .....	23
1.7 Research Flights in Hurricanes .....	25
1.7.1 Overview .....	25
1.7.2 Flight Patterns for Measuring Cloud-Aerosol Interactions .....	28
1.8 Flights Completed in Polluted Tropical Clouds .....	30
1.9 Conclusions and Recommendations for the Future .....	30
2. Aerosols, Cold-Pools, and Hurricane Intensity Modulation .....	33
2.1 Introduction .....	33
2.2 Model Improvements .....	34
2.2.1 Development of a Prognostic Scheme for Sea-salt Sources .....	34
2.2.2 Implementation of Scavenging Aerosol Sinks .....	34
2.3 Exploration of Methods to Mitigate the Intensity of Tropical Storms, Leading to Better Forecasts of Hurricane Intensity .....	34
2.4 Main Results .....	35
2.4.1 Vertical Motions, Supercooled Liquid Water, and Precipitation .....	35
2.4.2 Cold-Pools .....	36
2.4.3 Downdrafts .....	40
2.4.4 Surface Winds .....	40
2.5 Concluding Remarks About Targeted Insertion of CCN .....	41
2.6 Impact of the Sea-Salt Sources Sea-Salt Aerosol and Scavenging by Precipitation on the Storm Microphysics .....	46
2.7 Conclusions and Recommendations for the Future .....	51
3. Testing the Sensitivity of TC Intensity to Concentration of Small Aerosols .....	53
3.1 Introduction .....	53
3.2 Development of a High-Resolution Spectral Bin-Microphysics Model and its Justification .....	54
3.3 Development of a Unique Model for Investigation of Spray Effects .....	56
3.4 Development of the Model of the BL Which Resolves Large Eddies .....	59
3.5 Simulation of Aerosol Effects on the Intensity of a Land-Falling TC .....	59
3.5.1 Introduction .....	59
3.5.2 Model and Experimental Design .....	62

3.5.3 Results of Simulations.....	64
3.5.4 Discussion and Conclusions .....	68
3.6 Simulation of Aerosol Effects on TC Genesis .....	69
3.6.1 Aerosol Effects on the TD Intensity .....	69
3.6.2 Simulation of Structure and Microphysics of Developing TD.....	71
3.6.3 Comparison of Microphysical Structure of TD Simulated by the SBM and Bulk Parameterization Schemes .....	74
3.7 Conclusions and Recommendations for the Future .....	77
4. Development and Implementation of Innovative Physics Packages for New-Generation, High-Resolution, Coupled Hurricane-Wave-Ocean Models .....	79
4.1 Introduction.....	79
4.2 Sea State Dependence of Momentum Flux .....	79
4.3 Air-Sea Flux Budget.....	80
4.4 Wave-Current Interaction .....	80
4.5 Implementation of Sea Spray Parameterization into Coupled Hurricane-Wave-Ocean Models .....	81
4.6 Development of a Boundary Layer Model with Explicit Resolution of Large Eddies .....	84
4.6.1 The New BL Model Development and Validation.....	85
4.6.2 Comparison with 3D Large Eddy Simulation (LES) Model.....	86
4.6.3 The Effect of Coriolis Force on Marine Boundary Layer Roll Vortices .....	88
4.6.4 Interaction of the BL Roll Vortices and Internal Gravity Waves .....	90
4.6.5 Effect of BL Convection with Latent Heat Release on Large Scale Mean Flow.....	92
4.7 Proposed Methodology to Explicitly Represent Roll Vortices and Sea Spray Dynamics .....	93
5. Dissemination of Results and Developing Collaborations .....	96
5.1 Fostering Collaboration Between HAMP and Scientists at NOAA, the U.S. Navy, and NASA .....	96
5.2 Dissemination of Results .....	97
5.2.1 Participation in Scientific Projects, Meetings, and Conferences .....	97
5.2.2 Publications Resulting from this Work .....	98
5.2.3 Presentations .....	100
5.2.4 Conference Papers Submitted .....	100
6. Conclusions and Recommendations for the Future.....	101
6.1 Rosenfeld’s Conclusions and Recommendations .....	101
6.2 Cotton et al. Conclusions and Recommendations .....	102
6.3 Khain’s Conclusions and Recommendations .....	104
6.4 Ginis et al. Conclusions and Recommendations.....	105
6.5 Overall Conclusions and Recommendations.....	122
References .....	107

## List of Figures

Figure 1.1 Conceptual diagram adapted from Rosenfeld and Lensky (1998).....	21
Figure 1.2 Air pollution haze ingested into a spiral band of Typhoon Nuri.....	22

Figure 1.3 NASA/MODIS-Aqua aerosol optical depth (AOD) image .....	23
Figure 1.4 Satellite microphysical analysis of Typhoon Nuri .....	24
Figure 1.5 TRMM satellite VIRS image of the typhoon Nuri .....	26
Figure 1.6 Tropical cyclone, Gustav off the coast of South Carolina, from MODIS Terra .....	27
Figure 1.7 NASA/MODIS-Aqua aerosol optical depth (AOD) image for TC Gustav .....	28
Figure 1.8 GOCART calculated AOTs for 5 aerosol species and the total AOT .....	29
Figure 1.9 Desired flight tracks for rain-band clouds of a TC .....	31
Figure 2.1 Virtual flights over internal and external radii.....	35
Figure 2.2 SC liquid water at simulation time 39 h for the control run and seeded run .....	36
Figure 2.3 Comparison of SC liquid water .....	37
Figure 2.4 Comparison of updrafts .....	37
Figure 2.5 Comparison of mixing ratio of aggregates .....	38
Figure 2.6 Comparison of precipitation .....	38
Figure 2.7 Comparison of integral downward mass transport .....	41
Figure 2.8 Comparison of area covered by downdrafts.....	42
Figure 2.9 Largest simulated cold-pool and its associated downdraft .....	43
Figure 2.10 Comparison of buoyancy within the most intense downdrafts .....	44
Figure 2.11 Comparison of rain mixing ratio .....	45
Figure 2.12 Comparison of raindrop mean mass diameter .....	46
Figure 2.13 Comparison of hurricane intensity surface wind frequencies .....	47
Figure 2.14 Comparison of hurricane intensity surface wind frequencies .....	48
Figure 2.15 Average cloud droplet concentration in lower levels of region near the eye wall .....	49
Figure 2.16 Storm intensity metric.....	49
Figure 2.17 Total SC cloud droplet mass.....	50
Figure 3.1 Mass distribution functions at different heights .....	54
Figure 3.2 Droplet size distributions at different levels .....	55
Figure 3.3 Fields of vertical velocity and liquid water content.....	57
Figure 3.4 Field of rainflux at t=135 min. ....	58
Figure 3.5 Number and mass distributions of drops (blue) and aerosols inside of droplets (red) .....	60
Figure 3.6 Vertical profiles of horizontally averaged absolute humidity (a) and potential temperature (b) .....	61
Figure 3.7 Time dependences of sensible (a) and latent (b) fluxes in the LE (solid) and No_LE (dashed curve) runs.....	61
Figure 3.8 Time dependence of minimum pressure in numerical experiments and hurricane Katrina (August 2005) .....	64
Figure 3.9 Droplet concentrations and CWC in MAR and CAR-CON simulations.....	66
Figure 3.10 Graupel and snow concentrations in MAR and CAR-CON simulations.....	66
Figure 3.11 The fields of maximum wind speed 28 Aug. 21 z (upper panels), and 22 z. in runs MAR (left) and MAR_CON (right) .....	67
Figure 3.12 Fields of Lightning Potential Index (LPI) calculated in MAR (left) and MAR-CON (right) .....	68
Figure 3.13 The track of TD Debbie and the geometry of the model meshes.....	69
Figure 3.14 Time dependencies of minimum pressure in simulations of TD Debbie .....	70
Figure 3.15 Time dependence of minimum pressure in observations and simulations .....	71
Figure 3.16 Fields of maximum winds in simulations .....	71

Figure 3.17 Fields of maximum values of droplet concentration and CWC ..... 72

Figure 3.18 Fields of total liquid water content ..... 72

Figure 3.19 Fields depicting the maximum updrafts ..... 73

Figure 3.20 Fields of maximum values of snow and graupel ..... 73

Figure 3.21 Time dependencies of maximum wind speed in Debbie..... 74

Figure 3.22 Fields of the maximum of cloud water contents in simulations  
with SBM and WDM6 at t=72 h. .... 75

Figure 3.23 Fields of the maximum of rain water contents in simulations  
with SBM and WDM6 at t=72 h ..... 75

Figure 3.24 Fields of maximum snow (upper) and graupel contents  
(lower) in the WDM6 simulations at t=72 h..... 76

Figure 4.1 Flux and SST Adopted from Fan et al. 2009c ..... 81

Figure 4.2 A schematic of the coupled wind-wave-current modeling system and the  
URI air-sea interface module (ASIM) ..... 82

Figure 4.3 Surface wind vector, significant wave height, phase speed of dominant wind-forced waves,  
and wave energy dissipation ..... 82

Figure 4.4 Drag coefficient vs. surface wind speed ..... 83

Figure 4.5 Contour plot of vertical velocity ..... 86

Figure 4.6 Mean potential temperature profile ..... 87

Figure 4.7 Mean profile comparison of potential temperature, vapor mixing ratio,  
and along-roll velocity, and cross-roll velocity ..... 87

Figure 4.8 Total momentum flux profiles comparison..... 88

Figure 4.9 Mean velocity profiles ..... 89

Figure 4.10 Vertical velocity at 5 hours after turning on convection for the experiments..... 90

Figure 4.11 Vertical velocity at a quasi-steady state for the experiments ..... 90

Figure 4.12 Contour plots of vertical convective velocity from experiment C1 ..... 91

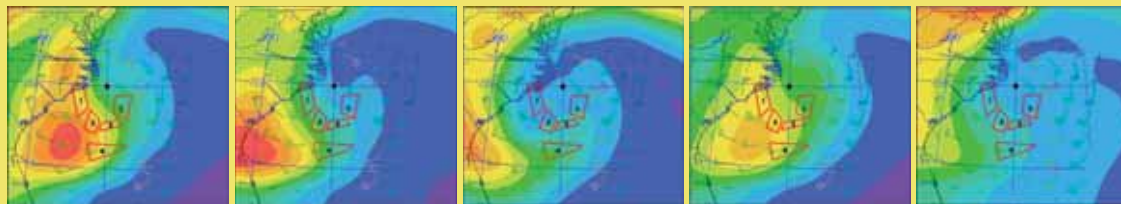
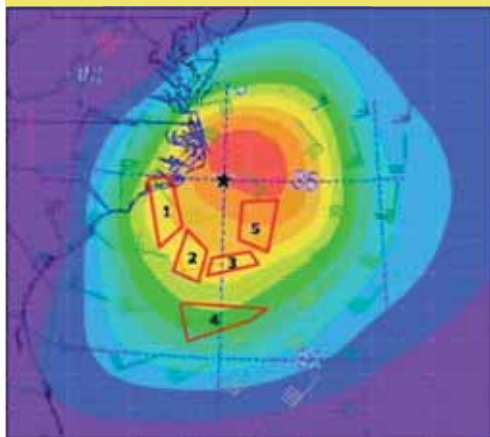
Figure 4.13 Experiment S2 T=2.5 hours ..... 93

Figure 4.14 Experiment S2 T=4 hours ..... 94

**List of Tables**

Table 2.1 Cold-pool analyses for different times, flight types,  
and varying aerosol release rates ..... 39

Table 2.2 Cold-pool analyses for flights varying aerosol release rates..... 40



## Executive Summary

The first year of the Hurricane Aerosol and Microphysics Program (HAMP) was highly productive scientifically. Aerosol and cloud measurements, statistical analyses, and numerical modeling using advanced microphysical schemes supported the hypothesis that tropical cyclones (hurricanes) are sensitive to aerosols that can act to decrease storm intensity. The work documented key elements of the conceptual model of hurricane processes that guides the HAMP research. The group developed a unique spectral bin microphysics (SBM) package and implemented it into the Weather Research Forecasting model (WRF). The advanced WRF/SBM model was shown to be superior to 12 bulk parameterization schemes in predicting storm intensities.

The major impact of this research on hurricane intensity prediction is that it highlights the importance of low-level cold-pools, particularly in the outer rainbands on hurricane intensity. It means that methods for diagnosing cold-pool strength and area in real time need to be developed for hurricane intensity prediction. In addition, operational forecast models need to be implemented that can explicitly represent the variability of TC cold-pools due to variations in wind-shear, environmental moisture, and aerosols. It was found also that the effect of aerosols on tropical cyclone intensity is as important as interactions with the ocean. The work comparing observations with model forecasts shows that improving forecasts of storm intensity will require the use of advanced microphysical schemes that take into account of the effects of aerosols.

The work has been widely disseminated and has enhanced the work of others through extensive interactions with the HAMP research team. Team members submitted 34 articles to referred journals (23 accepted to date), delivered more than 20 presentations and seminars at scientific meetings, and developed productive collaborations with NOAA's Global Systems Division, National Hurricane Center, Hurricane Research Division, and Aircraft Operation Center as well as with the Office of Naval Research and the Naval Postgraduate School. Continuation of this effort will produce the understanding needed to improve forecasts of hurricane intensities as storms develop.

The HAMP approach reported here has demonstrated that aerosols naturally modulate (increase and decrease) hurricane intensities and therefore aerosol distributions must be considered when trying to improve forecasting of hurricane intensity.

### Introduction

Natural disasters brought about by earthquakes, floods, fires, and severe storms are of universal concern. The disastrous hurricane season of 2005 and the devastation of Hurricane Katrina have increased attention on the hurricane threat in the United States. Once a hurricane reaches land, the damage and devastation can be immense. The destructive force of these storms is proportional to the cube of the wind speed. This means that for only 25% increase in wind speed, its destructive power doubles. Thus, accurate

forecasts of hurricane path and intensity are very important to the people living along the coast. To improve forecasts, the National Oceanic and Atmospheric Administration (NOAA) sponsors important research to better understand tropical cyclonic behavior and to keep the population aware of impending danger. Accurately predicting hurricane behavior is the goal of NOAA's Hurricane Forecast Improvement Project (HFIP). Improving our ability to forecast hurricane intensity is a major mission goal of NOAA.

Hurricane forecasts are also important to the Department of Homeland Security (DHS) because hurricanes pose a threat to national security and accurate forecasts will help DHS gauge its response to impending storms. To improve forecasts of hurricane intensity, the Homeland Security Advanced Research Projects Agency (HSARPA), a division of DHS Science and Technology Directorate, has embarked on what appears to be a hitherto missing key component of the hurricane research effort, HAMP.

The DHS approach in HAMP supplements the NOAA research programs and is unique in two respects.

- First, HAMP aims to document the suspected effect of aerosols on clouds and precipitation inside a hurricane. This work requires synergistic interactions between hurricane observations and model simulations. This unique approach is expected to lead to better understanding of hurricane processes and improved forecasts of hurricane intensity. Prior to the HAMP effort, groups tasked with improving hurricane forecasts have virtually ignored aerosols and the distribution of aerosols is not yet factored into hurricane forecasts.
- Second, HAMP adopts the view that a good way to understand a meteorological system is to perturb it in some way. This perturbation can be experimental in the real world and/or it can be done through numerical simulation of physical changes.

## The HAMP Hypothesis and Objectives

HAMP emphasizes aerosols because they have been implicated in the rate of energy transfer within hurricanes. The main sources of energy of these hurricanes or tropical cyclones (TC) are latent heat released in clouds and sensible heat transferred from the warm ocean. The intensity of a TC critically depends on the rate of latent heat release as well as on its spatial distribution within the storm. The latent heat release results from complicated microphysical processes in clouds. It is known that cloud composition, which in turn determines and precipitation forming processes and the resultant heating depend on atmospheric aerosols (pollution, dust, and salt). These aerosols affect the cloud composition by determining the concentration and size of water droplets and ice crystals in the cloud. Recent observational and numerical studies (using advanced microphysics schemes) indicate that higher concentrations of atmospheric aerosols dramatically intensify updraft velocities and latent heat release aloft in deep maritime convective clouds. This is coupled by greater evaporative cooling at the low levels. This redistribution of heat tends to decrease the intensity of the storm.

The core HAMP hypothesis is that higher concentrations of aerosols that can nucleate cloud droplets diminish the intensities of TCs. If this hypothesis is demonstrated to be true, then such aerosols must be considered when attempting to improve the forecasts of TC intensity.

The first stage of the HAMP effort tested the hypothesis concerning the sensitivity of TC intensity to aerosols. To test the hypothesis, observational data from satellites and aircraft were examined. Then observational data were compared to results from simulations. The second stage of the HAMP effort compared observational data to outputs of several TC models to test their ability to show the effects of aerosols on TC intensity. The third stage of the HAMP effort aimed to create an advanced TC model that considers TC–ocean interactions.

## Summary of Main Results

The key links in the hypothesis that guides HAMP research on the effect of aerosols on hurricane intensity are articulated by Prof. Dr. Daniel Rosenfeld in Chapter 1. To validate the hypothesis, satellite analyses were combined with cloud physics aircraft data measured in other related field programs.

The aircraft measurements validated the correctness of the microphysical representation of cloud-aerosol interactions and their impacts on rain forming processes in our model simulations. The satellite observations of TCs also demonstrated an effect similar to the hypothesis on the outer spiral cloud bands when pollution areas (aerosols) were ingested into the storms. Satellite and other remote-sensing documentation show the predicted invigoration and increased lightning activity of the polluted cloud (high aerosol concentration) bands. Satellite documentation also show wind-generated sea spray (aerosols) restoring rain formation processes in clouds as predicted by the hypothesis.

An initial quantification of the impact of aerosols on hurricane maximum wind speed was obtained by comparing the observed intensities of TCs with their predicted intensities using some of the operational models that do not account for the aerosols. In polluted situations, the observed TC intensities tended to be less than predicted by the models, indicating a negative effect of pollution aerosols on TC intensity. This quantification also indicates a somewhat surprising result that strongly absorbing aerosols such as black carbon might have invigoration effects on TCs.

The research groups of Prof. Dr. William Cotton and Prof. Dr. Alexander Khain compared observational data to outputs of several TC models to test their ability to show the effects of aerosols on TC intensity. Their work is described in Chapters 2 and 3 respectively. Current TC models use simplified descriptions of microphysical processes based on different bulk parameterization schemes, which are not sensitive to aerosols. Because of the lack of appropriate mathematical incorporation of microphysical processes, the improvement of the model resolution does

not lead to improvement of forecast skill of the TC models. This fact was clearly demonstrated in many presentations during the 29th Conference on Hurricanes and Tropical Meteorology in Tucson, Arizona in May 2010. Aerosols must be considered.

The Cotton group performed several simulations of development of an idealized TC under different loading of natural aerosol, as well as simulated introduction of aerosol perturbations into clouds at the periphery of a model TC. The simulations were performed using the RAMS mesoscale model with advanced bulk parameterization with binmimic components, making the scheme sensitive to aerosol effects. The results indicate that TCs developing in zones of high aerosol loading are weaker than those developing in clean air. Moreover, it is shown that introducing aerosols into clouds at the TC periphery leads to a significant TC weakening.

The research group of Prof. Dr. Isaac Ginis aimed to create an advanced TC model that considers TC–ocean interactions. As described in Chapter 4, one of the most complicated aspects of this problem is describing the effects of spray forming at the ocean surface under strong winds and the effects of spray generation on TC cloud microphysics. The HAMP work investigated the role of spray using micro-physically advanced models of the boundary layer (BL) in TCs. The group compared intensity predictions from 12 available bulk parameterization schemes with intensity predictions using the advanced WRF/SBM model that the HAMP group helped develop. That comparison demonstrated a significant advantage for the WRF/SBM model and a need for significant improvement of convective parameterization and of TC-ocean interaction.

The groups of Khain and Ginis each developed models of the BL at high winds. Both models indicate a dramatic role of large eddies (convective rolls, cells) on the BL thermodynamic structure and surface fluxes. It was shown that taking large eddies into account increases surface latent heat fluxes by a factor of two. It was also shown that large eddies transport spray to the upper levels, where spray droplets form precipitating clouds (cloud base at about 200 m). These results illustrate the need to use advanced

methods describing the BL, which would allow one to take into account effects of large eddies transporting large spray upward. The Ginis group implemented a new wave model into the TC model available.

As shown in Chapter 5, Dissemination of Results and Developing Collaborations, the HAMP team has produced an impressive array of peer-reviewed publications and conference presentations during its first year.

### ***Observations of Aerosol Effects on TC Cloud Dynamics and TC Intensities***

The first stage of the HAMP effort examined observational data from satellites and aircraft.

#### **Result 1: Aerosols affect microphysical processes (vertical velocities and timing of raindrop formation)**

During the summer field campaign in India, unique in-situ measurements of deep monsoon convective clouds were made. These clouds developed in a very moist atmosphere similar to that in a TC. The main difference between these clouds and the clouds in TCs is that monsoon clouds in India often develop in a polluted atmosphere containing a high concentration of aerosols. Actually these clouds represent naturally polluted tropical clouds. These measurements showed the dramatic effects of aerosols. First raindrops formed at levels above 5 km above cloud base (0.6 km). These results support the hypothesis that the ingestion by tropical clouds of soluble aerosols leads to invigoration of these clouds and to the intensification of latent heat releases in them. This is an important point. The data obtained are of great importance for testing different microphysical models.

#### **Result 2: Current models overestimate TC intensity when aerosols are present**

We compared observational data on actual TC intensities with predictions for those storms from the

two best forecast models now available at the Geophysical Fluid Dynamics Laboratory at NOAA (the GFDL Hurricane Prediction System model) and at NOAA (the statistical hurricane intensity prediction scheme (SHIPS) model). Our detailed statistical analysis showed that both models tend to overestimate TC intensities in highly polluted zones. If these aerosols from pollution and dust sources explain the variability of hurricane prediction errors, then incorporating the aerosol effects into hurricane prediction models should increase their accuracy. Our hypothesis projects that the processes in TCs of precipitation forming and evaporation are key to determining intensity changes. They must be simulated properly in order to achieve additional improvements in hurricane prediction models. Understanding the role of aerosols is crucial to improving forecast models.

#### **Model Forecasts and the Effects of Aerosols on TC Intensity**

The Cotton research group (Chapter 2) performed several simulations of development of an idealized TC. They used the Colorado State University Regional Atmospheric Modeling System (RAMS) mesoscale model with advanced bulk parameterization with bin-mimic components. This scheme is sensitive to aerosol effects. They performed simulations under different loading of natural aerosol and under simulated hygroscopic seeding of clouds at the periphery of a model TC. The results indicate that TCs developing in zones of high aerosol loading are weaker than those developing in clean air. Moreover, it was shown that ingestion by tropical clouds of soluble aerosols leads to invigoration of these clouds and to the intensification of latent heat releases in them. This leads to a significant TC weakening.

The Khain group (Chapter 3) developed a unique SBM package and implemented it into the Weather Research Forecasting model (WRF). The resulting WRF/SBM model was used to simulate the landfall of hurricane Katrina and the genesis of tropical depression (TD) Debbie. Then these simulations were compared to the actual events. It was shown that aerosols penetrating clouds at the TC periphery

intensify convective clouds there and lead to significant weakening of land-falling TCs. It was also shown that aerosol-induced convective intensification at the periphery of tropical depression Debbie hindered the TD genesis. Both of these findings are in agreement with the main HAMP hypothesis. These facts are very important because the incorporation of aerosol effects into TC forecast models should result in improved forecasts of TC intensities.

These results support the HAMP hypothesis and agree well with the results obtained by the other HAMP research groups.

### ***Microphysically Advanced Models of the Boundary Layer in TCs and the Role of Spray***

The Khain and Ginis groups both developed models of the BL at high winds. Both models indicate a dramatic role of large eddies (convective rolls, cells) on the BL thermodynamic structure and surface fluxes. It is shown that large eddies being taken into account increase surface latent heat fluxes by a factor of two.

It was also shown that large eddies transport spray to the upper levels, where spray droplets form precipitating clouds with cloud base at about 200 m. The results indicate the necessity to use advanced methods of the BL description, which would allow one to take into account effects of large eddies transporting large spray upward.

The Ginis group (Chapter 4) implemented a new air-sea interface model into the GFDL TC model available.

### **Collaboration and Coalition Building**

It is important to note that all objectives of HAMP are closely related to improving our ability to forecast TC intensity and TC genesis. From the beginning, a major goal of the HAMP team was to integrate its efforts with those of other groups that are working for improvements in the forecasts of TC intensity. HAMP researchers participated in key meetings, built coalitions with scientists having

mutual interests and activities, and provided access to the HAMP models to other scientists who would benefit from such access. This is described in Chapter 5. It is important to note that the seminal work of Khain and Ginis has been aided by access to an advanced supercomputer at the U.S. Army Engineer Research and Development Center. This computer is larger and faster than any currently available in NOAA and the Navy.

The HAMP effort began as an exploratory workshop in Boulder, Colorado, in February 2008, hosted by NOAA/GSD and sponsored by the Science and Technology Directorate of DHS. The workshop was requested by the Undersecretary of DHS to open dialogue on possible new scientific approaches to hurricane mitigation. It drew more than two dozen scientists from diverse locations and backgrounds. The workshop final report identified promising new research efforts on hurricane modeling. Several of these coalesced into the first phase of the HAMP project (reported here). Others were identified for future work if funds were available.

The HAMP research focused on the impacts of aerosols and cloud microphysics on changes in hurricane intensity. Coordination with NOAA/ESRL was maintained from the outset through a GSD-appointed Project Monitor, Ed Tollerud. Key members of the HAMP team, Ginis and Khain, made numerous visits to NOAA/HRD in Miami, Florida to coordinate with the NOAA/HFIP Program to gain feedback at key points in the analysis.

The team of Woodley at Woodley Weather Consultants and Dr. Joseph H. Golden of Golden Consulting Group, made HAMP presentations at annual meetings of the Office of the Federal Coordinator for Meteorology (OFCM) (multi-agency operational audience), and it organized a special panel discussion on HAMP issues at the 2008 American Meteorological Society (AMS) Conference on Weather Modification in Denver, Colorado. Golden organized a briefing by Dr. Rosenfeld on HAMP in February, 2010 for the Director of NHC, Mr. Bill Read and two NHC forecasters, Mr. James Franklin and Mr. Richard Pasch in Boulder, Colorado. Their feedback during that meeting to Rosenfeld resulted in further study of

the impacts of aerosols on hurricane intensity changes in the GFDL dynamical model and the SHIPS statistical model used at NHC. A scientific session on HAMP research was organized by the entire HAMP team for the AMS Tropical Meteorology and Hurricane Conference in Tucson, May, 2010.

We believe it is vital to continue coordination of HAMP research with the HFIP Program and collaboration with its field components like the 2010 NOAA/NASA/NSF Genesis and Rapid Intensification Processes (GRIP) experiment.

Woodley and Golden continue to work closely with HRD scientists, especially Mr. Robert Black and Dr. Paul Willis, on acquiring field measurements of aerosols and cloud microphysics in tropical disturbances, including tropical storms and hurricanes in the Atlantic. HAMP-funded instrumentation has been delivered to NOAA's Aircraft Operation Center (AOC) for installation on one of the P3 aircraft. A cloud condensation nuclei (CCN) counter owned by Georgia Institute of Technology (Georgia Tech)/NASA scientists has been installed on one of the P3s. The HAMP team has developed a data-sharing arrangement with Georgia Tech for acquiring aerosol/microphysics data in Atlantic tropical systems for the summer of 2010. Woodley and Rosenfeld obtained such measurements for the field campaign in India during 2009 and 2010. Golden visited with HRD scientists to coordinate desired P3 aircraft flight tracks, and to discuss collaboration on development of a new small unmanned aircraft system (UAS) with Dr. Joe Cione, HRD. (Up to the final draft of this report, we have been unable to achieve scheduling of the desired P3 flight tracks into suitable Atlantic TCs with decision-makers at HRD and AOC.) Dr. Golden has also visited NHC to coordinate HAMP research on hurricane intensity change forecasting.

## Conclusions and Recommendations for the Future

These findings underline the importance of precipitation forming and evaporation processes in TC clouds and the need to simulate them and the resultant cold pools properly in order to obtain additional

improvements in TC prediction models. These results show that the

- a) Effects of aerosols should be taken into account in the prediction of TC intensity, and
- b) Results support the HAMP hypothesis that the introduction of small aerosol particles into the clouds at their bases at its periphery act as CCN and can weaken the storm intensity.

Thus, air pollution that comes from the land into a TC can affect substantially the cloud microstructure and suppress the warm rain forming processes there. This can lead to invigoration of the affected clouds at the periphery of the storm, which is manifested by greater lightning activity and stronger precipitation reflectivities above the freezing level. The rain is restored further inside the storm by a possible combination of natural cloud seeding by sea spray and washing down of the aerosols by the rain.

The research reported here has made a significant contribution to the understanding of hurricane microphysics and our ability to improve some forecast models, but much more can be accomplished if we continue to build on the work completed in 2009/2010.

A second year of research funded for the HAMP team could address the following needs and improve forecasting of hurricane intensity through consideration of the effects of aerosols.

1. Refine inclusion of aerosols and explicit microphysics in the current HAMP models.
2. Provide for inclusion of aerosols and microphysics in the operational models used for hurricane intensity forecasting, e.g. the GFDL and SHIPS models.
3. Acquire NOAA P3 aircraft data on aerosols and microphysical parameters in Atlantic tropical systems, including hurricanes and use these data for selected cases to test/validate HAMP models and impacts of aerosols on hurricane intensity changes.
4. Develop a proper formulation of the effects of aerosols in the models requires additional research involving in situ measurements of aerosols and cloud properties to be conducted with the

hurricane monitoring airplanes in storms ingesting air masses with various aerosols.

5. Further develop the spray model by creating advanced parameterization of spray effect on surface fluxes and on the structure of the BL.

6. Conduct simulations of different TC using WRF/SBM model. Investigation of aerosol effects on intensity of hurricanes and on TC genesis under different environmental conditions.

7. Modify the SBM codes (development and implementation of a new parallelization method) with the purpose of significant decrease of the computer time of WRF/SBM simulations.

8. Simulate the effects of introduction of CCN aerosols into clouds at the TC periphery. Estimate the impact of varying amounts of CCN aerosols and various particle sizes on the storm intensity.

9. Calibrate current two-moment bulk parameterizations to improve representation of convection and aerosol effects in current TC forecasting models in collaboration with HRC (of GFDL).

10. Examine impacts of aerosols on hurricane intensity change relative to other important factors, such as vertical wind shear, moisture, and sea-surface temperatures.

11. Investigate how black carbon aerosols introduced at low levels in a hurricane environment can impact TC intensity. Also investigate how black carbon aerosols introduced above the anvils and over a large area extending beyond the storm impact its intensity.

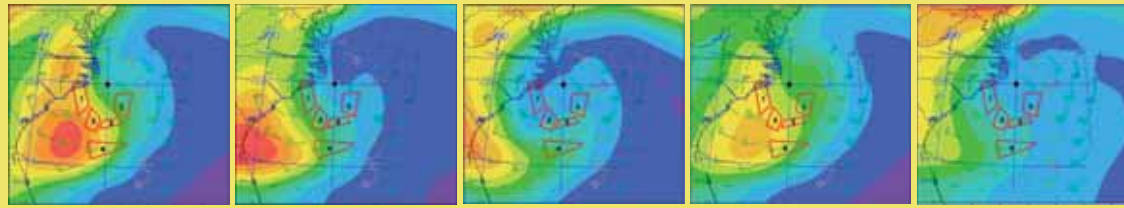
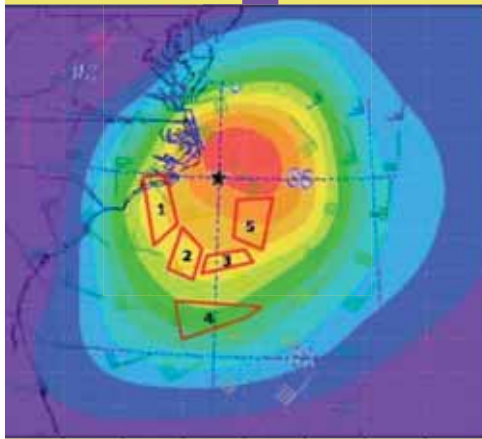
12. Continue to build coalitions with groups tasked with the improvement of TC intensity. For example, there is a good possibility if HAMP is continued of collaboration with the Navy's development of a new operational TC prediction model, Coupled Ocean and Atmosphere Mesoscale Prediction System (COAMPS)-TC at its facilities in Monterey. We plan to hold a joint HAMP/Navy Workshop in the Washington, DC area in early December, 2010 to explore such collaboration. The Navy has expressed interest in utilizing some of the new HAMP microphysical and aerosol expertise in its COAMPS model.

13. Apply the HAMP TC models to test new

cases defined by the NHC Science Operations Officer, Dr. Landsea, as "problem cases" for current NHC operational hurricane intensity change models in the 2010 hurricane season.

If Phase 2 funding for HAMP is approved, these important activities will take place in 2011.





## Satellite Observations of Pollution Aerosols Suppressing Warm Rain and Invigorating Spiral Cloud Bands of Tropical Cyclones<sup>1</sup>

### 1.1 Introduction

The hypothesis that CCN aerosols decrease the intensity of tropical cyclones has been supported by numerous simulation studies. It was also supported by statistical analyses showing that aerosols can explain part of the variability of storm prediction errors. Here we present observational support to key links in the conceptual model describing the way by which aerosols might be affecting the intensity of the storms.

Satellite observations show that pollution aerosols reduce the cloud drop size and suppress the formation of warm rain processes in the external spiral cloud bands of the tropical storms, which in turn invigorates the convection in the clouds and induces cloud electrification. These effects are countered by the sea spray raised by the strong winds closer to the center of the storms, which introduce giant CCN. These observations reinforce the already available simulation and statistical analysis, which support the hypothesis of CCN aerosols reducing the intensity of TCs by invigorating the peripheral clouds at the expense of the intensity of the convection in the eye wall.

1. Principal Author: Prof. Dr. Daniel Rosenfeld, Hebrew University of Jerusalem, Israel; With contributions from: Mr. Tal Halevi and Ms. Michal Clavner

### 1.2 Impact of Aerosols on the Dynamics and Electrification of Deep Tropical Convective Clouds

The suppression or delay of precipitation by aerosols can have a substantial dynamic effect on the clouds of all depths, from expanding the cloud cover of marine stratocumulus (Albrecht, 1989; Rosenfeld et al., 2006; Wood et al. 2010) to invigorating deep tropical convection (Rosenfeld et al. 2008a and references therein; Koren et al. 2010). In this study we extend the observations to the CCN impacts on maritime clouds that constitute TC, and discuss the possible effects on these storms.

Previous studies have shown that increased aerosol quantities can slow the drop coalescence and hence suppress the formation of warm rain below the freezing level (Gunn and Phillips, 1957). Heavy smoke from forest fires in Indonesia and in the Amazon was observed to reduce cloud droplet size and so delay the onset of precipitation from 1.5 km above cloud base in pristine clouds to more than 5 km in polluted clouds (Rosenfeld, 1999; Rosenfeld and Woodley 2003; Andreae et al. 2004). Elevating the height for onset of precipitation keeps the cloud water in the cloud up to greater heights, and instead of early rain out the water is raised to the super-cooled (SC) levels. The freezing of the SC water onto ice hydrometeors releases additional latent heat and leads to invigoration of the updrafts, causing more

intense thunderstorms (Andreae et al. 2004). Cloud electrification takes place mostly at temperatures below  $-13^{\circ}\text{C}$ , when collisions of ice crystals and graupel occur in the presence of super-cooled cloud drops (Takahashi, 1978; Saunders, 1993; Black et al., 1999; Cecil et al. 2002; Sherwood et al. 2006). Increased CCN concentration induces greater updrafts, larger SC water content and ice hydrometeors, which are the main ingredients for cloud electrification. The phenomena of invigoration due to aerosols in polluted clouds over ocean is supported by observations (Koren et al. 2010) of deep tropical clouds growing taller in areas containing greater aerosol quantities as measured by the aerosols optical thickness (AOT) observed directly by satellites and as calculated by the Goddard Chemistry Aerosol Radiation and Transport (GOCART) hindcast model (Chin et al. 2000).

### 1.3 Possible Impact of Aerosols on the Dynamics of Tropical Cyclones

Fierro et al. (2007) showed in numerical simulations that the disappearance of lightning in the TC central zone and its intensification at the TC periphery can be a good indicator of a TC decaying, since the lightning signifies the intensification of the convection at the outer bands of the TC on expense of the intensity of the convection in the eye wall. Khain et al. (2008) conducted simulations, which showed that aerosols change the cloud microstructure and the dynamics to foster lightning formation. It was simulated that as the TC approaches landfall, the increased aerosol concentrations induce the transition of the lightning within the eye wall to the lightning at the TC periphery, signifying the decay of the TC intensity.

The idea of modifying TCs by aerosols through their impacts on precipitation forming processes originated with project STORMFURY (Willoughby et al. 1985). It was postulated that glaciogenic (ice forming) seeding of convective clouds just outside the eye wall would freeze their SC water, so that the released additional latent heat of freezing would invigorate the seeded clouds and disrupt the convergence of air into the eye wall and so weaken the maximum TC wind speed. STORMFURY was inconclusive, to a

large extent because most TCs apparently do not have sufficient SC water. The pristine maritime air that typically converges to TCs has small concentrations (few hundred  $\text{cm}^{-3}$ ) of CCN, which form respectively low concentrations of large cloud drops that are fast to coalesce into raindrops. Therefore, much of the cloud water precipitates from the rising air before reaching the freezing level, thus leaving little potential for SC water.

Based on the hypothesis of aerosols invigorating convection, as reviewed by Rosenfeld et al. (2008), Rosenfeld et al. (2007) simulated the impacts of aerosols suppressing coalescence in TC clouds and suggested that the basic idea of STORMFURY – invigoration of the periphery on expense of the center – might still work by adding CCN aerosols to the air ingested by a TC. The early rainout can be delayed by high concentrations of CCN aerosols, which form a larger number of smaller cloud drops that are slower to coalesce into raindrops.

TC weakening was observed to occur in the presence of Saharan Air Layer, which contains large quantities of dust aerosols (Dunion and Velden 2004). However, the effect could not be ascribed uniquely to the aerosols. These observations prompted numerical simulations testing the impact of CCN activity of desert dust on TC intensities (Cotton et al. 2007, Zhang et al. 2007). This was simulated by adding  $2000 \text{ CCN cm}^{-3}$  in the area where the storms formed compared to simulations with  $100 \text{ CCN cm}^{-3}$  (considered to be “clean of pollution”) and  $1000 \text{ CCN cm}^{-3}$ . In the simulation with the  $2000 \text{ CCN cm}^{-3}$  the CCN aerosols weakened the storm substantially, with peak winds lowered by  $25 \text{ ms}^{-1}$  and central pressure higher by 25hPa. Independently, Rosenfeld et al. (2007) obtained similar results by simulating the invigoration achieved due to turning off the warm rain forming processes at the periphery of a TC. They showed that the suppression of warm rain led to invigoration at the periphery coupled by enhanced evaporation and cooling at the low levels that led to weakening of the TC. However, wind-induced sea spray containing salt aerosols that serve as giant CCN restored the warm rain and reduced the simulated TC-weakening effect. Subsequent model simulations provided additional

support to this mechanism and emphasized the role of cold-pools of air due to evaporative cooling that weaken the storms (Khain et al. 2008; Zhang et al. 2009).

#### **1.4 Quantitative Relations Between Aerosol Amounts and TC Intensity**

Rosenfeld et al. (2010) used observed TC data and forecasted TC data to statistically analyze the relationships between TC intensity to aerosol quantities at the TC's periphery. They separated the aerosol's effect on TC intensity from all other effects by using data of TC prediction models (GFDL (Bender et al. 2007) and SHIPS (DeMaria et al. 2005)) that take into account all meteorological and sea surface temperature properties, but not the aerosols. Their hypothesis was that if greater aerosol amounts actually act to decrease storm intensity, the forecast model would tend to over predict the observed intensities of the more "polluted" storms. Rosenfeld et al. (2010) tested this hypothesis by examining the prediction errors of the maximum sustained wind velocities ( $dV_{max}$ ) and their statistical relationship with GO-CART's calculated AOTs at the TC peripheries. The results showed that an increase of 0.01 in the AOT of sulfate or organic carbon aerosols is associated with a reduction of nearly 0.5 kt in  $dV_{max}$ . Dust did not appear to have much of an effect, probably because of its weak small CCN activity.

This statistical analysis supports the findings of numerical studies (Rosenfeld et al. 2007, Cotton et al. 2007, Zhang et al. 2007; Khain et al. 2008; Zhang et al. 2009), and therefore, this association is likely to be a cause and effect relationship in accordance with the HAMP hypothesis that CCN aerosols decrease TC intensity. These findings underline the importance of precipitation forming and evaporation processes in TC clouds and the need to simulate them and the resultant cold-pools properly in order to obtain additional improvements in TC prediction models.

#### **1.5 Conceptual Model of the Ways by Which Aerosols Might be Affecting TCs**

Rosenfeld et al. (2007) formulated a conceptual model of the ways by which the CCN aerosols might be affecting the TC intensity. This conceptual model was further refined based on additional simulations and observations since 2007. Our present understanding is summarized in the following links in the conceptual chain:

1. Small CCN aerosols in the form of particulate pollution and/or desert dust nucleate larger numbers of smaller cloud drops that slow the coalescence of the cloud drops into rain drops.
2. The CCN aerosols present in the peripheral clouds of the hurricane slow the rain forming processes there.
3. The delayed formation of rain decreases the amount of early rainout from the rising air; hence more water can ascend to freezing levels, where it forms ice precipitation particles.
4. The greater amount of freezing water aloft releases extra latent heat that invigorates the convection. The invigoration and the added SC water are manifested in greater cloud electrification and lightning discharges.
5. The greater vigor of the clouds draws more ascending air at the periphery of the storm, thereby bleeding the low-level airflow towards the eye wall. The weakened convergence towards the center causes the central pressure to rise; less air ascends in the eye wall, and respectively lower maximum wind speed.
6. The intensified ice precipitation at the peripheral clouds melts and evaporates at the lower levels, thereby cooling the air that converges into the center of the storm.
7. Additional low-level cooling occurs when the cloud drops that did not precipitate and did not ascend to the freezing level re-evaporate.
8. The storm is further weakened by cooling of the low-level air that converges to the center, in addition to the air bleeding effect that was discussed in the first five points. The cooler air has

less buoyancy and hence dampens the rising air in the eye wall, thereby weakening further the convergence and the maximum wind speed of the storm.

9. Wind raised sea spray induces large cloud and drizzle drops that partially restores the warm rain processes and has a contradictory effect to the delaying effect of CCN aerosols on rain forming processes. Therefore the CCN aerosol effect would be effective mostly in the peripheral clouds of the storm, where the winds are still not very strong. Strengthening of the winds there would reduce the sensitivity of the storm to the weakening effect of the CCN aerosols.

## 1.6 Observations of Aerosols Impacts on Cloud Bands in TCs

### 1.6.1 The Observational Methods

The conceptual model is supported by model simulations and statistical analysis relating the aerosols to TC intensities. Here we provide observations of pollution aerosols that interact with TCs and clearly affect their cloud microstructure and electrification, in ways that are directly related to key links in the conceptual model.

Here we use satellite observations of aerosols, the vertical profiles of cloud microstructure, and lightning flashes in order to locate increased aerosol quantities. In order to quantify the aerosols, the aerosol optical depth (AOD) was obtained from NASA's Moderate Resolution Imaging Spectroradiometer (MODIS) standard aerosol products as well as the AOT simulated by the hindcast GOCART model. Additional information on the vertical distribution of the aerosols was obtained from the Cloud Aerosol Lidar with Orthogonal Polarization (CALIOP) on board the CALIPSO satellite. The cloud microstructure was inferred by relating the cloud top particle effective radius ( $r_e$  in  $\mu\text{m}$ ) to cloud top temperature ( $T$  in  $^{\circ}\text{C}$ ), using the method of Rosenfeld and Lensky (1998). The combination of  $r_e$  from cloud tops at different  $T$  reproduces the vertical evolution of cloud top  $r_e$  with its vertical growth (Lensky and Rosenfeld

2006). The evolution of the cloud composition and particle size in the vertical cross section of a cloud can be used to infer the precipitation properties: non-precipitating, drizzle, warm rain, mixed-phase, or ice precipitation processes. A particularly intriguing prospect is the ability of detecting how cloud composition and precipitation are affected by natural (e.g., desert dust) and anthropogenic aerosols (e.g., smoke from burning vegetation, urban and industrial air pollution) (Rosenfeld and Lensky, 1998; Rosenfeld, 1999 and 2000; Rosenfeld et al. 2001, 2002, 2007, 2008b; Rosenfeld and Woodley 2003; Rudich et al. 2002 and 2003). This is illustrated in Fig. 1.1.

The  $T$ - $r_e$  relation can be retrieved from the MODIS onboard Terra and Aqua satellites and from the Visible and Infra Red Scanner (VIRS) onboard the Tropical Rainfall Measuring Mission (TRMM) satellite. Also used in this study are the TRMM Precipitation Radar (PR) that provides the 3-dimensional structure of the precipitation reflectivity, and the Lightning Imaging Sensor, which measured the lightning flashes that occur during 90 seconds in the field of view of TRMM during its overpass.

### 1.6.2 Typhoon Nuri on 21 August 2008

Two storms presented here provide clear examples of the aerosol effects on TC cloud microstructure. The first example is for Typhoon Nuri, which hit Hong Kong on 21 August 2008. This is a good example because it drew heavy air pollution from mainland China, which was visibly seen from space as haze that partially obscured the land surface (Fig. 1.2). The haze is clearly seen in Fig. 1.3 as a red strip of MODIS AOT > 0.9. According to the CALIOP lidar (See to the south of point A in Fig. 1.3) the haze was at the lowest 2-3 km of the atmosphere. This haze converged into a cloud band that spiraled towards the center of the Typhoon. The polluted clouds reduced the cloud drop size in that band to less than half in comparison to the cloud drops at the same height in the non-polluted clouds. The height for reaching the precipitation threshold of median  $r_e \approx 15 \mu\text{m}$  (Lensky and Drori 2007) in the polluted clouds increased from the  $12^{\circ}\text{C}$  isotherm level to about  $-13^{\circ}\text{C}$  (see

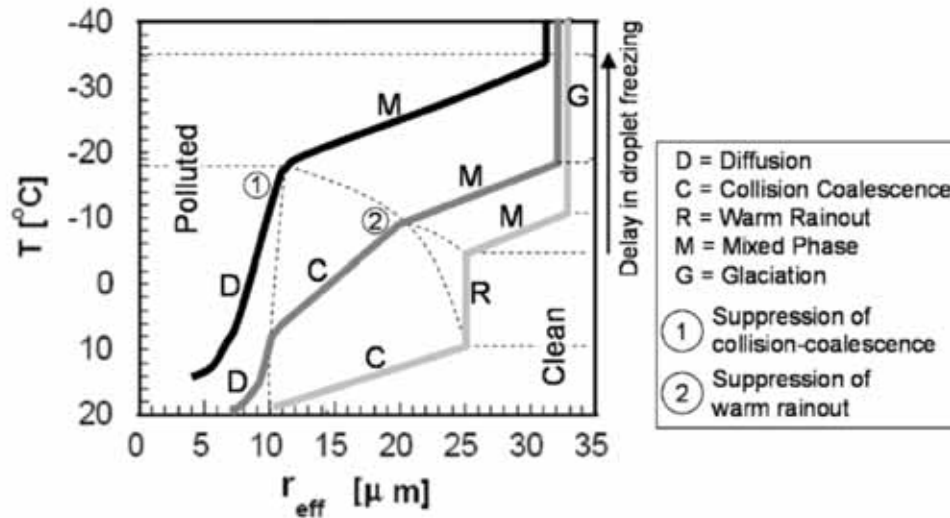


Figure 1.1 Conceptual diagram adapted from Rosenfeld and Lensky (1998)

The diagram describes five microphysical stages: droplet growth by diffusion, collision-coalescence, warm rainout, ice-water mixed phase and glaciated phase. These stages are common to deep convective clouds and their response to the concentration of pollution aerosols. The bottom curve (light grey) shows the case of maritime environment with low CCN concentration and the possibility of warm rain processes. The middle curve (grey) corresponds to commonly found continental cases, where the larger number of CCN aerosols suppresses the warm rain process. The top curve (black) represents extremely polluted cases where the very large number of CCNs produce smaller and more numerous droplets at the cloud base suppressing the onset of collision-coalescence processes, and postpones the start of droplet freezing to much lower temperatures, in comparison to the less polluted case (grey line). These three situations are the examples of not polluted (light grey), polluted (grey) and extremely polluted (black) cases therefore, intermediate situations to the above curves occur.

the  $T-r_c$  relations for rectangles 1 and 2 in Fig. 1.4, respectively). This is a dramatic difference between the polluted clouds to the pristine clouds in the same TC. The pristine clouds (rectangles 2 and 6 in Fig. 1.4) produced early warm rain and lost much water at the rainout regime (see schematic representation in R in Fig. 1.1) before glaciating quickly above the  $0^\circ\text{C}$  isotherm level, as indicated by the sharp increase of  $r_c$  there. The  $r_c$  of the polluted clouds remained well below  $10\ \mu\text{m}$  below the  $0^\circ\text{C}$  isotherm, implying negligible cloud drop growth by coalescence, which means strong suppression of warm rain. The sharp increase of  $r_c$  above the  $-13^\circ\text{C}$  isotherm indicates that mixed phase precipitation forming processes occurred there, leading to glaciation at about  $-22^\circ\text{C}$ , as seen by the  $r_c$  values reaching its saturation value.

According to the TRMM PR, the polluted cloud band developed high reflectivities well above the freezing level, associated with numerous lightning

flashes (See Fig. 1.5). This is in sharp contrast to the other bands that ingest pristine maritime air. The highest reflectivities there were weaker than in the polluted cloud band by 5 to 10 dBZ and were confined to below the freezing level at heights of about 5 km. The pristine microphysically maritime cloud bands did not produce any detectable lightning, indicating scarcity of SC water and ice particles.

The base temperatures of the polluted and clean clouds were similar, as indicated by the warmest cloudy pixels. There are no other meteorological reasons that could conceivably serve as a potential alternative explanation to the indicated microphysical differences between the polluted and pristine cloud bands in such close proximity.

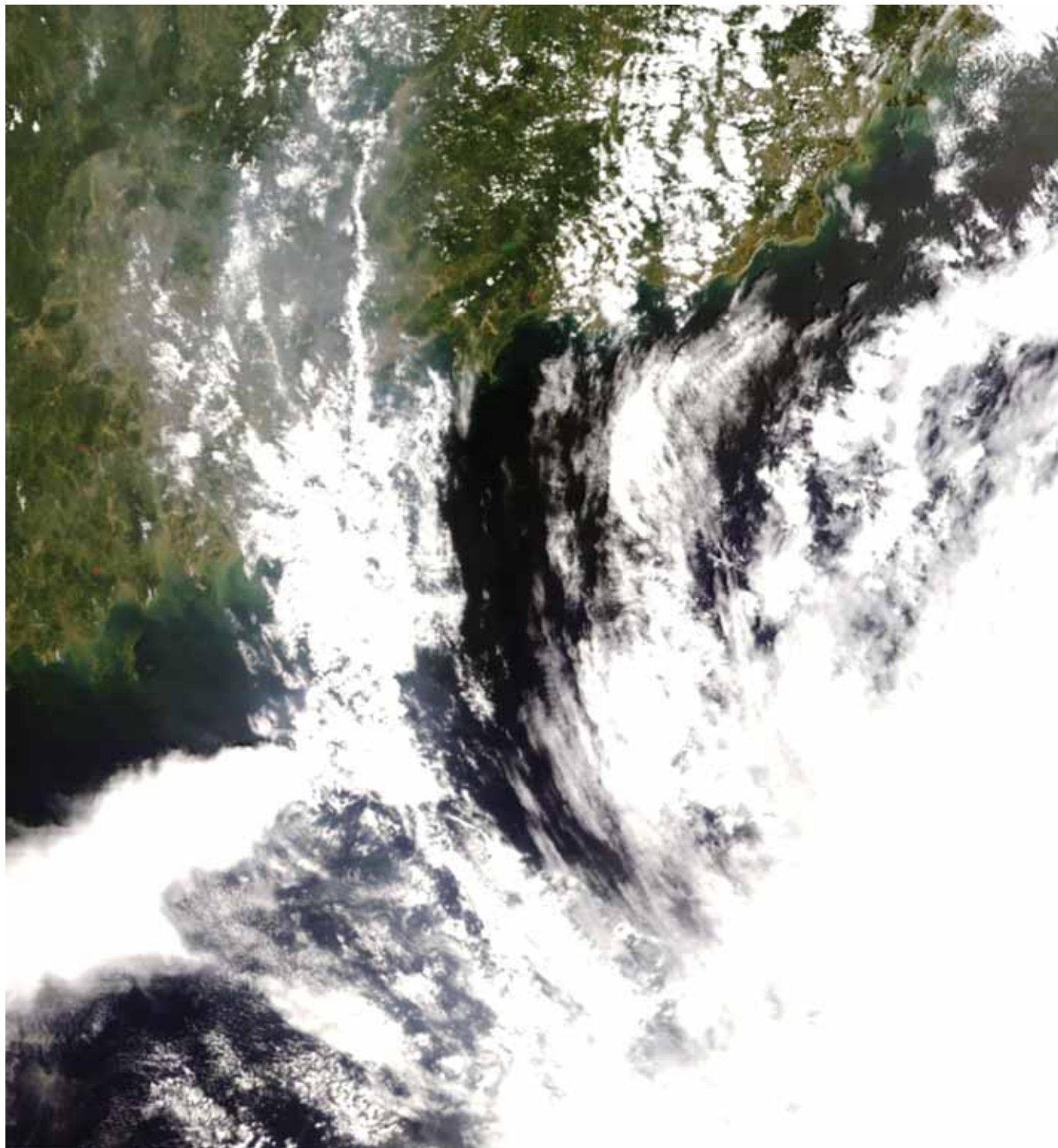


Figure 1.2 Air pollution haze (left top corner) ingested into a spiral band of Typhoon Nuri (bottom right corner)

While approaching Hong Kong, the haze, originating from mainland China obscures partially the land terrain and brightens the sea surface to the south, due to increased scattering of incoming solar radiation. Clean maritime air converges to the storm from the East China Sea at the upper right of the image. This is a true color image taken by Terra's MODIS from 21 August 2008 02:55 UTC. The image size is approximately 850 km in the north-south and 1000 km in the east-west directions.

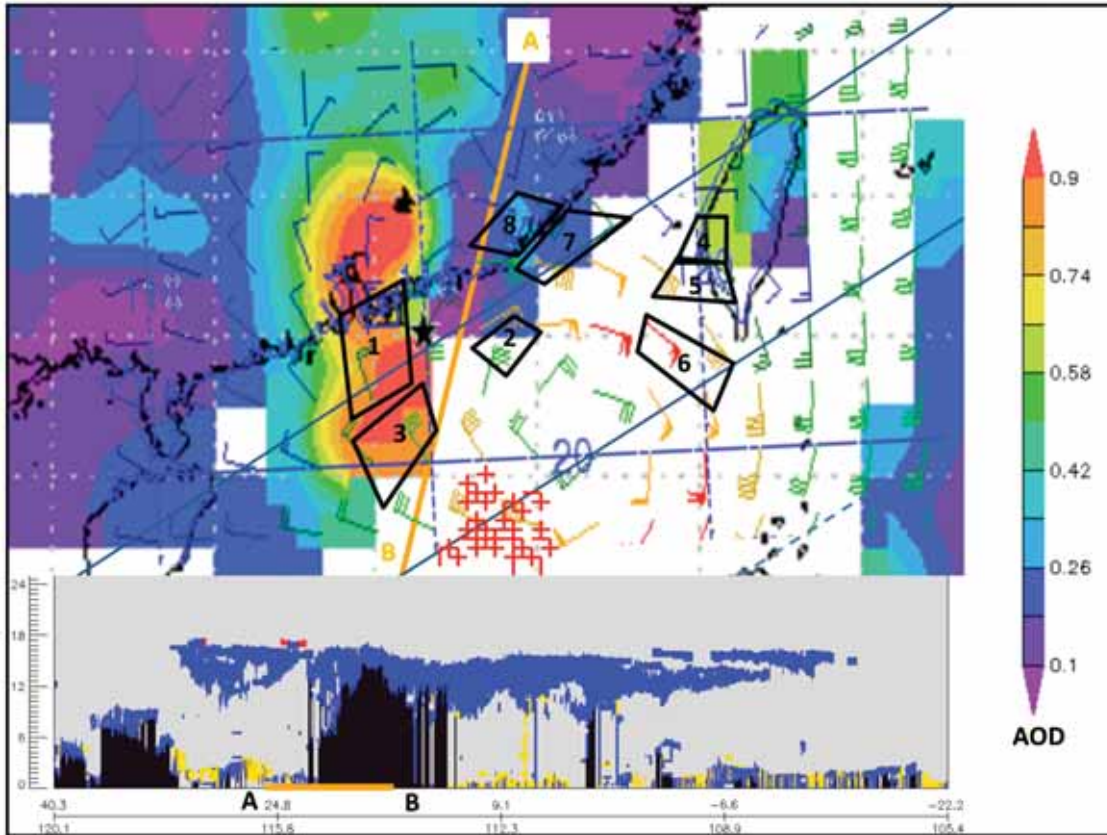


Figure 1.3 NASA/MODIS-Aqua aerosol optical depth (AOD) image

A surface wind flag map is superimposed, as calculated from NCEP reanalysis, for the same area shown in Fig. 1.2. Rectangles and their numbers match those on Fig. 1.3. Black solid lines delimit the TRMM-PR swath and black dashed lines delimit the TRMM-passive microwave swath, shown in Fig.1.5. Lightning flashes in this figure are denoted by the red crosses. The lower inset is the CALIPSO-Lidar vertical feature mask along the line AB, which is presented on the AOD image by the orange solid line and the short orange line in the lower inset. The color blue in the inset figure indicates clouds, the orange – aerosols, the red – stratospheric clouds and the black – total attenuation of the signal. The horizontal scale is latitude (above the line) and longitude (below the line) and the vertical scale is altitude (km). The layer containing the aerosols near point A is confined between the surface and about the height of 4 km, therefore it is evident that the aerosols feed the base of the clouds, allowing them to affect the cloud microphysics. The areas containing higher AOT $>0.9$  (red area) attributed to anthropogenic pollution emitted from the industrialized areas in China noticeably coincide with the polluted cloud band in Fig. 1.2. The wind advects the polluted continental air mass off-shore into the typhoon. The lightning activity occurs in the area to which the wind appears to drive the polluted aerosol laden air. The aerosol AOD could not be calculated in the location of the lightning due to the cloud canopy obscuring the AOD retrievable data.

### 1.6.3 Hurricane Gustav off the South Carolina Coast on 10 September 2002

The second case, TC Gustav, near the east coast of the United States, shows how air pollution is drawn into the storm. This storm is similar to the first case in this respect, but is less conspicuous because the levels of air pollution over China exceed by

far the levels that are observed over the United States in this case. The clouds that form in the air that comes off the south eastern shores of the United States appear with substantially reduced  $r_c$  (rectangle 4 of Fig. 1.6) compared to the clouds closer to the storm center (rectangles 3 and 5 of Fig. 1.6), or compared to the clouds in the maritime flow in the first case (rectangles 2 and 6 of Fig. 1.4). The MODIS AOD shows only moderate values of about 0.15, which in-

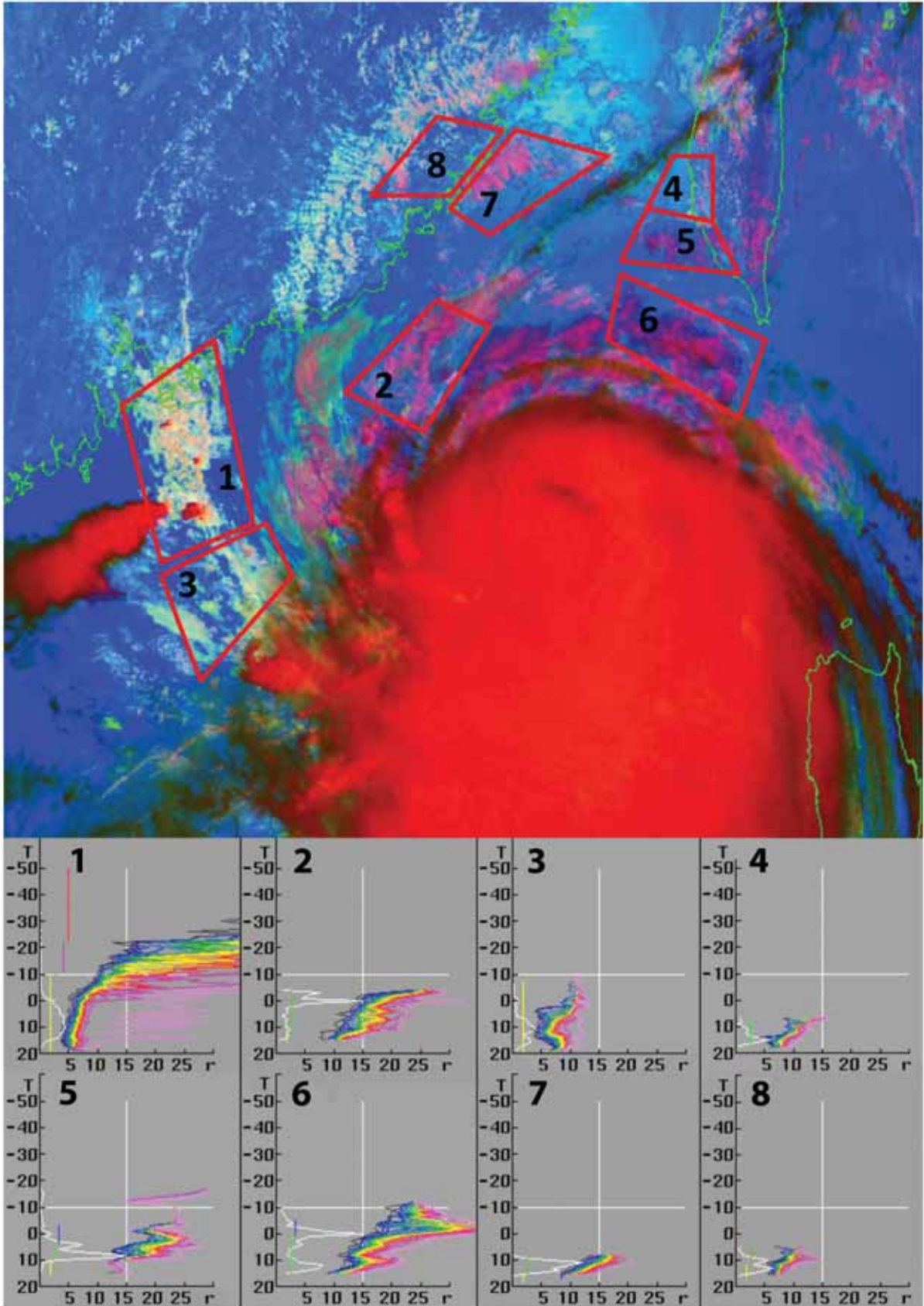


Figure 1.4 Satellite microphysical analysis of Typhoon Nuri

A NASA/MODIS-Terra image from 21 August 2008 02:55 UTC, for the same area as in Fig. 1.2. The colors in the figure signify the solar reflectance at different wavelengths: red for visible reflectance, green for 3.7- $\mu\text{m}$  reflectance (approximating cloud top particle effective radius,  $r_e$ ), and blue for the inverse of 10.8- $\mu\text{m}$  brightness temperature. The rectangles enclose areas corresponding to the graphs below the satellite image, which present the evolution of  $r_e$  [ $\mu\text{m}$ ] on the x-axis as a function of cloud top temperature [ $^{\circ}\text{C}$ ] on the y-axis. The significance of the colors and the interpretation of the T- $r_e$  relations are first described in Rosenfeld and Lensky (1998) and are schematically shown in Fig. 1.1. In this figure, rectangles 1 and 3 mark the spiral band present in the polluted air mass. The yellow colors of the clouds indicate small  $r_e$ , which is caused by the increased number of air pollution aerosols nucleating a large number of small cloud drops. The microphysical effects of aerosols are presented coherently in the T- $r_e$  plot of rectangle 1, showing that  $r_e$  reaches the 15  $\mu\text{m}$  precipitation threshold only above the  $-10^{\circ}\text{C}$  isotherm height indicating the suppression of warm rain in this spiral band of the typhoon. The precipitation initiates as ice hydrometeors above the  $-10^{\circ}\text{C}$  height. In contrast, the clouds in rectangle 2 are located in pristine air mass that is advected from the Eastern China Sea are indicated by the magenta color signifying large  $r_e$  at high T, which is typical for maritime clouds. This is also shown quantitatively in the T- $r_e$  number 2, where the 15  $\mu\text{m}$  precipitation threshold is already reached at altitudes below the  $10^{\circ}\text{C}$  isotherm level, an occurrence typical for maritime clouds in pristine air. Typhoon Nuri is a good example that shows warm rain precipitation from clouds in the pristine air mass, but its prevention in the nearby polluted clouds due to increased CCN quantities.

creases to about 0.3 towards the center of the storm, probably due to the strong surface winds, reaching 45 knots (Fig. 1.7). The GOCART AOT replicates this pattern of carbonaceous and sulfate aerosols coming off the southeastern United States and ingested into the TC, being replaced by sea salt inside the storm (Fig. 1.8). Because Gustav did not yet reach a hurricane stature (at that time it was a tropical storm with maximum winds of 50 kt), the cloud canopy was not fully developed, and so the cloud tops of the convective feeders can be seen inside the storm and not only at the outer spiral bands, which is the case in well-formed TCs (Fig. 1.6). This allows us to track the microphysical changes that the polluted clouds undergo when they approach the center of the storm, where the winds are stronger, demonstrated in Fig. 1.6. In this figure, the T- $r_e$  relations show that at the periphery (rectangle 4), the  $r_e$  remains under 15  $\mu\text{m}$  until the height of  $-5^{\circ}\text{C}$  indicating suppressed warm rain. In comparison, it can be seen that closer to the center of the storm (rectangle 3) the  $r_e$  reaches 15  $\mu\text{m}$  already at the height of about  $13^{\circ}\text{C}$ , indicating active warm rain processes at much lower heights than in rectangle 4.

## 1.7 Research Flights in Hurricanes

### 1.7.1 Overview

The HAMP effort uses model simulations and observational studies that make use of aerosol measurements to reach its goal. The observations are used to document TC structure and behavior before and after the ingestion of aerosols. Then the observations are used to validate the model simulations of changes brought about by the aerosols. Aerosol measurements within TCs can be obtained from satellite imagery and from direct sampling by aircraft within the storm using particle measuring devices mounted on the reconnaissance plane. The HAMP team saw such a need for these measurements that it purchased a CCN counter and PCASP aerosol instrument at a cost of \$162,000. This instrumentation has since been shipped to NOAA for installation on its P-3 aircraft for the 2010 Atlantic hurricane season. Unfortunately it was not possible to mount the PCASP instrument on any of the NOAA aircraft, so no measurements of giant CCN and sea spray at low altitudes could be made. The two cases presented earlier in this chapter show the value of taking such measurements.

Members of the HAMP team have been working with various scientists and groups to promote the summer observational field effort, trying to be helpful and not intrusive to the other parties involved. A

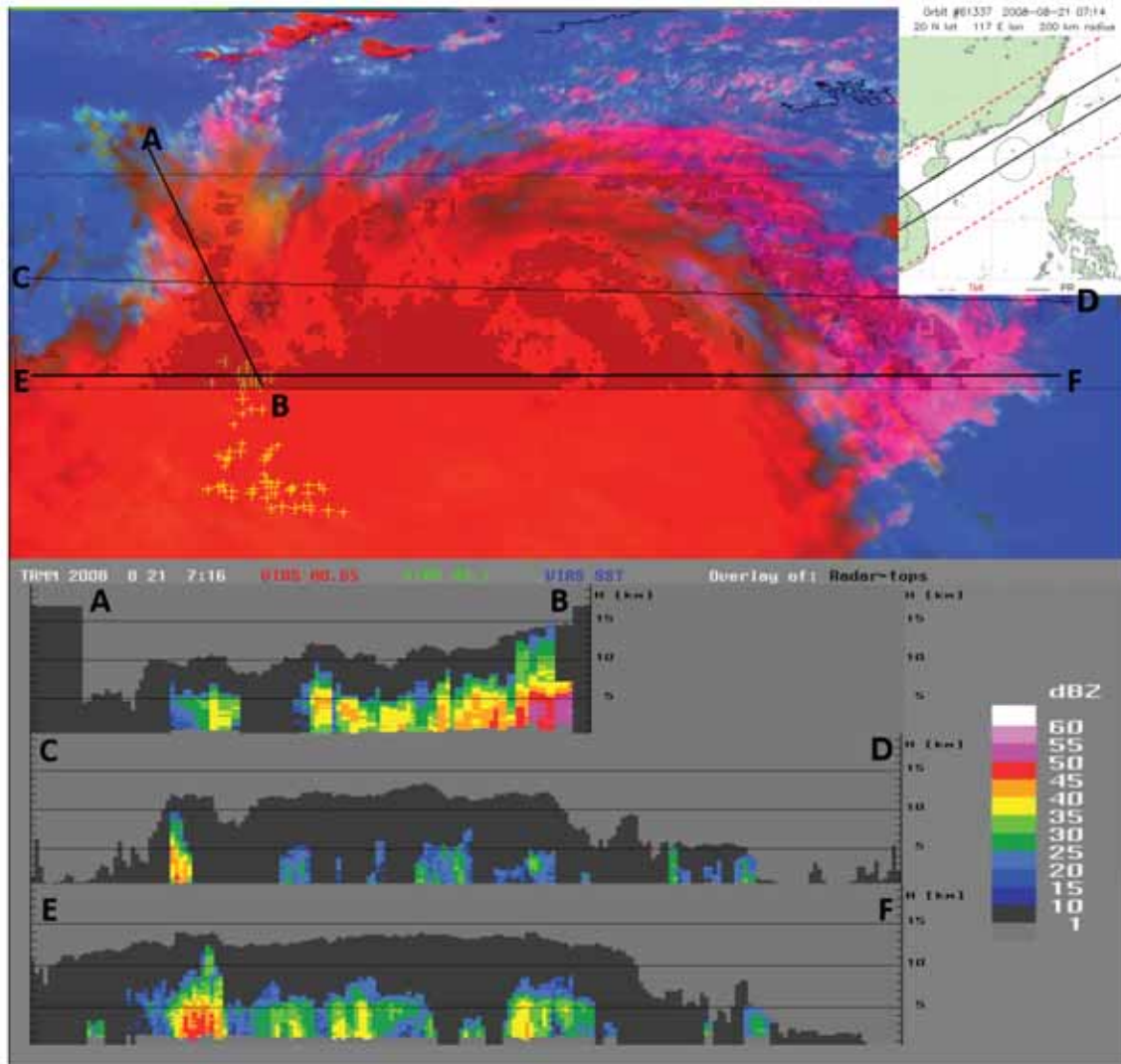


Figure 1.5 TRMM satellite VIRS image of the typhoon Nuri

From 21 August, 2007, 0716 UTC (the color scheme is the same as in Fig. 1.4). The geographic coverage of the TRMM overpass is given at the inset at the upper right corner. The center two lines delineate the swath of the precipitation radar (PR). Lightning flashes are denoted in the upper inset by the yellow crosses. The lower inset contains three vertical cross sections along the lines AB, CD and EF, which are represented on the VIRS image by black solid lines and the respective letters, where the left end is point A and the right end correspond to point B, etc. The colors in the lower inset represent the precipitation reflectivity in dBZ, as measured by the TRMM PR. The swath of the PR is delimited on the main figure by the two uppermost and lowermost black lines. Areas in the lower inset with gray overlay are PR detected precipitation from the spiral bands of the storm, which are present under the high cloud canopy. Note the lightning activity along the area where the polluted spiral band enters the typhoon, indicating large amounts of SC water, ice particles and strong updrafts. The larger aerosol quantities are also evident in the high PR reflectivity and at higher levels (colder temperatures), where lightning is active, at the TC periphery. Elsewhere the reflectivities in the storm are much lower and quickly decay above the freezing level, which is at about the height of 5 km, signifying the microstructure of pristine conditions.

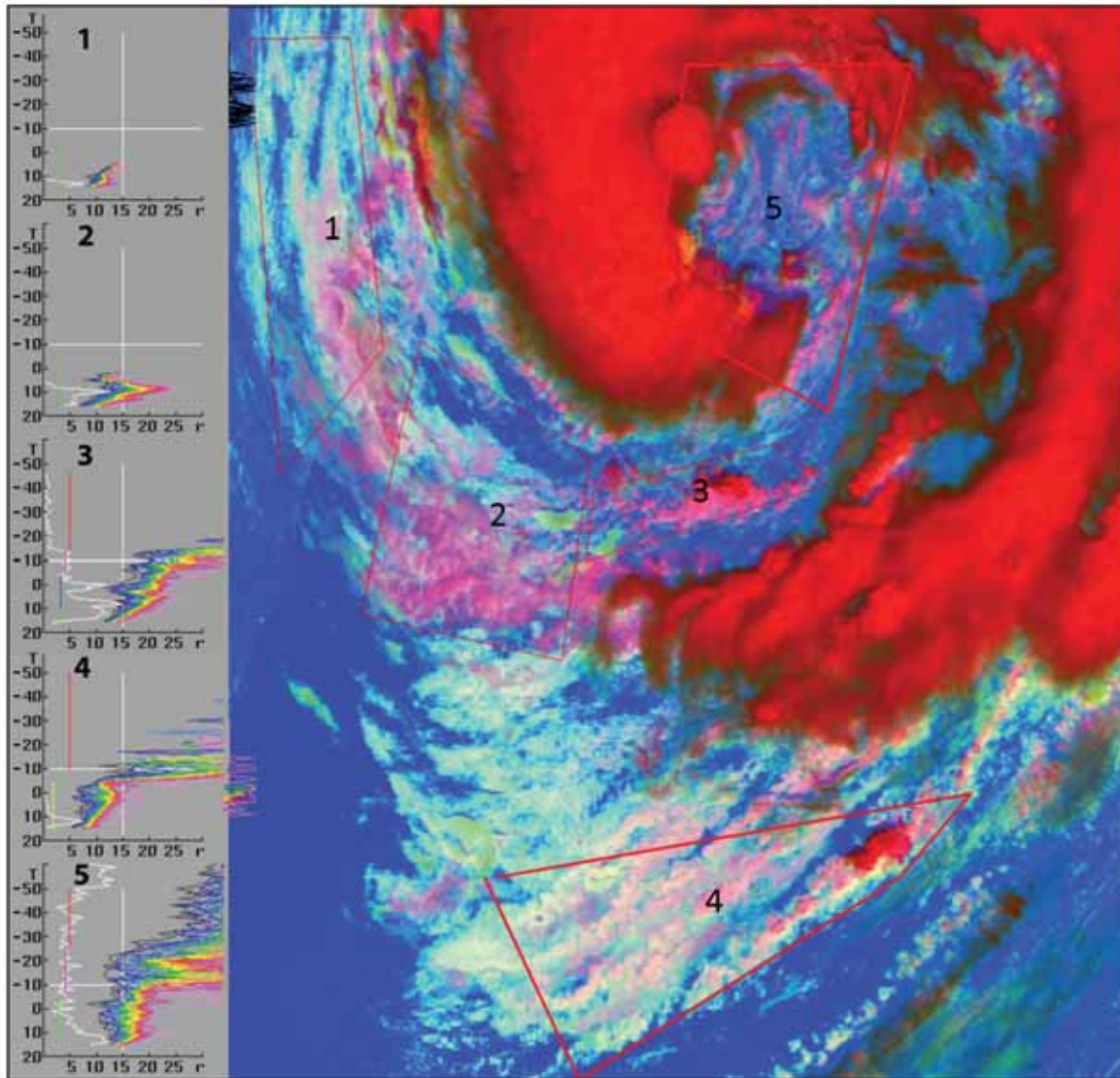


Figure 1.6 Tropical cyclone, Gustav off the coast of South Carolina, from MODIS Terra

Same as in Fig. 1.4, but for Gustav on 10 September 2002 15:40 UTC. The geographic location is evident in Fig. 1.7. Off shore flow brings polluted air from the southeastern USA into the storm. The polluted air forms clouds with small drops over the ocean, as seen in rectangle 4, where the clouds grow to the  $-5^{\circ}\text{C}$  isotherm before they reach the precipitation threshold  $\text{Re}$  of 15 micron. The not yet fully developed cloud shield of the growing storm permitted the tops of the growing clouds to be seen in the inner spiral bands and in the region of the eye (rectangles 1, 2, 3, and 5). According to the redder colors and the  $\text{TRe}$  relation in rectangle 3, cloud drops constituting the clouds closer to the center of the storm are by far larger, indicating washout of the aerosols and/or the effect of the sea spray, induced by the storm's winds, creating large drops, which restores the warm rain processes. However, in region 5, which encompasses part of the developing eye, where convection should be the strongest, the  $\text{Re}$  is not the largest.

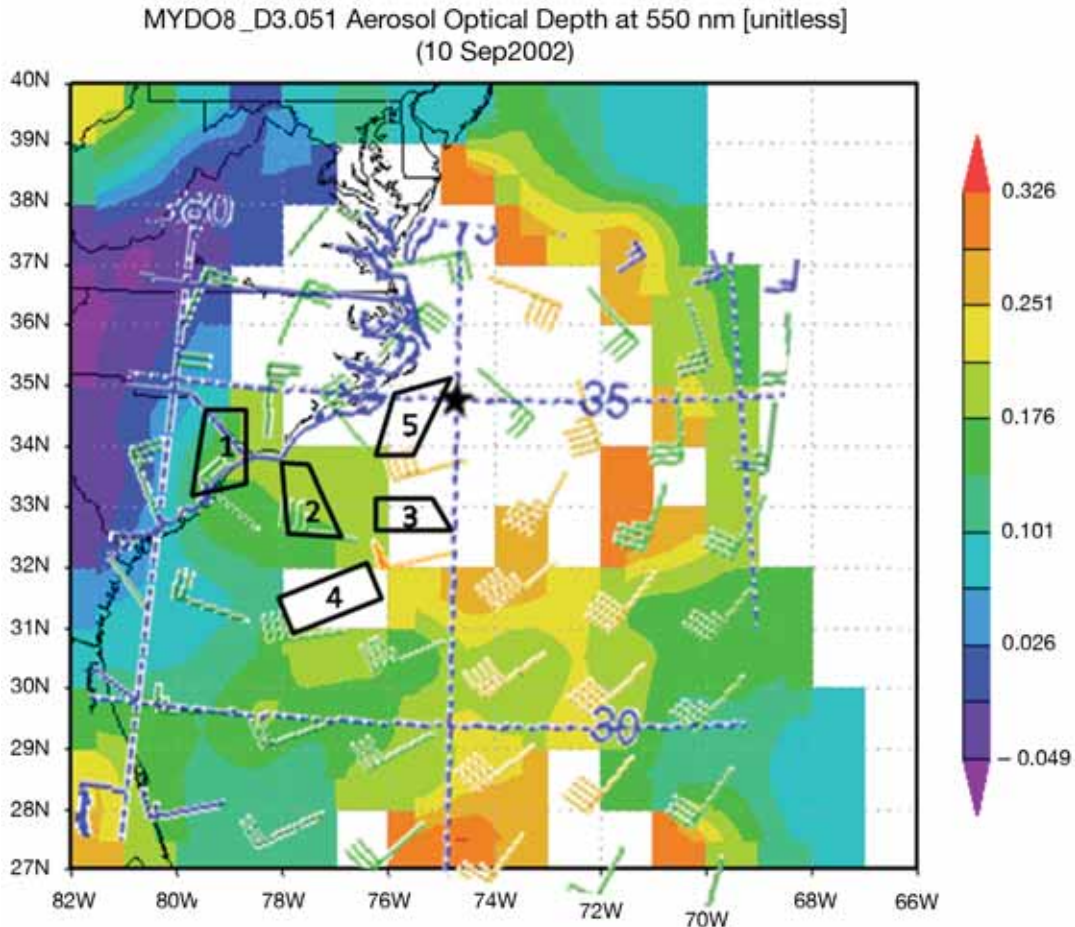


Figure 1.7 NASA/MODIS-Aqua aerosol optical depth (AOD) image for TC Gustav

On September 10th 2002, same as Fig. 1.3, the TC ingests the polluted air mass from the southeast United States, as can be seen from the higher AOD values in the bottom left corner and the wind contours advecting this air mass into the storm. Rectangle 4, having a location determined according to Fig. 1.6, lacks satellite retrieved AOD data due to the masking the clouds but it can be inferred from the data points adjacent to it. The highest AOT values coincide with the highest surface winds, indicating that it might be related to sea spray

major challenge at this writing was the implementation of flight plans that would give the best chance of HAMP securing some of the needed measurements. These flight plans require flight at cloud base that is lower than the P-3 aircraft typically fly. The desired flight plan and procedures are presented in Fig. 1.9. These are detailed and specific, so it would be best to have a member of the research team on the aircraft to direct at least a portion of the flight to implement the desired flight patterns. Seating on the flights was limited because of seat commitments to other individuals, so real-time flight direction by a HAMP team member was not possible as of early September 2010.

### *1.7.2 Flight Patterns for Measuring Cloud-Aerosol Interactions*

Given here are the considerations for aircraft flight planning strategy and the flight patterns, as were summarized and provided to the P3 flight scientists.

The objective is to measure the aerosols below cloud base, and their impacts on initiation of rain in growing convective clouds. It is observed that larger CCN concentrations delay the initiation of rain to greater heights in the clouds. Greater surface winds raise more sea spray aerosols that seed the clouds

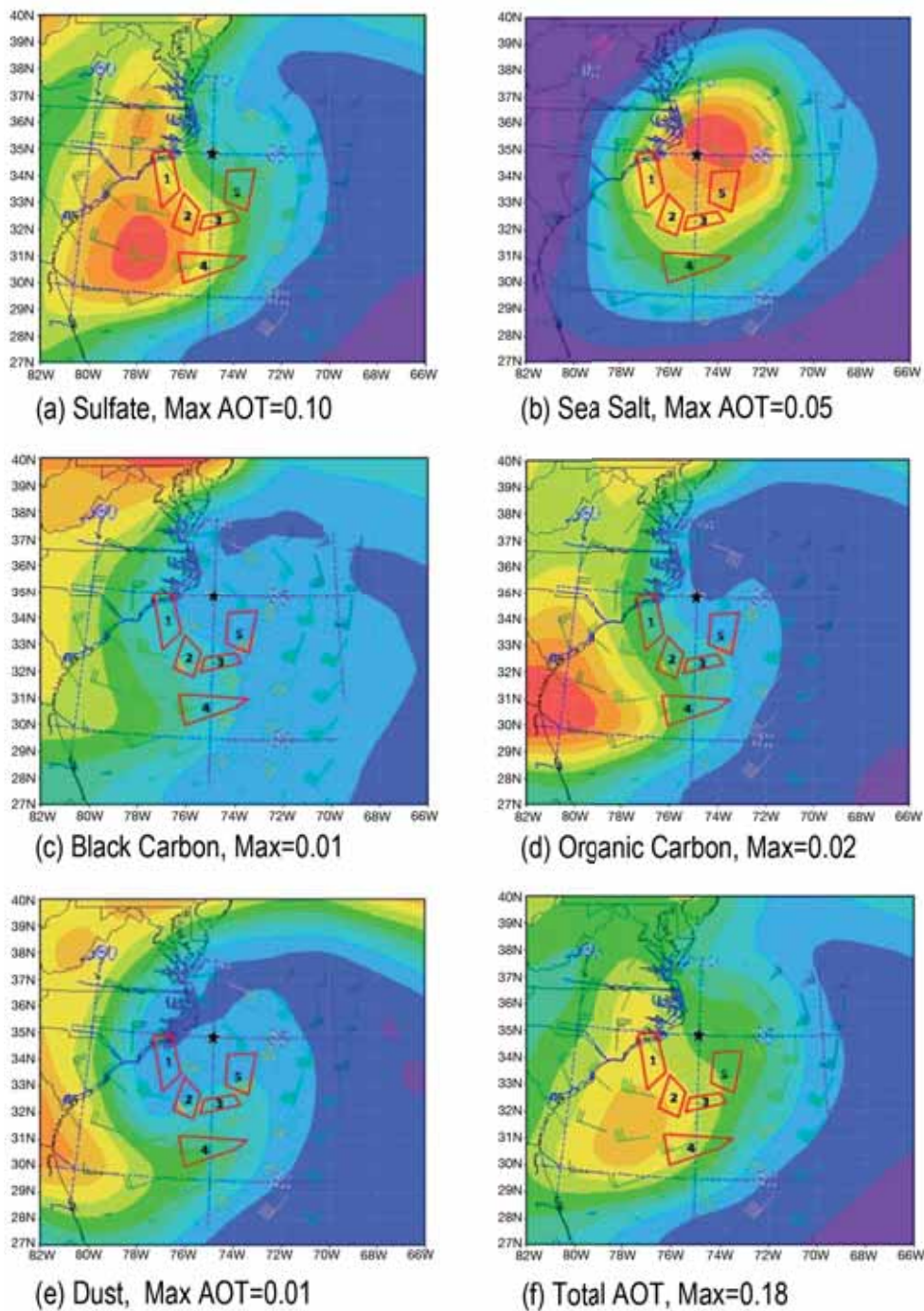


Figure 1.8 GOCART calculated AOTs for 5 aerosol species and the total AOT

For 10 September 2002; carbonaceous aerosols are evidently advected from SE USA coinciding with the polluted parts of the storm as reflected by the clouds seen in Fig. 1.6. The sea salt AOT increases correspondingly to the wind speeds, indicating the increased winds induce larger sea spray. Note that since the sources of sulfates are in part by air pollution from land and in part by emissions from the ocean, the sulfate's concentration increases towards the center of the storm coinciding with the increased wind velocity.

and start the rain sooner. Our task is to measure the combined effects of small CCN and sea spray aerosols on the precipitation forming processes as we progress along the spiral bands to stronger winds, up to the safety limit. This requires that:

- These flights must be conducted visually, therefore only during daylight time.
- Preference should be given to events with high pollution or dust aerosols, because the majority of the situations are with relatively clean maritime air.
- Flights will be conducted from the very outer fringes of the spiral bands inward, up to the point where surface winds will be deemed by the pilots to be too strong for this flight pattern.
- CCN and cloud measurements well within the eye are highly desirable, and will be measured down to the lowest safe flight level there.

The specific flight patterns for conducting measurements of the aerosols and clouds in the very outer spiral bands are given and illustrated in Fig. 1.9. In order to achieve good measurements, the measurements should be made of the aerosols and clouds in the very outer spiral bands:

1. Select a segment with new growth of convective clouds with tops at varying heights that are not under higher precipitating clouds.
2. Measure the aerosols and CCN spectrum below the cloud bases, but not in rain.
3. Measure non precipitating well defined lowest cloud base, such that the surface is barely visible, for at least 20 seconds cumulative time in cloud. Do consecutive higher passes not lower than 1000' below the tops of non-precipitating clouds, at steps of 500', 1000', 2000', above cloud base, and then every 1000 to 1500' higher, until reaching height where most of the cloud water has already converted into precipitation, even in young growing convective towers.
4. Descend to below cloud base and continue along the spiral band for another such vertical profile, where the winds have increased for justifying that additional profile, and so on.
5. Important: The vertical profile must be done

above the area that was measured for aerosols, drifting with the winds.

## 1.8 Flights Completed in Polluted Tropical Clouds

Aircraft observations in India have demonstrated that heavy air pollution can suppress warm rain in deep tropical clouds up to and above the freezing level, as hypothesized. Aircraft measurements over the sea show that added giant CCN, apparently from sea spray, restore some of the rain in the polluted clouds. These aircraft measurements validated the correctness of the microphysical representation of cloud-aerosol interactions and their impacts on rain forming processes in our model simulations. Satellite measurements showed that similar processes occur when heavy air pollution interacts with clouds that constitute the outer spiral bands of TCs. An initial quantification of the impact of aerosols on hurricane maximum wind speed was obtained by comparing the observed intensities of TCs with their predicted intensities using models that do not account for the aerosols. This quantification indicates that strongly absorbing aerosols such as black carbon have invigoration effects on hurricanes. The observational and simulation effects are consistent with each other, and provide strong support to the hypothesis of aerosols impacts on hurricanes.

## 1.9 Conclusions and Recommendations for the Future

The hypothesis that CCN aerosols decrease the intensity of tropical cyclones has been supported by numerous simulation studies. It was also supported by statistical analyses showing that aerosols can explain part of the storm prediction errors variability. Here we present observational support to key links in the conceptual model describing the way by which aerosols might be affecting the intensity of the storms. The main observations are:

- Pollution aerosols were observed to reduce the cloud drop size and suppress the warm rain forming processes in the external spiral cloud

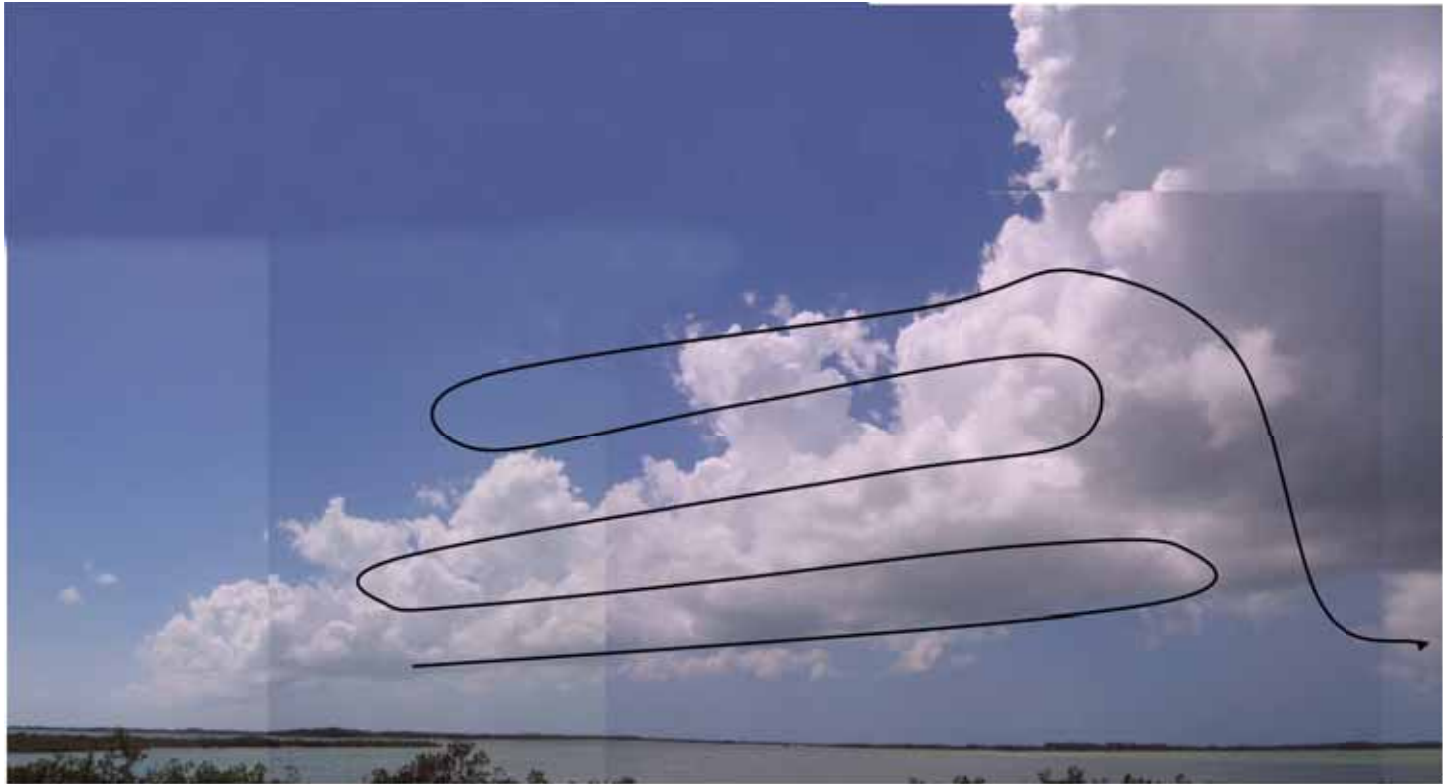


Figure 1.9 Desired flight tracks for rain-band clouds of a TC

bands of the storms; whereas adjacent unpolluted spiral bands had much larger cloud drops and produced readily warm rain.

- The polluted rain bands produced stronger precipitation radar reflectivities extending to greater heights, whereas in the adjacent pristine rain bands only moderate reflectivities were confined to below the freezing level. This supports the hypothesis link that the aerosols cause invigoration of the convection at the periphery of the storm.

- Frequent lightning flashes were observed in the polluted spiral cloud band, but none anywhere else in the storm. This further supports the invigoration hypothesis.

- The cloud drop size in polluted clouds increased substantially when the clouds moved inward to the storm in the areas with higher winds over the sea surface. This supports the link in the hypothesis that the sea spray raised by the high winds seeds the polluted clouds and restores the

warm rain processes in them when they move inward to areas with high wind speeds.

In summary, this study has added observational support to the already available simulation and statistical studies, which support the hypothesis that CCN aerosols reduce the intensity of tropical cyclones. Additional research involving in situ aircraft measurements in tropical cyclones that ingest heavy air pollution is necessary to further substantiate and validate the remote sensing observations and inferences.

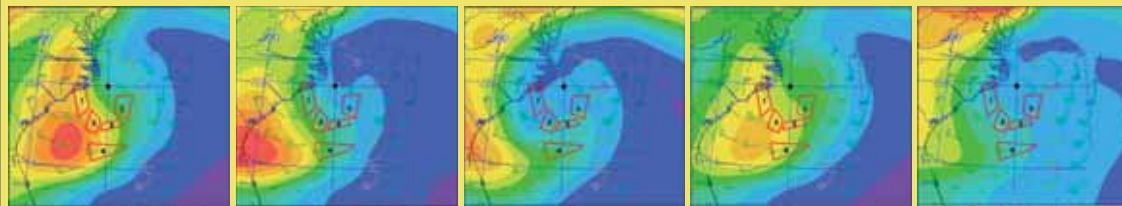
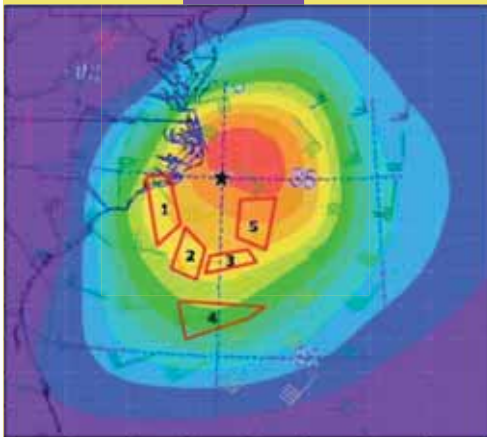
These results show that a) effects of aerosols should be taken into account in the prediction of TC intensity, and b) the results support the HAMP hypothesis that small soluble aerosol particles ingested into clouds at a storm's periphery can reduce the intensity of the TC, as might be the case in a TC approaching a polluted landmass.

Continuing the progress made by the HAMP team requires the following additional activities.

1. Coordinate with NOAA to incorporate consideration of aerosols into the SHIPS statistical hurricane prediction model.
2. Analyze existing data that are being measured in the present flights of the P3, which are not optimized for the HAMP objectives, and extract relevant information to validate models.
3. Coordinate with NOAA on the usage of the hurricane surveillance P3 airplanes for measuring the aerosols, cloud microstructure, precipitation

forming processes, and the impacts on cold-pools in hurricanes.

4. Conduct a field campaign that will be coordinated with a simulation effort for validating the HAMP simulations.
5. Validate further the satellite retrievals of cloud microstructure in hurricanes.
6. Examine the microstructure of the low clouds and aerosols in the eye.



## Aerosols, Cold-Pools, and Hurricane Intensity Modulation<sup>2</sup>

### 2.1 Introduction

Zhang et al. (2007; 2009) examined the impacts of dust acting as CCN inserted into a hurricane environment. The simulations by Zhang et al. (2009) revealed a non-monotonic response such that increases in CCN concentrations weakened the storm, while further increases in CCN concentrations either strengthened or had no impact on it. That study did not reveal why such peculiar behavior should occur. We hypothesize that much of that variability was due to the variable intensity of outer rainband convection when the enhanced CCN advected into that region. Moreover, the environmental CCN are not always transported from the storm environment into outer rainband convection as it is at the mercy of the local flow in those regions. Furthermore the hurricane is a huge aerosol scavenging machine such that virtually none of the dust made its way into the interior of the storm owing to strong washout.

Motivated by simulations of Zhang et al., Cotton et al. (2007) hypothesized that pollution-sized aerosols ingested into hurricanes could lead to a chain of responses leading to the eventual reduction of the storm intensity. In the outer rainbands, increasing CCN concentration results in reduced collision/

coalescence, increased SC water aloft, enhanced convection (latent heat of freezing) and ultimately enhanced precipitation and low level cooling (evaporation). The increase in low level cold-pool coverage in the outer rainband region blocks the flow of energy into the storm core inhibiting the intensification of the tropical TC. However, the amount of suppression of the strength of the TC depends on the timing between the transport of CCN to the outer rainbands and the intensity and lifecycle stage of the outer rainband convection. The outer rainband convection needs to be strong in order for the transport of SC liquid water aloft to take place. Note that Rosenfeld et al. (2007) arrived at a similar hypothesis using an entirely different dynamic model with simplified bulk microphysics.

While much of the motivation of this work was to investigate the potential for hurricane mitigation by seeding with small hygroscopic aerosol, the results contribute to our understanding of the importance of outer rainband convection and associated rainfall-induced cold-pools on hurricane intensity. As such, it is a complimentary investigation to the recent study by Riemer et al. (2010) in which they find that shear-induced downdrafts in the outer rainband convection of a hurricane can flush the BL with low  $\theta_e$  air, which in our language interferes with the flow of enthalpy into the storm interior resulting in a weakening of the storm. While aerosol modulation of outer rainband convection is much more subtle than shear-induced

---

2. Principal Author: Prof. Dr. William Cotton, Colorado State University, Colorado, USA; With contributions from: Dr. Gustavo G. Carrió.

changes, our results show a storm response that is consistent with that driven by wind shear.

We used the Regional Atmospheric Modeling System (RAMS) developed at Colorado State University (Cotton et al. 2003) that simulates “virtual flights” during which CCN particles are released as an aircraft flies at an altitude slightly lower than cloud base and at several seeding times and using different aerosol release rates. Results clearly support the aforementioned hypothesis, as seeding flights increased the quantities of SC liquid water, peak updrafts, and lowered the temperature of the cold-pools. More importantly, the peak surface winds show a significant sensitivity to both the seeding time and the aerosol release rates. Moreover, the results suggest there is an optimum CCN release rate; too much CCN thrusts more water substance into the storm anvils, lowering storm precipitation efficiency and short-circuiting the reduction in surface winds.

A brief description of model improvements that had to be made to perform the proposed studies is given in Section 2.2. The numerical experiments testing methods to mitigate the intensity studies are described in Section 2.3 while the corresponding results and some concluding remarks are given in Sections 2.4 and 2.5, respectively. In addition we are performing a study focused on the effects of sea-salt sources and scavenging by precipitation on the evolution of idealized tropical storms (TS). These additional studies and their preliminary results are summarized in Section 2.6.

## 2.2 Model Improvements

### *2.2.1 Development of a Prognostic Scheme for Sea-salt Sources*

We developed a prognostic scheme to take into account sea-salt surface sources based on a set of diagnostic (empirical) formulae (O’ Dowd, 1999). The scheme used a Newtonian relaxation technique and it is able to predict the generation of sea-salt particles in three size ranges: the film, jet, and spume sea-salt modes. These modes have been added to our research version of RAMS as full prognostic vari-

ables, and therefore they are advected, diffused and have sources and sinks. The film and jet modes have also been interfaced with the microphysical modules to act as cloud condensation nuclei (CCN) and giant CCN, respectively. These schemes were tested in an interactive-nested-multi-grid framework and used for hurricane studies.

### *2.2.2 Implementation of Scavenging Aerosol Sinks*

We added separate routines to consider the scavenging of sea-salt particles by rain and drizzle drops. Scavenging efficiencies are not averaged and are considered dependent on the drop sizes for both precipitating liquid species and therefore the process is “weighted” by the corresponding size distributions. These routines (separately) compute the scavenging of CCN, giant CCN as well as the film, jet, and spume sea-salt modes by drizzle and raindrops spectra. To reduce the uncertainty linked to drop-particle collision efficiencies; we based the scheme on empirical data (Chate et al. 2007 and personal communication) linking scavenging coefficients to rainfall rates at every model grid cell (computed from the drizzle and raindrop spectra). As in the previous case, the model improvements were tested in an interactive-nested-multi-grid framework and used for hurricane studies.

## **2.3 Exploration of Methods to Mitigate the Intensity of Tropical Storms, Leading to Better Forecasts of Hurricane Intensity**

We designed a series of simulations for which the time of the “virtual flights” as well as the aerosol release rates are varied. RAMS was configured to have three two-way interactive nested grids with 40 vertical levels. The horizontal grid spacings were 24 km, 6 km, and 1.5 km for grids 1 to 3, respectively. The corresponding domain sizes were 1536 km × 1526 km, 612.5 km × 612.5 km, and 304 km × 304 km. The centers of all grids and that of the storm were approximately coincident (~ 15N, 40W). The corresponding

time steps were 60 s, 20 s, and 2.5 s. The idealized TC simulations were similar to those of Zhang et al. (2007; 2009) except for recent updates in the model.

For this study we implemented a prognostic scheme (based on the O’ Dowd diagnostic formulae (1997) to take into account sea-spray sources for the film, jet, and spume modes, which act as CCN and giant CCN, respectively. The values predicted by the O’ Dowd formulae for the current surface winds were nudged at first model level. In addition, we added modules to take into account the scavenging of various types of aerosols by drizzle and raindrops. These routines (separately) compute scavenging of CCN, giant CCN as well as the film, jet, and spume sea-spray modes by drizzle and raindrops spectra. Scavenging coefficients are calculated as functions of aerosol size and precipitation rates at each model grid cell; they use curves derived from empirical data (Chate, personal communication). These data relate the scavenging coefficient for each sea-salt mode to the precipitation rate.

In order to examine the chain of responses to the introduction of enhanced CCN concentrations in TCs, we performed a rather large number of multi-grid numerical experiments. Those simulations were homogeneously initialized with clean (maritime) concentrations and used a code that simulates the flight of a plane and increases the CCN concentrations as an aircraft flies following different trajectories. Flight times varied between simulation times 36 and 42h for the runs corresponding to results presented in this paper. The aerosol release rates during these virtual flights were also varied. However the numerical experiments will be identified by the CCN concentration in the grid cells along the trajectory. All virtual flights were performed at an altitude slightly lower than cloud base height ( $\sim 2000$  m) and the aircraft speed was  $150 \text{ ms}^{-1}$ . Fig. 2.1 schematically represents two internal radius and external virtual flights some runs combined internal and external flights.

## 2.4 Main Results

### 2.4.1 Vertical Motions, Supercooled Liquid Water, and Precipitation

The time evolution of the simulated TCs soon after the corresponding seeding flights exhibited a common pattern with regard to vertical motion, SC liquid water mass, and precipitation. In general, updraft maxima simulated within the outer rain-bands and the altitude at which they occur increased approximately 3 hours after the corresponding seeding flight. This invigoration of the convection along the aerosol plume was associated with an important increase in the SC liquid water contents that enhances the production of aggregates and eventually precipitation.

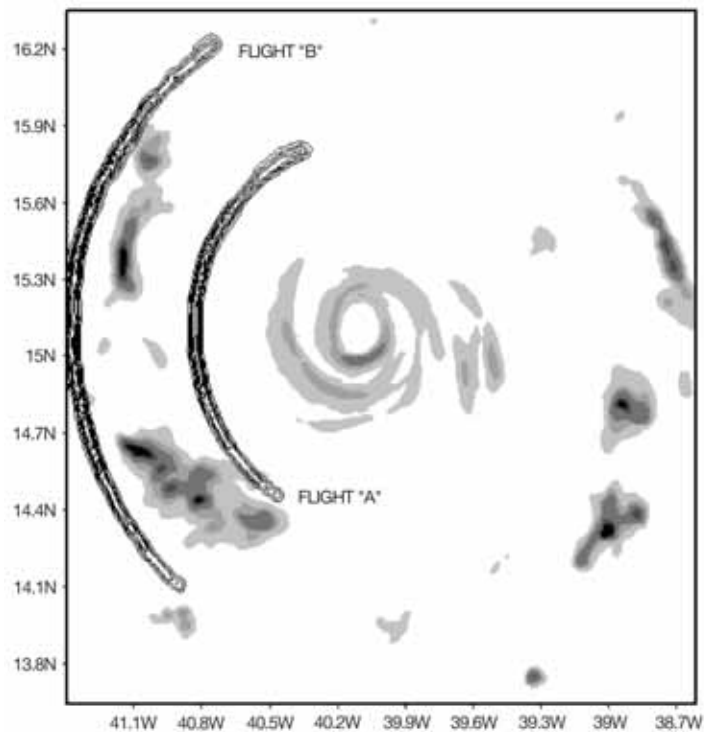


Figure 2.1 Virtual flights over internal and external radii

For the combined trajectory, the aircraft would fly north following flight “A” and then south along flight “B”. Black contours denote aircraft flight paths and shaded areas locate convective activity (liquid water path).

Figures 2.2-2.5 illustrate this chain of early effects on the TC evolution for an external radius flight at time 39h and  $8000 \text{ cm}^{-3}$  along the trajectory. The latter experiment, as discussed in the following subsections produced the most dramatic impact on storm evolution. Figures 2.2 and 2.3 compare the SC liquid water mixing ratios simulated for this virtual flight (panels b) to that of the control run (panels a) for the time of the flight (simulation time 39h) and 3 hours later (42h), respectively. Naturally, no differences can be seen at SC levels at the time the aerosols are released right below cloud (Fig. 2.2). The expected aerosol plume location is approximately indicated by an arrow in Fig. 2.2(b). Along this aerosol plume, important differences in the simulated SC liquid water isosurfaces are evident when comparing these two runs three hours later [Fig. 2.3(a) and (b)]. For instance, the integral mass of SC liquid water at simulation time 42h (computed as the spatial integration of the SC liquid water contents) was almost 30% higher than that of the control run.

Vertical motion was significantly affected along the aerosol plume as can be seen in Fig. 2.4 that shows updraft isosurfaces. The altitudes at which up-

draft maxima occurred were between 800 and 1900m above those of the control run between simulation times 42 and 45 h, (not shown). The rapid freezing of these larger amounts of SC droplets via riming produces a significant increase in the production aggregates as can be seen in Fig. 2.5 that gives the mixing ratios of this species for simulation time 42h.

The precipitation accumulated between time 39 and 43h (the four hours following the virtual flight) is compared in Fig. 2.6. A significant impact is evident over the aerosol plume. The integral volume of precipitation during these four hours after the virtual flight simulation was approximately 15 % higher than that corresponding to the control run. However, differences in the integral volumes between simulation times 43 and 72 h were slightly negative (not shown).

#### 2.4.2 Cold-Pools

We computed probability density functions (PDFs) of cold-pool size for numerical experiments using grid 3 model outputs every 30 minutes. Cold-pools were defined as groups of contiguous grid cells that had temperatures at least  $4^\circ\text{C}$  lower than the

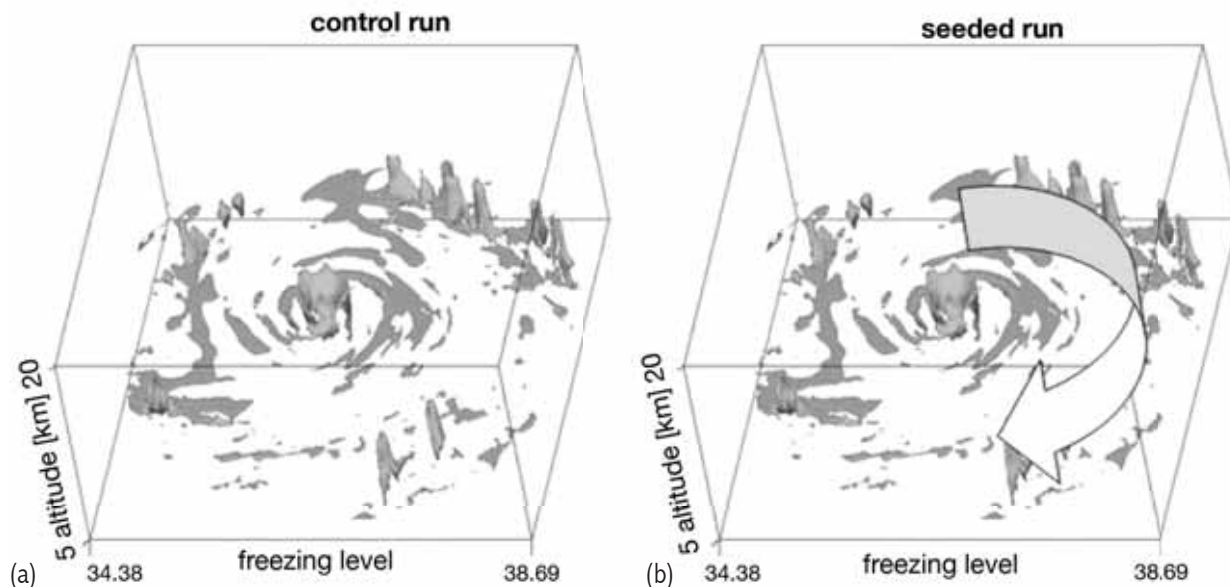


Figure 2.2 SC liquid water at simulation time 39 h for the control run and seeded run

Isosurfaces correspond to the  $1\text{gkg}^{-1}$  level. The arrow denotes the approximate location of the aerosol plume. The base of the shown subdomain is the freezing level.

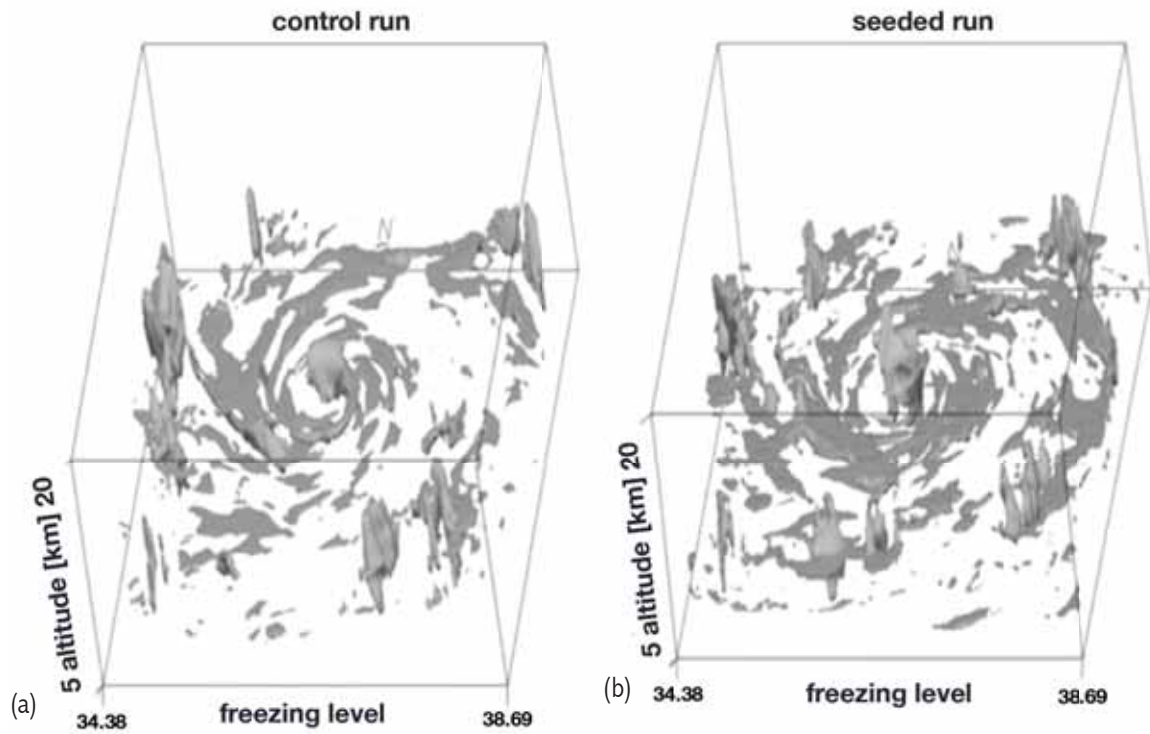


Figure 2.3 Comparison of SC liquid water

Simulation time 42h, three hours after the seeding flight. Isosurfaces correspond to the  $1 \text{ gkg}^{-1}$  level.

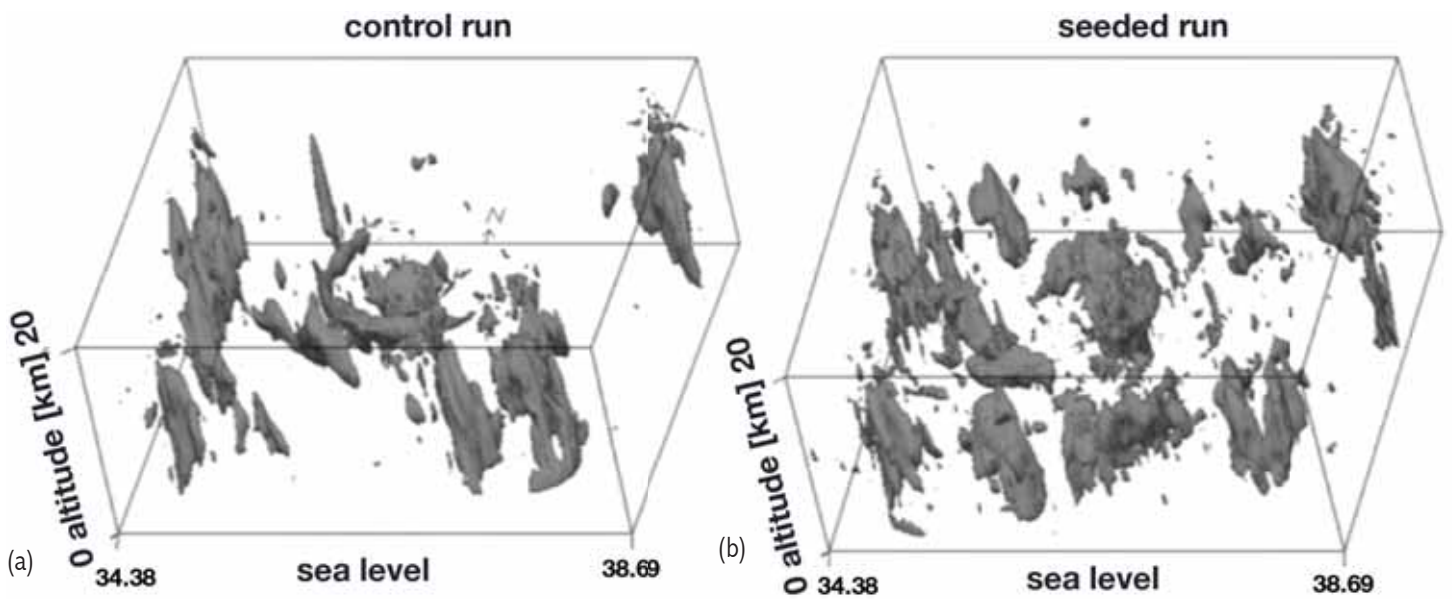


Figure 2.4 Comparison of updrafts

Simulation time 42h, three hours after the seeding flight. Isosurfaces correspond to the  $5 \text{ m s}^{-1}$  level.

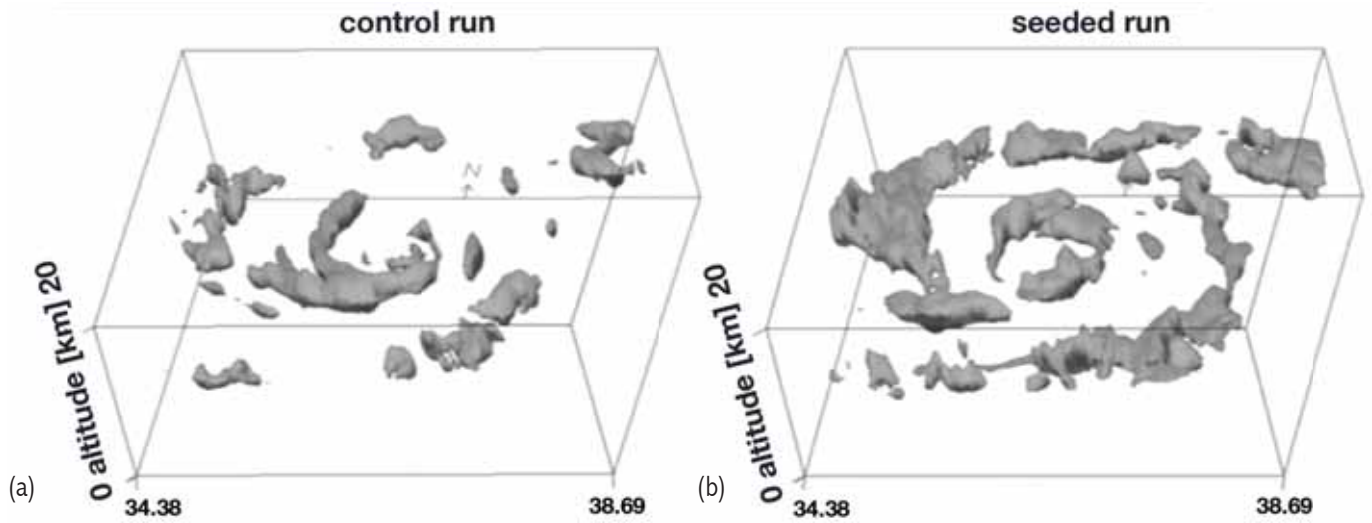


Figure 2.5 Comparison of mixing ratio of aggregates

Simulation time 42h, three hours after the seeding flight; isosurfaces correspond to the  $1.2 \text{ gkg}^{-1}$  level.

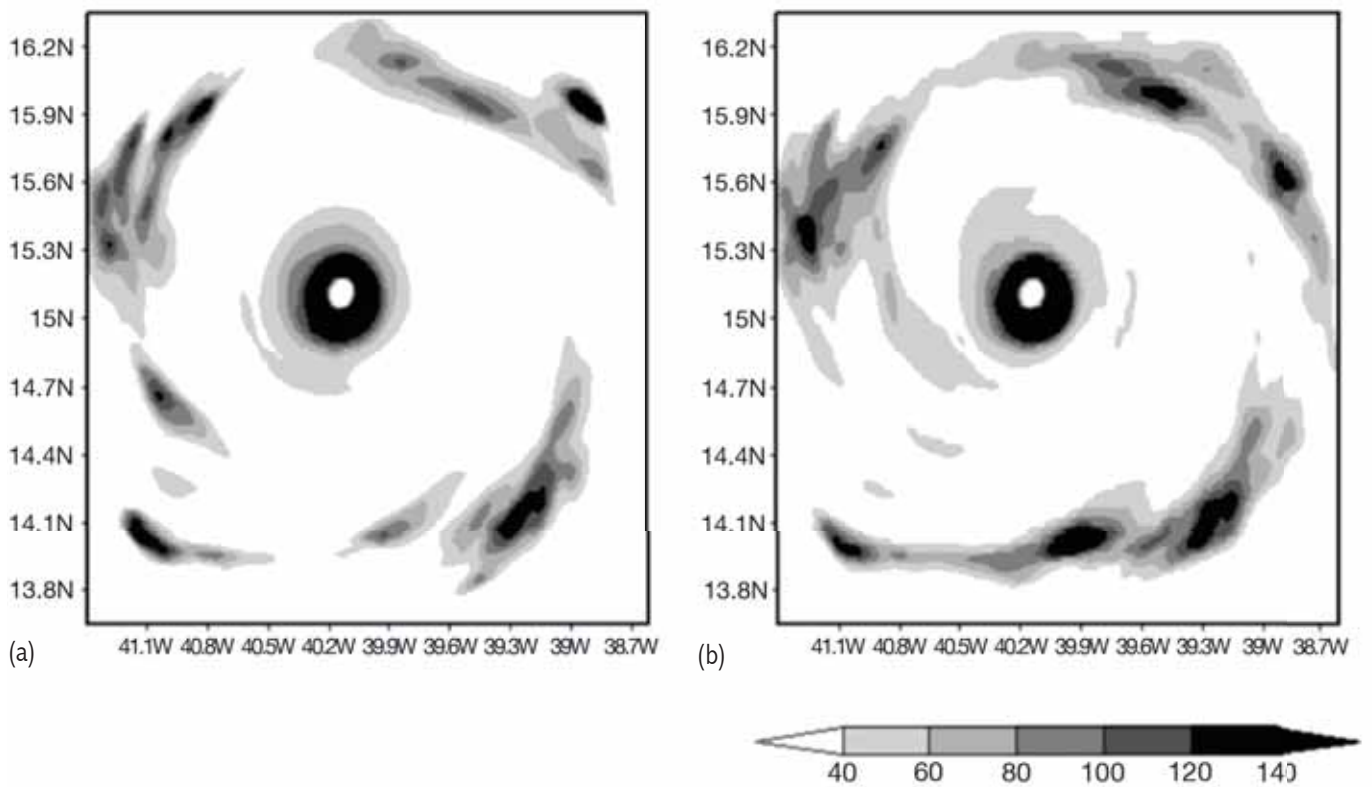


Figure 2.6 Comparison of precipitation

Accumulated between hours 39 and 43 for the control run and the seeded run in panels (a) and (b), respectively. Shaded areas represent precipitation in mm.

horizontal domain-average at the corresponding time. The main results are summarized in Table 2.1 for different seeding times, trajectory types, and aerosol release rates. In general, simulated seeding flights produced cold-pool distributions with expected (mean) areas considerably higher than that of the control run. It must be noted that, the expected cold-pool area is four times larger than that of the control run for the virtual flight used for comparisons in the previous subsection (shaded row in Table 2.1).

The PDFs of cold-pool area also showed differences in their tails, indicating higher frequencies of large cold-pools sizes. For instance, the maximum simulated area shows a considerable increase for all sensitivity runs except for the flight at 39h and 4000 cm<sup>-3</sup>. Not only is the cold-pool size affected by seeding but so also its minimum temperature. We computed those minima, relative to the current horizontal average over the finest grid. In most cases this difference ( $\Delta T_{pool}$ ) was higher (in absolute value) than that corresponding to the control run (again, the virtual flight at 39h and 4000 cm<sup>-3</sup> is an exception).

Moreover, seeding flights reduced the temperature of the entire lower layer. The horizontally-averaged temperature over the finest grid for the first model level above ground relative those of the control run for the last 24h of the simulation ( $\Delta T_{G3}$ ) gave negative differences for all runs. These differences (up to 0.14°C) may seem small, however, it

must be noted that they are temporal averages over the entire finest grid. These differences are the cause of the storm intensity weakening. Moreover, the seeding effects on expected and maximum cold-pool areas are actually underestimates because they have been computed relative to each run's horizontally-averaged values.

We performed several other experiments using the virtual flight trajectory of the experiment highlighted in Table 2.1 to cover a CCN concentration range from 2000 to 16000 cm<sup>-3</sup>. The corresponding results are given in Table 2.2. It is interesting to note the clearly monotonic behavior of various quantities when CCN concentrations vary between 2000 and 8000 cm<sup>-3</sup>. However, it can be seen that there is a change of response above 8000 cm<sup>-3</sup>. In particular, the area of the largest cold-pool simulated for the 8000 cm<sup>-3</sup> run is six times higher than that of the control run. However, from that peak value, it decreases approximately 3, 7, and 10% for the 10000, 12000, and 160000 cm<sup>-3</sup>, respectively. The overall cooling ( $\Delta T_{G3}$ ) is also less important for the latter runs. In order to further analyze the peculiar response of cold-pools, we examined the changes in the structures down-drafts in the following subsection.

Time	Type	CCN [cm <sup>-3</sup> ]	Expected area [km <sup>2</sup> ]	Maximum area [km <sup>2</sup> ]	$\Delta T_{pool}$ [°C]	$\Delta T_{G3}$ [°C]
-	-	0	26.3	49.5	-5.29	0.00
36	int	8000	50.6	288.0	-5.68	-0.06
36	ext	8000	67.1	180.0	-5.45	-0.05
42	ext	8000	76.1	292.5	-6.77	-0.03
39	both	8000	49.8	141.8	-5.38	-0.06
36	both	8000	26.8	67.5	-5.29	-0.03
42	both	8000	100.4	357.7	-5.57	-0.02
39	ext	8000	69.5	357.8	-5.68	-0.14
39	ext	6000	88.9	299.3	-5.66	-0.13
39	ext	4000	25.9	49.5	-5.10	-0.05

CCN [ $\text{cm}^{-3}$ ]	Mean area [ $\text{km}^2$ ]	Max area [ $\text{km}^2$ ]	$\Delta T_{\text{pool}}$ [ $^{\circ}\text{C}$ ]	$\Delta T_{\text{G3}}$ [ $^{\circ}\text{C}$ ]
0	26.3	49.5	-5.29	0.00
2000	26.2	49.5	-5.19	-0.05
4000	25.9	69.5	-5.32	-0.05
6000	88.9	299.3	-5.66	-0.13
8000	69.5	357.8	-5.68	-0.14
10000	72.3	352.4	-5.72	-0.12
12000	68.0	333.2	-5.68	-0.12
16000	65.7	327.7	-5.67	-0.11

### 2.4.3 Downdrafts

We computed the overall downward mass flux and compared the corresponding time-averaged vertical profiles for various numerical experiments considering seeding flights at simulation time 39h. Downward mass fluxes exhibit a clearly monotonic behavior when the CCN concentrations (along the trajectory) are increased up to  $8000 \text{ cm}^{-3}$  with differences up to 15% compared the control run [Fig. 2.7(a)]. Conversely, an opposite response is observed in Fig. 2.7(b) when CCN concentrations are above this threshold. Nonetheless, downward mass fluxes for both 12000 and  $16000 \text{ cm}^{-3}$  runs exceed that of the control run.

Figures 2.8a and b show that the enhanced downward fluxes are not linked (only) to more intense downdrafts but also to larger areas covered by them. The response is again clearly monotonic up to  $8000 \text{ cm}^{-3}$ . Even though all virtual flights produced a downdraft areal coverage lower than the control run, the values for numerical experiments using 12000 and  $16000 \text{ cm}^{-3}$  were between those simulated for  $8000 \text{ cm}^{-3}$  and the control run.

We generated statistics selecting the downdrafts linked to the three cold-pools of larger area for each model output time (every 30min). As an example, Fig. 2.9 illustrates a detail of the lowest 4000 meters of the downdraft (dark gray) associated to the largest cold-pool (light gray) simulated for these numerical experiments (virtual flight at 39h,  $8000 \text{ cm}^{-3}$ ).

Figures 2.10-2.12 compare average vertical profiles of the aforementioned downdraft composites for various runs. All runs considering virtual flights sensitivity produced buoyancy values higher (more negative) than those of the control run. Buoyancy within the lowest 1000 meters exhibits a monotonic response to CCN concentrations lower or equal to  $8000 \text{ cm}^{-3}$  [Fig. 2.10(a)]. However, further enhancing aerosol concentrations produces the opposite effect [Fig. 2.10(b)]. Figures 2.11(a) and (b) are analogous to Figures 2.10(a) and (b) but they give rain mixing ratio vertical profiles. It can be seen that rain mixing ratios exhibit an identical pattern of response. However, this change of behavior is not observed when comparing the mean mass diameters of raindrops within the most intense downdrafts (Fig. 2.12). In this case, raindrop diameters monotonically decrease when increasing CCN concentrations from 2000 to  $16000 \text{ cm}^{-3}$ .

### 2.4.4 Surface Winds

Surface winds exhibited the same pattern of response that was observed for the area and intensity of cold-pools and downdrafts, as well as the buoyancy and the rain mixing ratio within the latter. Fig. 2.13 compares surface wind frequencies corresponding to seeding flights numerical experiments to those of the control run. The frequencies of the highest surface winds for the control run are approximately 6 times larger than those corresponding to the  $8000 \text{ cm}^{-3}$  run. For category 5 wind speed range, reductions of

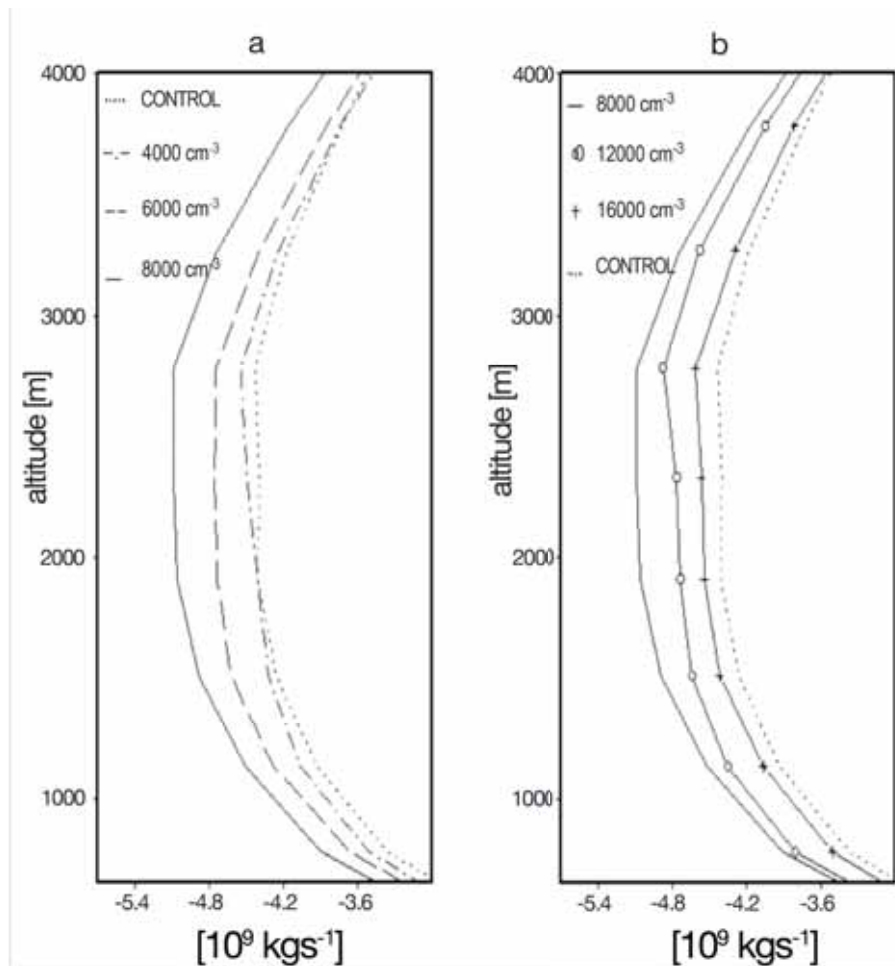


Figure 2.7 Comparison of integral downward mass transport

Computed for the control run and the seeded run in panels a and b, respectively. Vertical profiles correspond to temporal averages over the 24-hour period after the flight.

30, 50, and 60% were simulated for runs using 4000, 6000, and 8000  $\text{cm}^{-3}$ , respectively. These experiments also produced an approximate reduction of 30% for surface winds within category 4 and a minimum reduction 20% was simulated for all other hurricane categories. Fig. 2.14 is analogous to Fig. 2.13 but for the higher [CCN] range along the virtual flight trajectory. This figure shows that the reduction in the frequency of category 5 winds falls from 60% to 35 and 7% when comparing the 8000, 12000 and 16000  $\text{cm}^{-3}$  runs, respectively.

## 2.5 Concluding Remarks About Targeted Insertion of CCN

We performed a series of multi-grid cloud-resolving simulations to examine the response of a simulated hurricane to the targeted insertion of CCN. The modeling framework included improved microphysical modules that included a bin-emulating treatment of riming processes, sea-salt surface sources in three modes, sinks for cloud nucleating particles due to scavenging by precipitation, and a code that simulates the targeted insertion of CCN by aircraft.

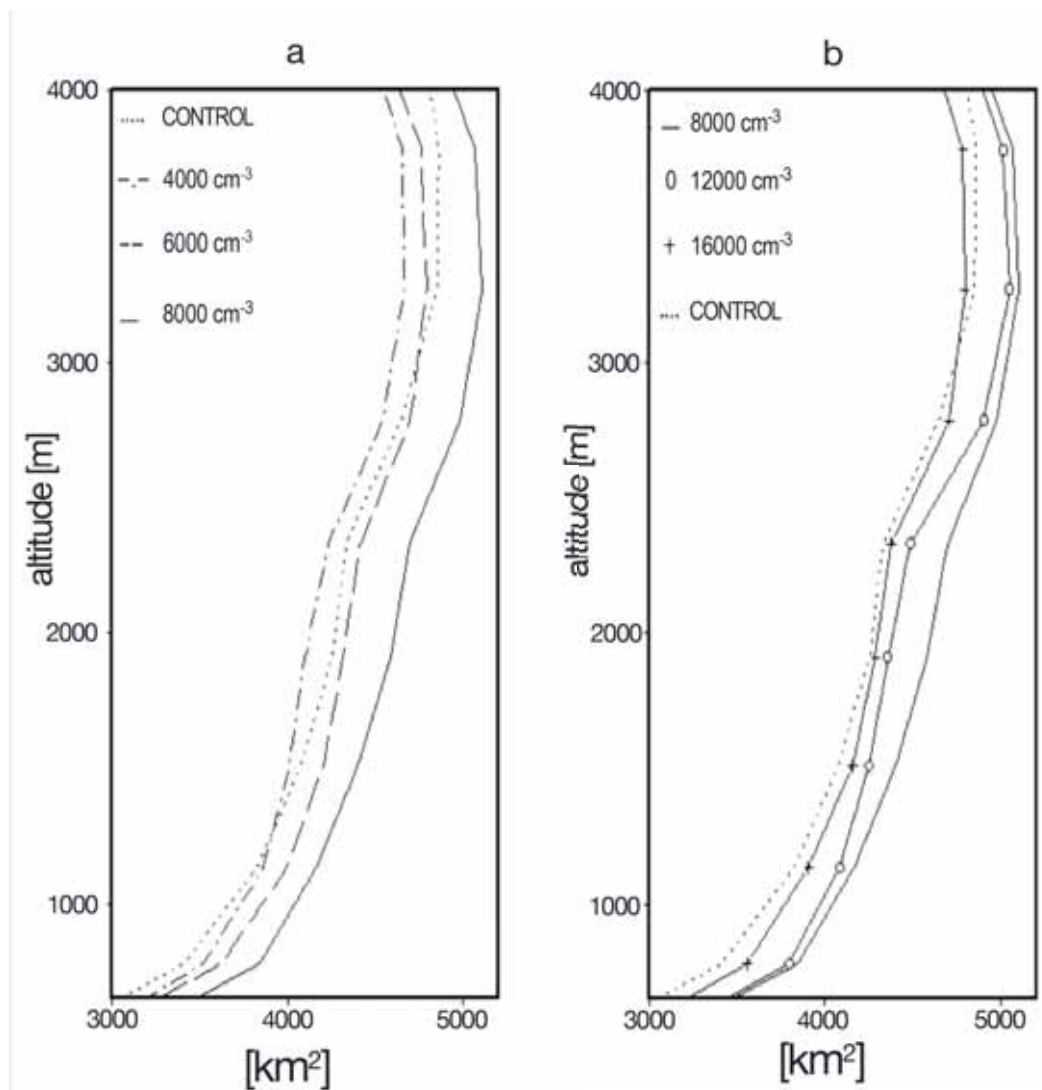


Figure 2.8 Comparison of area covered by downdrafts

Computed for the control run and the seeded run in panels (a) and (b), respectively. Vertical profiles correspond to temporal averages over the 24-hour period after the flight.

The results of these numerical experiments clearly support the hypothesis described in Section 1. Virtual flights cause a reduction of collision and coalescence, resulting in more SC liquid water to be transported aloft. This SC liquid water enhances latent heat of freezing, which produces higher updraft maxima at higher altitudes. Results also suggest that the higher evaporative cooling from enhanced rainfall rates in the outer rainbands produces stronger

and more widespread cold-pools. These cold-pools, covering larger areas, interfere with the flow of enthalpy into the storm core and therefore weaken the storm. Reimer et al. (2010) also finds evidence that the invigoration of convective activity in the outer rainbands leads to a reduction in TC intensity. That study focused on the role of vertical wind shear on the TC inflow layer.

Given the long history in hurricane research that implicates strong vertical shear as being det-

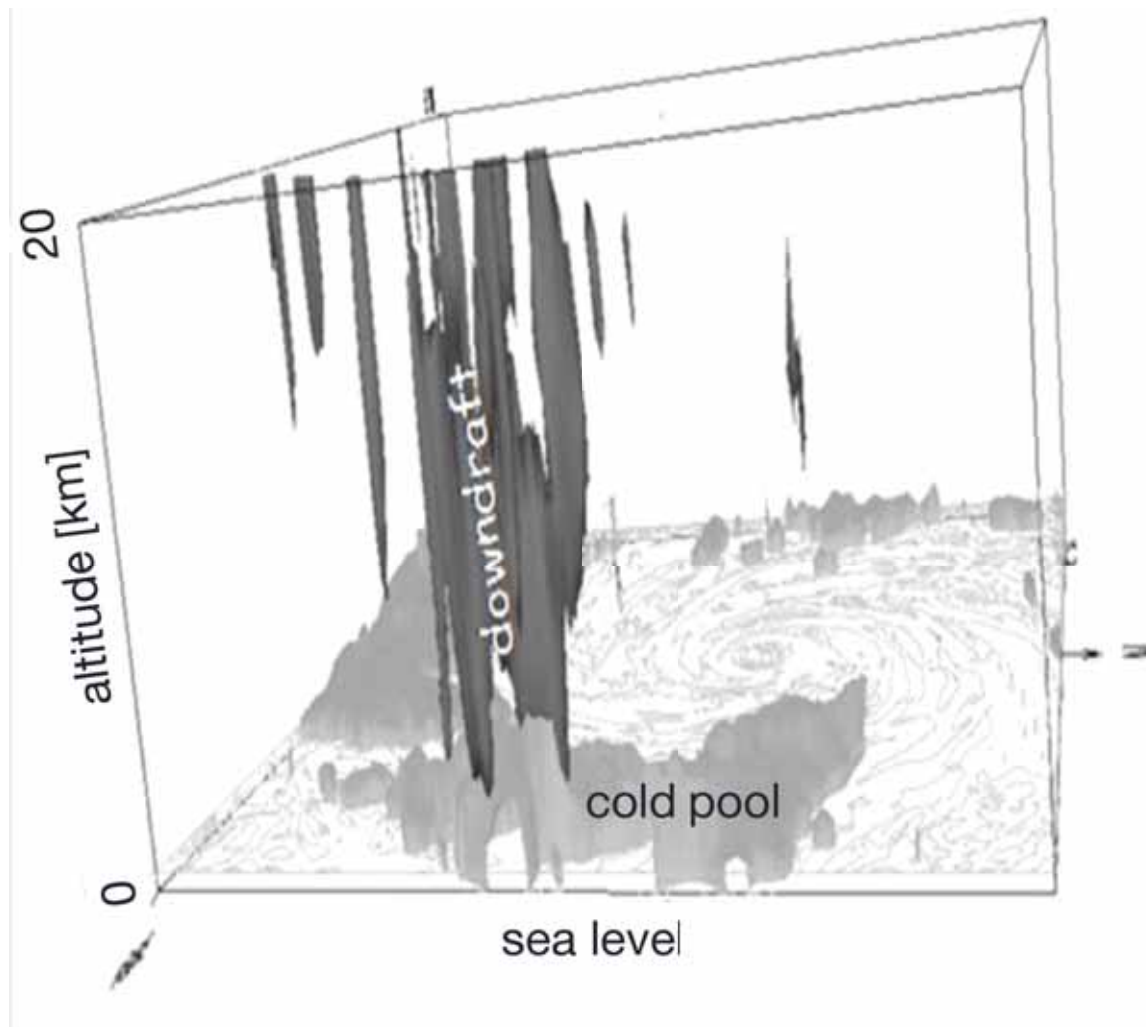


Figure 2.9 Largest simulated cold-pool and its associated downdraft

The isosurface representing the cold-pool (light gray) corresponds to a temperature difference of  $-4^{\circ}\text{C}$  with respect to the horizontal average (for each level). Downdraft isosurface (dark gray) correspond to  $-2\text{ms}^{-1}$ .

rimental to storm intensity, we speculate that the aerosol signal we see in these idealized simulations is secondary to the more dominant role that environmental shear plays. Likewise, we suspect that variability in moisture content of the storm plays a more dominant role over aerosols in modulating cold-pools and hence storm intensity. Again, there is a rich history in hurricane research that suggests that rapid

intensification of a storm coincides with moistening of the storm interior to almost saturation.

The increase in cold-pool spatial physical dimensions as well as the temperature difference with respect to their surrounding environment was clearly linked to the enhanced aerosol concentrations, mainly due to the monotonic response they exhibited when increasing CCN concentrations up to  $8000\text{ cm}^{-3}$ . A similar monotonic response was observed for the

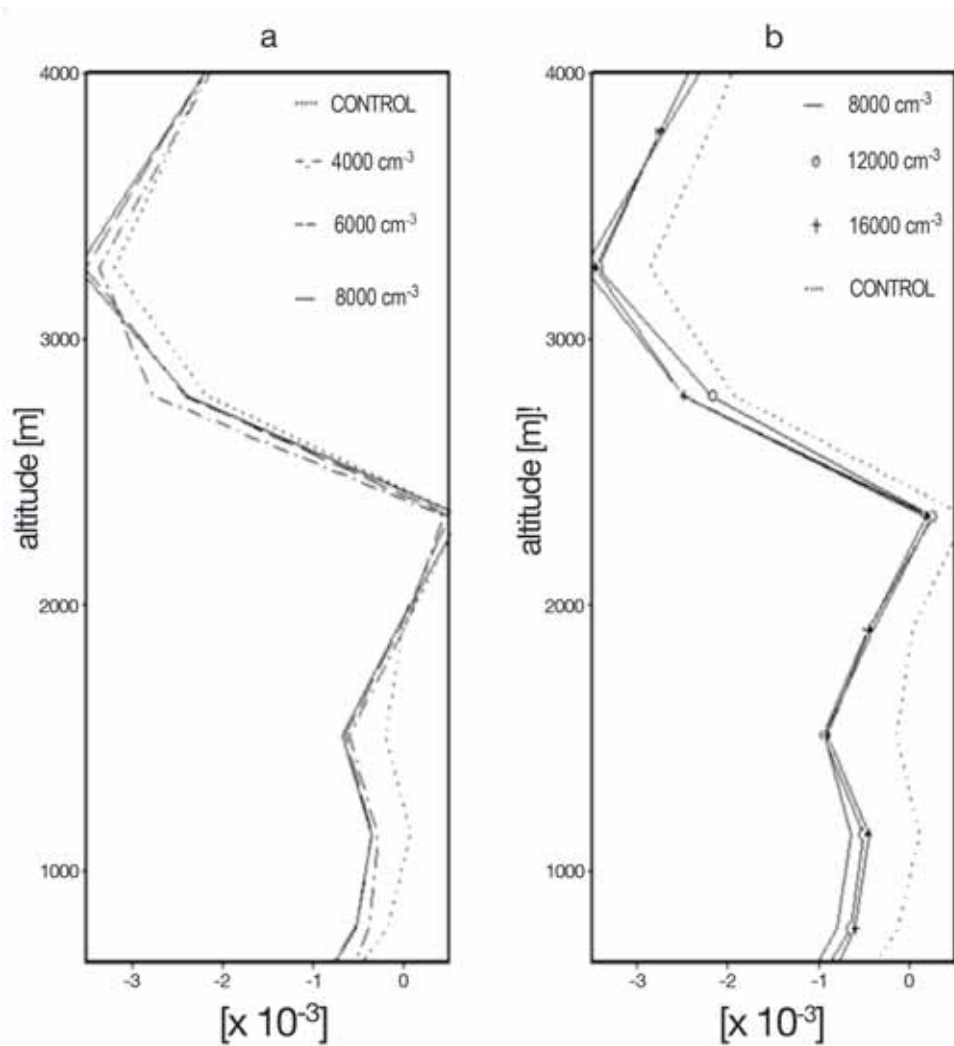


Figure 2.10 Comparison of buoyancy within the most intense downdrafts

For the control run and the seeded run in panels (a) and (b), respectively.

overall downward flux, the area covered with downdrafts as well as the buoyancy, rain mixing ratio, and (decreasing) raindrop size within the downdrafts associated with the largest cold-pools. Moreover, simulated reduction in frequencies of high surface winds behaved in a similar manner. Nonetheless, with the exception of raindrop sizes, all of the aforementioned quantities exhibited a different response when we considered concentrations above  $8000 \text{ cm}^{-3}$  along the flight trajectories. This change of behavior is consistent with the mechanism suggested by Carrió et al. (2010) and Carrió and Cotton (2010). Briefly, fur-

ther enhancing CCN concentrations reduces the size of SC droplets, which reduces riming growth of ice particles, which results in the transport of a greater fraction of the ice-phase water mass to anvil levels as pristine ice crystals instead of being precipitated to the surface. In this way, the importance of the entire chain of processes leading to the eventual reduction of surface winds is reduced as the cold-pools are weakened.

In summary, the primary impact of aerosols on TC genesis and intensity is by altering the strength of cold-pools. The idea that cold-pools are an im-

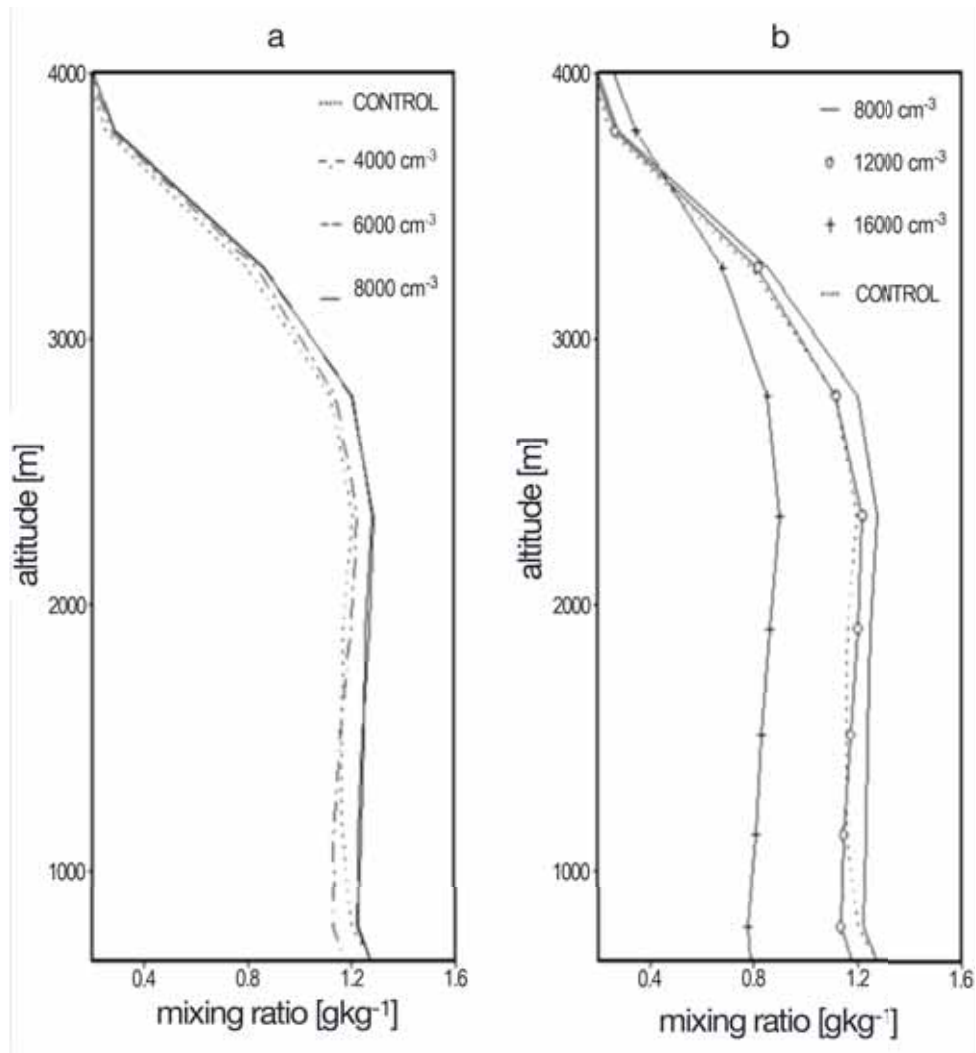


Figure 2.11 Comparison of rain mixing ratio

For the control run and the seeded run in panels (a) and (b), respectively.

portant modulator of TC intensity is consistent with observations that TC rapid intensification follows the formation of a nearly saturated core (results in weak cold-pools). It is also consistent with strong vertical wind shear as being a detriment to TCs (strong shear enhances entrainment of dry air increasing cold-pool strengths) as shown by Reimer et al. (2010). We speculate that during TC genesis vigorous cold-pools can lead to vertical decoupling between a mid-level MCV and low-level vorticities similar to what we find with tornadoes (Lerach et al. 2009). Furthermore,

vigorous cold-pools in mature TCs can interfere with the flow of enthalpy into the storm core.

An implication from this research for hurricane intensity prediction is that greater attention has to be given to cold pools. A remote sensing method of TC cold-pools would be ideal to map cold-pool variability in TCs. Furthermore, in order to simulate and predict aerosol impacts on TCs, models need high enough resolution and microphysics to represent convective-scale dynamical responses to aerosols as well as environmental properties affecting cold-pools

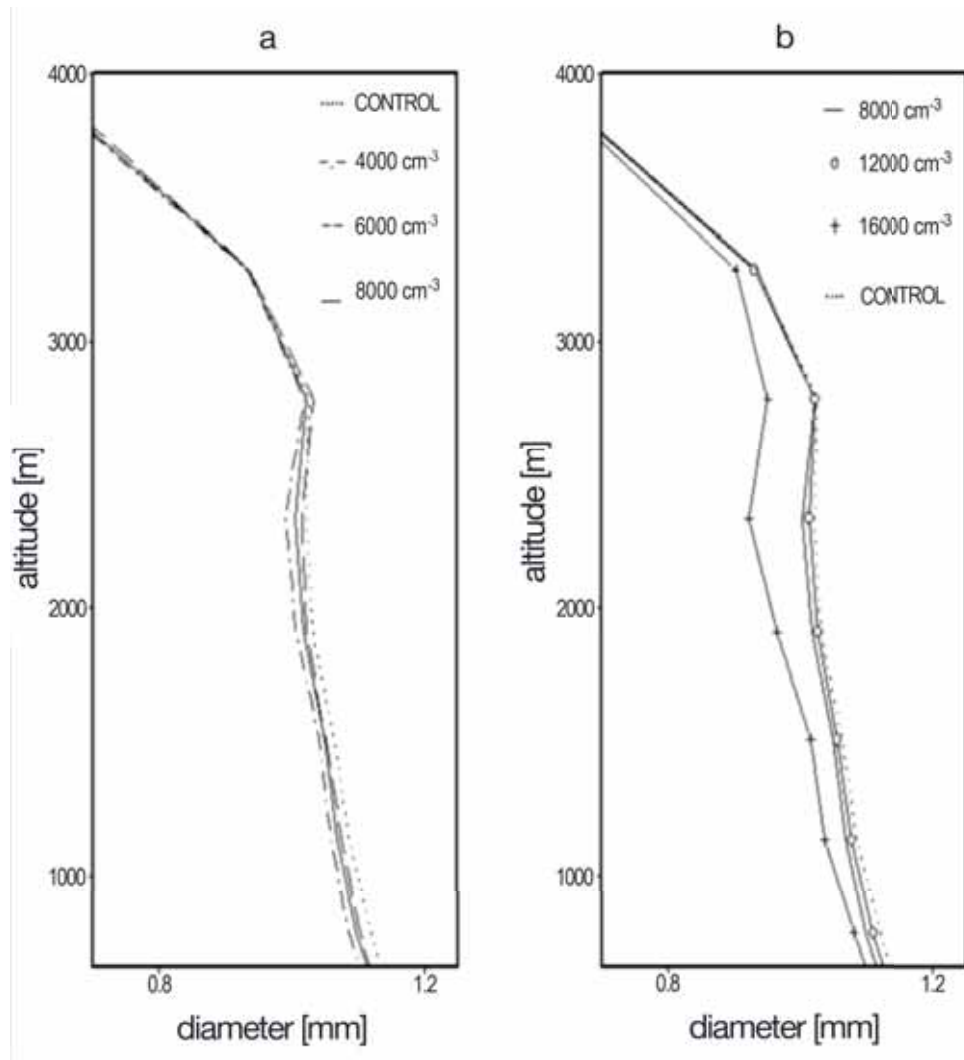


Figure 2.12 Comparison of raindrop mean mass diameters

For the control run and the seeded run in panels (a) and (b), respectively.

## 2.6 Impact of the Sea-Salt Sources Sea-Salt Aerosol and Scavenging by Precipitation on the Storm Microphysics

In order to see the effects of only the sea-salt aerosol source routine the two simulations SA0SC0 and SA1SC0 were compared. Comparing the two simulations that have the sea-salt aerosol scavenging routine disabled eliminates interactions between the two new aerosol routines thus making the impact of the sea-salt aerosol source routine more definitive. Since the storm developments of two different

simulations can occur at different simulation times, the results are presented in time series format so that relevant sections can be compared regardless if they do or do not occur simultaneously.

Fig. 2.15 shows the average cloud droplet concentration in a region near the eye wall, which was the volume defined to be 20 km to 30 km radius from the eye of the storm going from the surface up to a height of 1200 m. The data are shown for the final 48 hours of the simulation (which runs from 0 to 72 hours). Note that the average cloud droplet concentration tends to be the same for the two simulations up until the last 12 hours (from simulation time

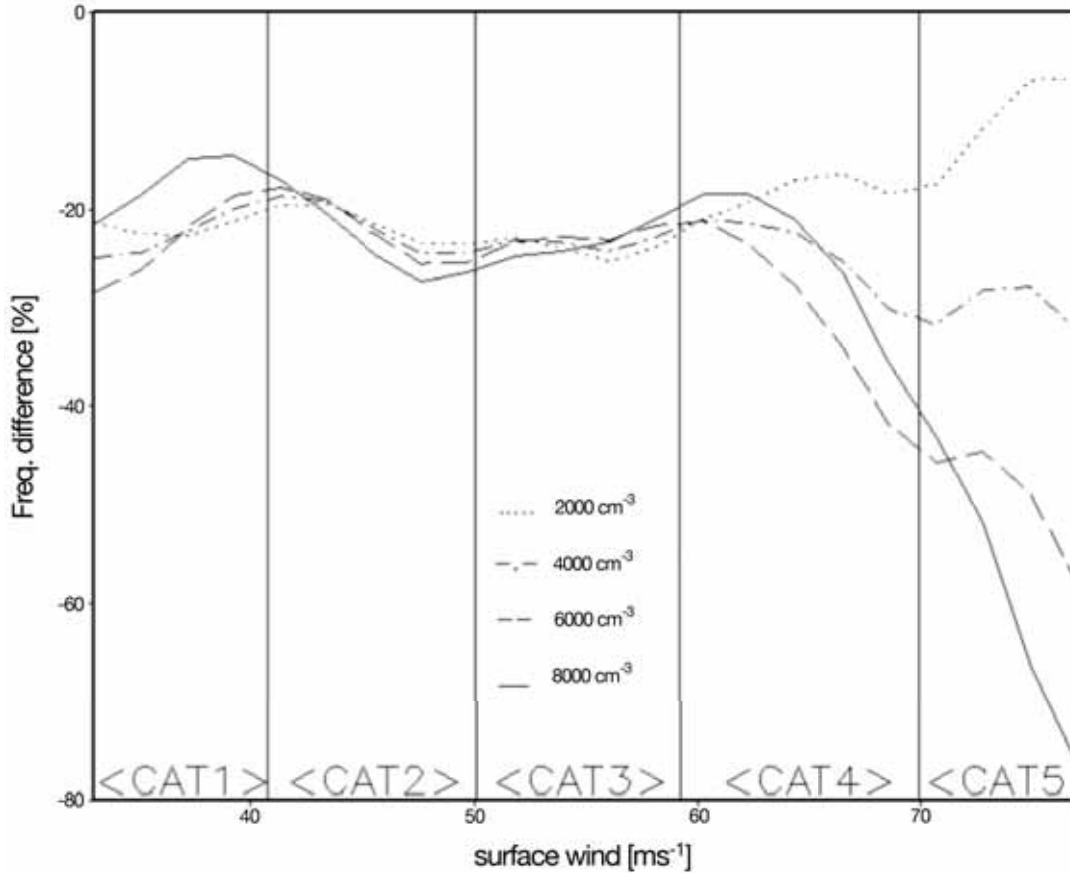


Figure 2.13 Comparison of hurricane intensity surface wind frequencies

For flights with CCN concentrations BELOW  $8000 \text{ cm}^{-3}$ . Curves represent percent differences with respect to the control run.

60 to 72 hours). At the 60 hour point (0Z 25 AUG) the simulation with the sea-salt aerosol source routine enabled (SA1SC0) starts showing a more rapid increase in the average cloud droplet concentration reaching a higher peak value than the simulation with the source routine disabled.

Fig. 2.16 shows a metric that represents the overall intensity of the storm. The metric is based on the areal coverage of surface wind speeds of hurricane strength ( $33 \text{ ms}^{-1}$ ) or greater. Note that in both simulations a very similar progression of storm intensity occurs. Also, note that the time scales are marked differently than the plots in Fig. 2.15 whereas in Fig. 2.16, the entire 72-hour simulation is shown.

As the storms intensify, high speed winds cover more of the surface. These winds are strong enough

to create sea spray, which in turn creates sea-salt based aerosols. The progression of the storm intensity is nearly the same for both simulations and the SA1SC0 simulation has a noticeably larger amount of cloud droplets in the lower levels near the eye wall. Therefore, it appears that the sea-salt aerosol source routine is correctly simulating the process of the surface wind creating sea spray. That process subsequently creates more aerosols, which then cause higher cloud droplet concentrations.

As before, the two simulations with the sea-salt aerosol source routine disabled were used for investigating the effects of the sea-salt scavenging routine in order to isolate the effects of the sea-salt scavenging routine. Fig. 2.17 shows the total SC cloud droplet mass for the simulations with the sea-salt scaveng-

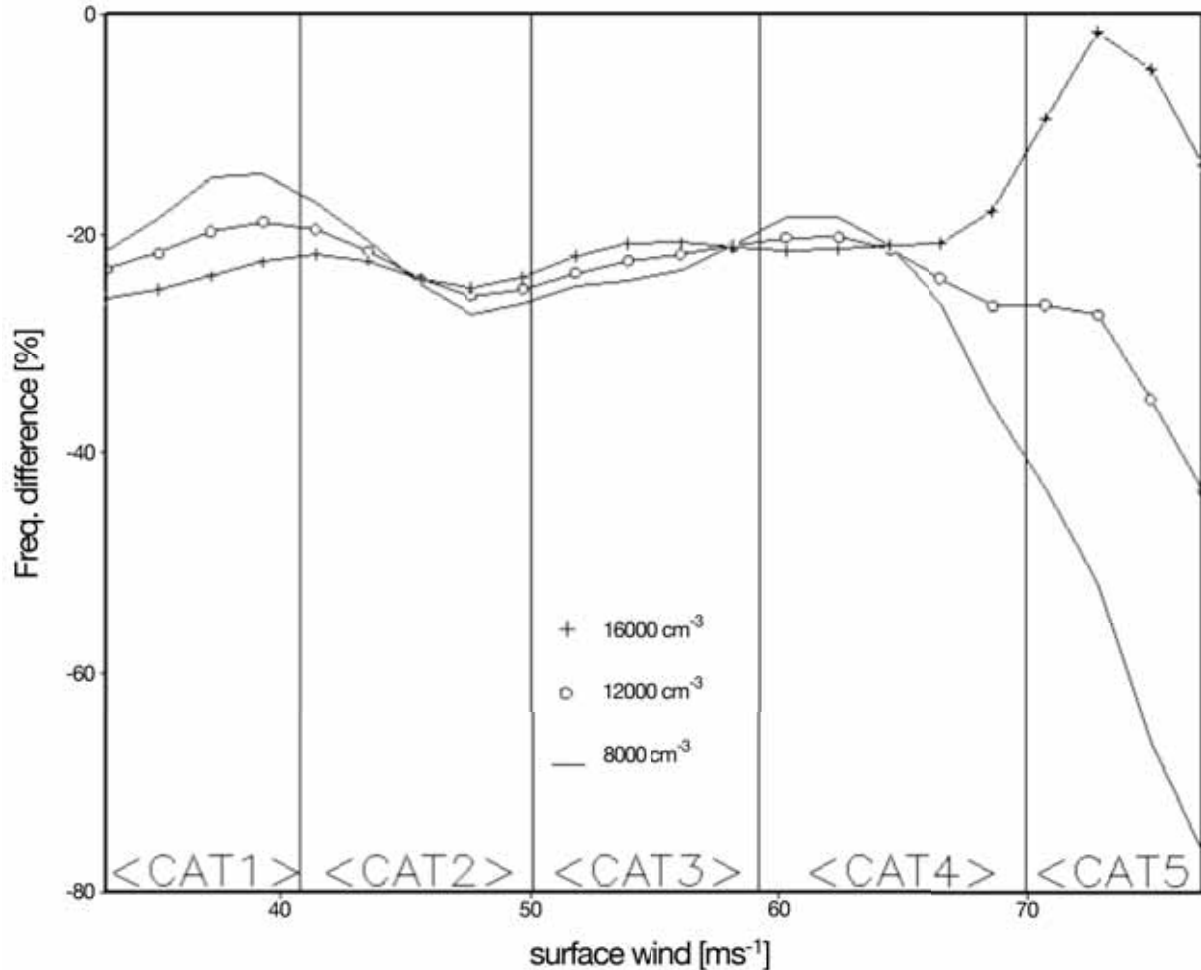


Figure 2.14 Comparison of hurricane intensity surface wind frequencies

For flights with CCN concentrations ABOVE  $8000 \text{ cm}^{-3}$ . Curves represent percent differences with respect to the control run.

ing sink routine disabled and enabled. Note that in the simulations with the scavenging routine disabled the amount of SC cloud droplet mass fluctuates until around 6Z 24 AUG (40 hours simulation time). At this point the total mass appears to settle on a somewhat steady value of roughly  $6 \times 10^{13} \text{ g}$ . In the simulation with the scavenging routine enabled however, a low frequency oscillation appears after 6Z 24 AUG with a period of about 18 hours.

We hypothesize that this behavior is a result of an interaction of the buildup of CCN and scavenging that goes as follows. The introduction of CCN in the rainband region suppresses the cloud droplet collision/coalescence processes by changing the droplet

size distribution to a large number of small droplets with similar diameters. In the rainband regions where convection is active, these droplets are carried aloft above the freezing level, which increases the amount of SC cloud droplets. This enhances updrafts due to the release of latent heat as these droplets freeze, which ultimately increases the precipitation rate. Then the increased precipitation will scavenge more CCN out of the atmosphere, which allows an increase in collision/coalescence to take place, reducing the SC cloud droplets aloft, reducing the updrafts and ultimately reducing the precipitation. Once the precipitation diminishes the scavenging decreases and

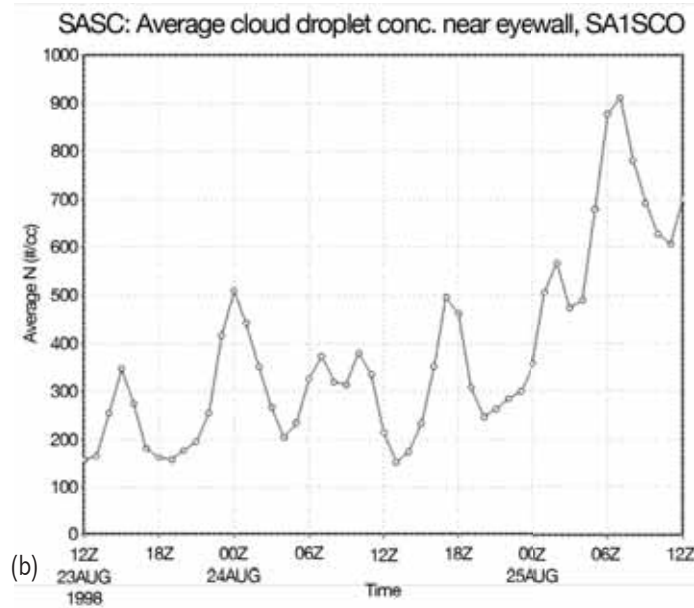
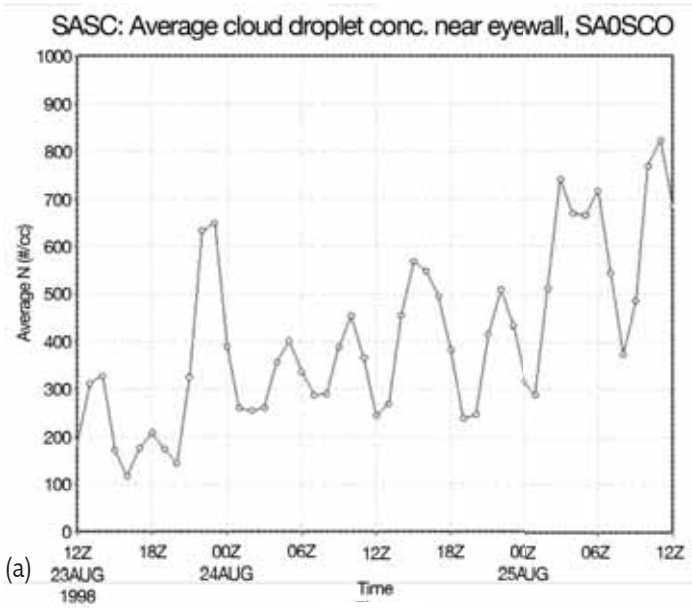


Figure 2.15 Average cloud droplet concentration in lower levels of region near the eye wall

SA0SCO (Left) has the sea-salt aerosol source routine disabled, SA1SCO (Right) has the sea-salt aerosol source routine enabled.

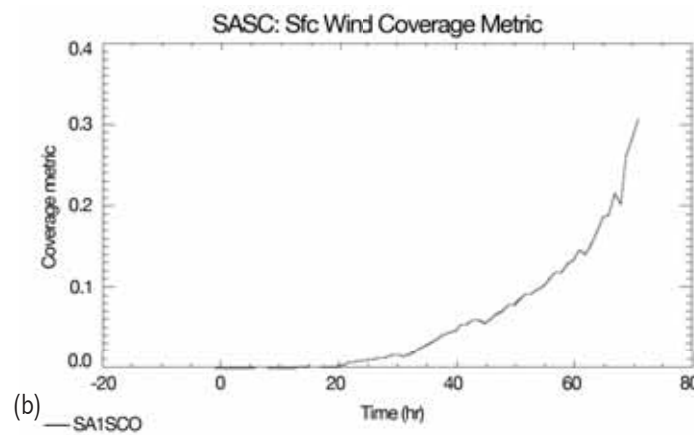
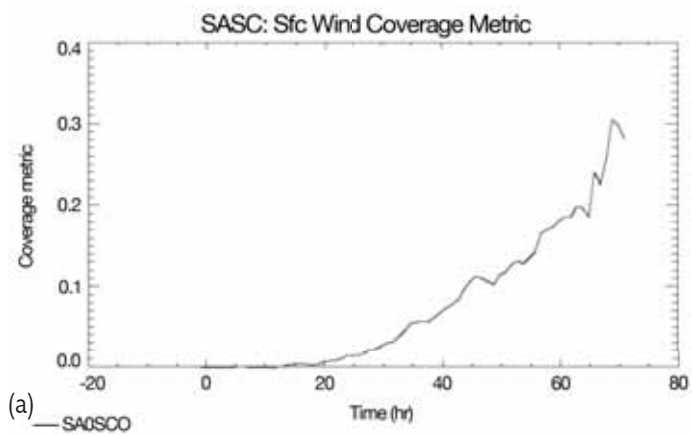


Figure 2.16 Storm intensity metric

Based on aerial coverage of hurricane force or greater surface winds. SA0SCO (a) has the sea-salt aerosol source routine disabled, SA1SCO (b) has the sea-salt aerosol source routine enabled.

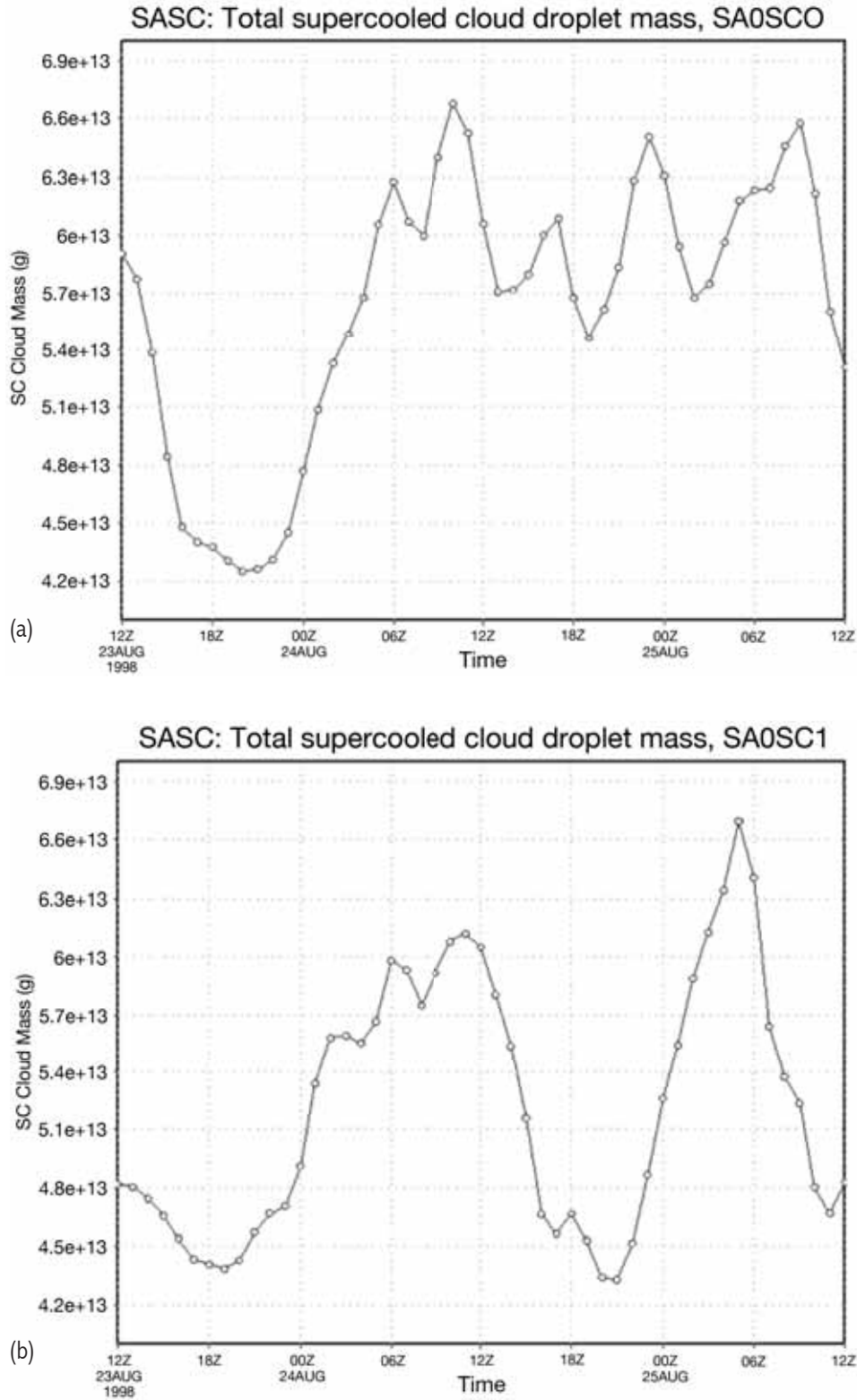


Figure 2.17 Total SC cloud droplet mass

SA0SCO (a) has the sea-salt scavenging sink routine disabled, SA0SC1 (b) has the sea-salt scavenging sink routine enabled

allows the CCN to build up again thus starting the cycle over again.

In summary, we have run four simulations each one a different combination of enabling or disabling the two new microphysics routines, which handle sea-salt aerosol source and aerosol scavenging sink (via precipitation). By comparing each routine enabled versus both routines disabled, we can isolate the effects of the routine being examined. This was done for both routines, which yielded interesting results.

The sea-salt source routine showed a noticeable increase in cloud droplet concentration near the eye wall region after the storm had reached hurricane force winds. This seems to indicate that the routine is correctly simulating the effects of increasing surface wind speed causing more sea spray, which increased the amount of CCN injected into low levels, which then caused the amount of cloud droplets to increase.

After the storm attained a strong intensity, the scavenging sink routine showed a low frequency oscillation in the total amount of SC cloud droplet mass when enabled versus a relatively steady state in the amount of SC cloud droplet mass when disabled. This oscillation occurs due to interactions between the CCN concentrations building up in the rainband region, which ultimately cause more precipitation that then scavenges CCN out of the atmosphere. The increase of CCN at the beginning of this cycle suppresses collision/coalescence, which allows more SC cloud droplets to move aloft that then enhance updrafts from the latent heat release due to the droplets freezing, which finally increases precipitation. This increase in precipitation then scavenges the CCN, which then allows the collision/coalescence processes to increase, which then diminishes the amount of SC cloud droplets aloft causing the updrafts to weaken (not be enhanced at least) and precipitation to decrease. This then lessens the scavenging, which allows the CCN amounts to build up again, thus starting the cycle over again.

This is clearly a work in progress and there is further investigation to be done. The results seem to indicate that there are subtle but important effects being modeled only when the new sea-salt source and sea-salt scavenging sink routines are included in the

simulation. We are planning on submitting this work in an upcoming publication once the investigation is completed.

## **2.7 Conclusions and Recommendations for the Future**

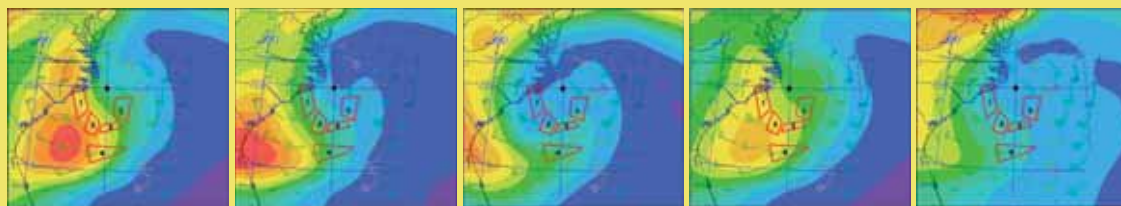
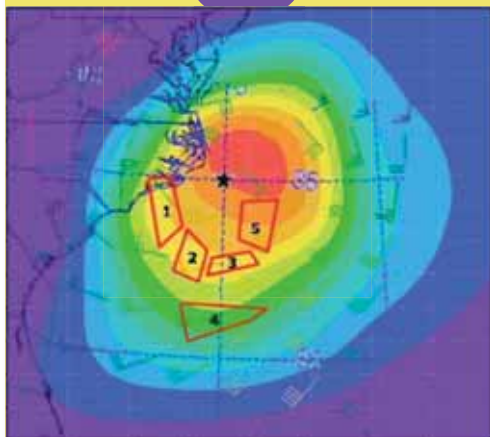
This research has clearly shown that aerosols can have an appreciable impact on tropical cyclone intensity. The results show that the aerosol impacts are greatest in the outer rainbands of a TC and that the mechanism is linked to the strength of cold-pools. These results are consistent with the findings of Reimer et al. (2010) who found that varying wind shear impacted TC intensity by varying the strength of cold-pools in the outer rainbands. The major impact of this research on hurricane intensity prediction is that it highlights the importance of low-level cold-pools, particularly in the outer rainbands on hurricane intensity. It means that methods for diagnosing cold-pool strength and area in real time need to be developed for hurricane intensity prediction. In addition, operational forecast models need to be implemented that can explicitly represent the variability of TC cold-pools due to variations in wind-shear, environmental moisture, and aerosols.

A natural question then is how responsive is a TC to varying CCN as vertical wind shear increases? Likewise, how responsive is a TC to varying aerosol and moisture amounts in the TC environment and the central core region? This is a natural question to ask as we expect that with higher amounts of moisture in the storm environment it will become increasingly difficult for aerosol to modulate storm intensity. These are questions that can be answered in the idealized storm studies that we have done so far.

Following that, we need to investigate how actual mature case study storms vary in intensity with targeted insertion of CCN. The targeted insertion approach should be used because it provides a more definitive representation of “cause and effect” without the confusing issues about whether or not the aerosol entered outer rainband convection at the right time and place.

Because the recent statistical studies by Clavner, an MS student under the supervision of Rosenfeld,

suggest that black carbon aerosols intensify hurricanes in contrast to Professor Gray's hypothesis, we also plan to investigate how black carbon aerosols introduced at low levels in a hurricane environment can impact TC intensity. We will also investigate how black carbon aerosols introduced above the anvils and over a large area extending beyond the storm impact its intensity. We anticipate that at the conclusion of this research we can state with some confidence how hurricane intensity is modulated both by hygroscopic aerosols and by light-absorbing black carbon aerosols.



## Testing the Sensitivity of TC Intensity to Concentration of Small Aerosols<sup>3</sup>

### 3.1 Introduction

Latent heat release in clouds is the main source of energy of a TC. The intensity of a TC critically depends on the rate of latent heat release as well as on its spatial distribution within the TC region. The latent heat release is the result of microphysical processes in clouds: condensational growth/evaporation of drops, deposition/sublimation of ice, drop freezing/ice melting, liquid drop-drop, ice-drop and ice-ice collisions, differential sedimentation of particles, etc. These processes depend on atmospheric aerosols determining the concentration and size of droplets and the concentration of ice crystals. Current TC models use simplified descriptions of microphysical processes based on different bulk-parameterization schemes. In these schemes, the exact equations describing microphysical processes are replaced by semi-empirical relationships with a great number of empirical parameters and coefficients to be tuned. Because of the lack of appropriate description of microphysical processes improvement of model resolution does not lead to improvement of forecast accuracy of TC models. This fact was clearly demonstrated in many presentations during the 29th Conference on

3. Principal Author: Prof. Dr. Alexander Khain, Hebrew University of Jerusalem, Israel; With contributions from: Scientific researchers: Dr. B. Lynn, Dr. A. Pokrovsky, Dr. M. Pinsky; Students: N. Ben-moshe; J. Spund; L. Magaritz; System manager: H. Zvi Kruglyak.

Hurricanes and Tropical Meteorology, Tucson, May 2010.

Recent observational and numerical studies showed that atmospheric aerosols dramatically affect the dynamics and microphysics of deep convective clouds. This means that aerosols can, in principle, affect the intensity of a TC. We assume that ingestion by tropical clouds of small soluble aerosols at the TC periphery leads to invigoration of these clouds and to the intensification of latent heat releases in them. This can invigorate the convection at the TC periphery and weaken the TC. This hypothesis dramatically differs from that of STORMFURY, where glaciogenic seeding of vigorous SC cloud towers within the eye wall was proposed. The STORMFURY hypothesis was not supported by observations within TCs and could not be justified by corresponding numerical modeling.

The main purposes of the present study were a) to test the hypothesis about the sensitivity of TC intensity to the concentration of small aerosols that play the role of CCN; and b) to test the hypothesis that ingestion by tropical clouds of soluble aerosols at the TC periphery leads to weakening of the storm. Note that the justification of these hypotheses required a principally new microphysics, which takes into account effects of aerosol on cloud dynamics and microphysics.

Tropical cyclones obtain their energy via latent and sensible heat fluxes. It is now well recognized that TC-ocean interaction is one of the most important factors affecting TC intensity. However, many uncer-

tainties remain in the description of such interaction. One of the most complicated problems is related to description of effects of spray forming at the ocean surface at strong winds. Most of existent models describing spray effects are 1D models, which do not take into account transport of spray by large eddies in the BL. At the same time in most LES models of the BL it was shown that large eddies play the dominant role in the vertical transport of heat, moisture, and momentum and increase surface fluxes of these quantities (e.g. Ginis et al. 2004). Accordingly, an important additional objective of the work was c) to determine the role of spray using an advanced microphysical model of the BL, which takes into account the effect of large eddies.

The points (a-c) determine the objectives of the study performed by our group during the first stage of the HAMP project.

### 3.2 Development of a High-Resolution Spectral Bin-Microphysics Model and its Justification

During the past decade a cloud model with SBM has been developed by our group at Hebrew University. This model is known as the Hebrew University Cloud Model (HUCM). The SBM is based on solving an equation system for size distribution functions of different hydrometeors (water drops, plate, columnar and branch-type crystals, snow, graupel and hail) as well as of aerosol particles (AP) serving the role of cloud condensation nuclei (CCN). Each size distribution is defined on the mass grid containing 43 (in a 2D model version) and 33 (in a 3D model) bins. This model has been used for simulation of individual clouds, cloud ensembles, squall lines, hail storms, etc.

In order to investigate the effects of AP on dynamics, microphysics and precipitation as well as to

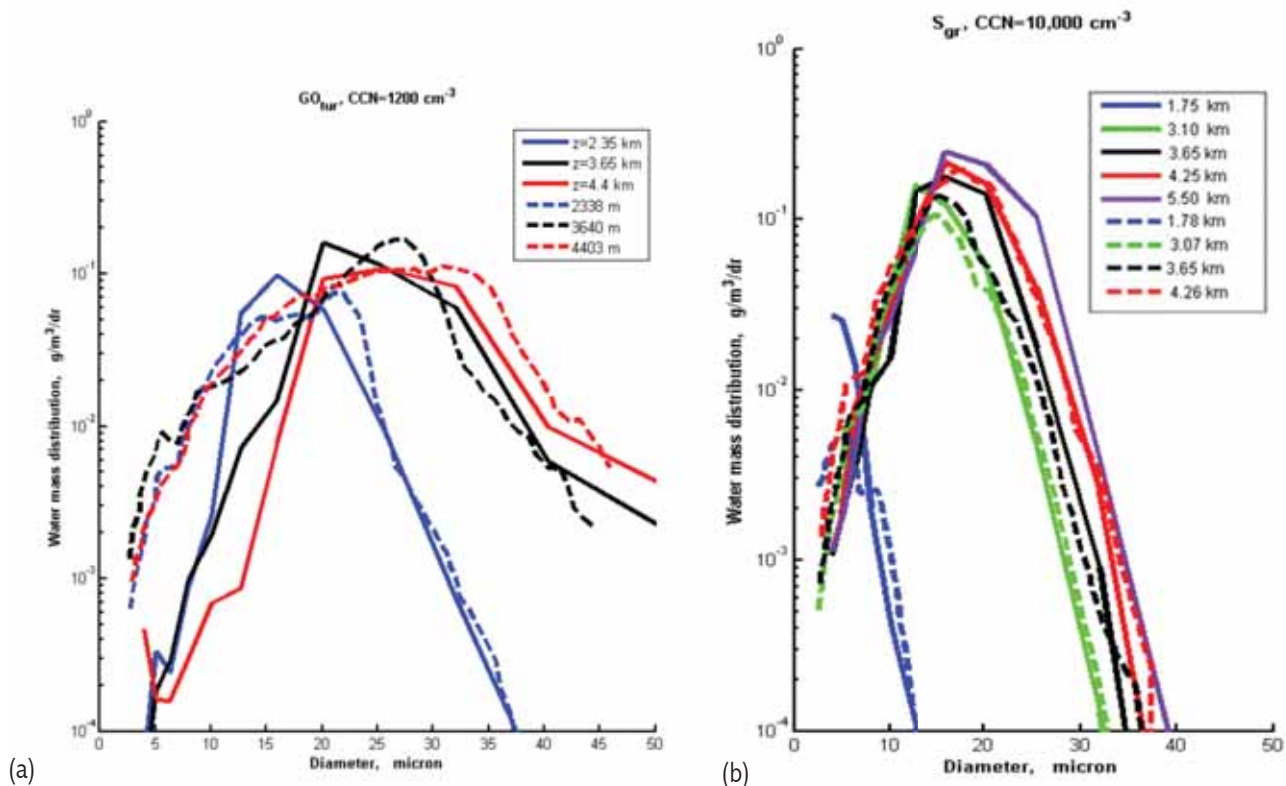


Figure 3.1 Mass distribution functions at different heights

Calculated in the green-ocean (left) and smoky (right) simulations (solid lines). The distributions measured in situ at 5 Oct 2002 in the green-ocean clouds at nearly the same height levels are plotted by dashed lines (after Andreae et al. 2004 and Freud et al. 2008).

justify the model's ability to reproduce in situ measured droplet size distributions and other microphysical parameters, significant efforts have been made to develop a 2-D HUCM spectral microphysics model with high resolution (from a few hundred of meters to 50 m). A set of simulations with resolution of 50 m was performed. In situ measurements during the LBA-SMOCC campaign in the Amazon region were chosen (Andreae et al. 2004; Freud et al. 2008) for simulation. Fig. 3.1 shows size distributions measured in situ and calculated by the model in relatively clean air (green-ocean clouds) and highly polluted atmosphere in zones of forest fires (smoky clouds).

One can see very good agreement of simulated distributions with those measured in situ. Fig. 3.1 shows a dramatic effect of aerosols on the shape and width of the droplet size distributions. Droplet size distributions in polluted air are substantially narrower, which led to a delay in raindrop formation. First

raindrops form in smoky clouds by  $\sim 2$  km higher than in clouds developing in clean air.

A new model version with the resolution 50 m x 50 m was used for simulation of deep convective clouds observed on 24 August 2009 during a field experiment in India. This case study was recommended for simulation within the framework of the HAMP Project to test the ability of the models used to reproduce observed development of precipitation. The unique features of the measured deep cloud were a) high air humidity, so that cloud base was below 1 km; b) extremely high CCN concentration, which was close to  $10000\text{ cm}^{-3}$  (at 1% of supersaturation). Such kind of clouds can be expected over the tropical oceans (in particular, at the TC periphery) in zones of penetration of continental aerosols.

In spite of high humidity, first rain drops were observed at heights of about 5 km. The hypothesis was that such a high level of the first raindrops for-

### Size distribution functions measured in deep convective cloud during field experiment in India 24 August 2009

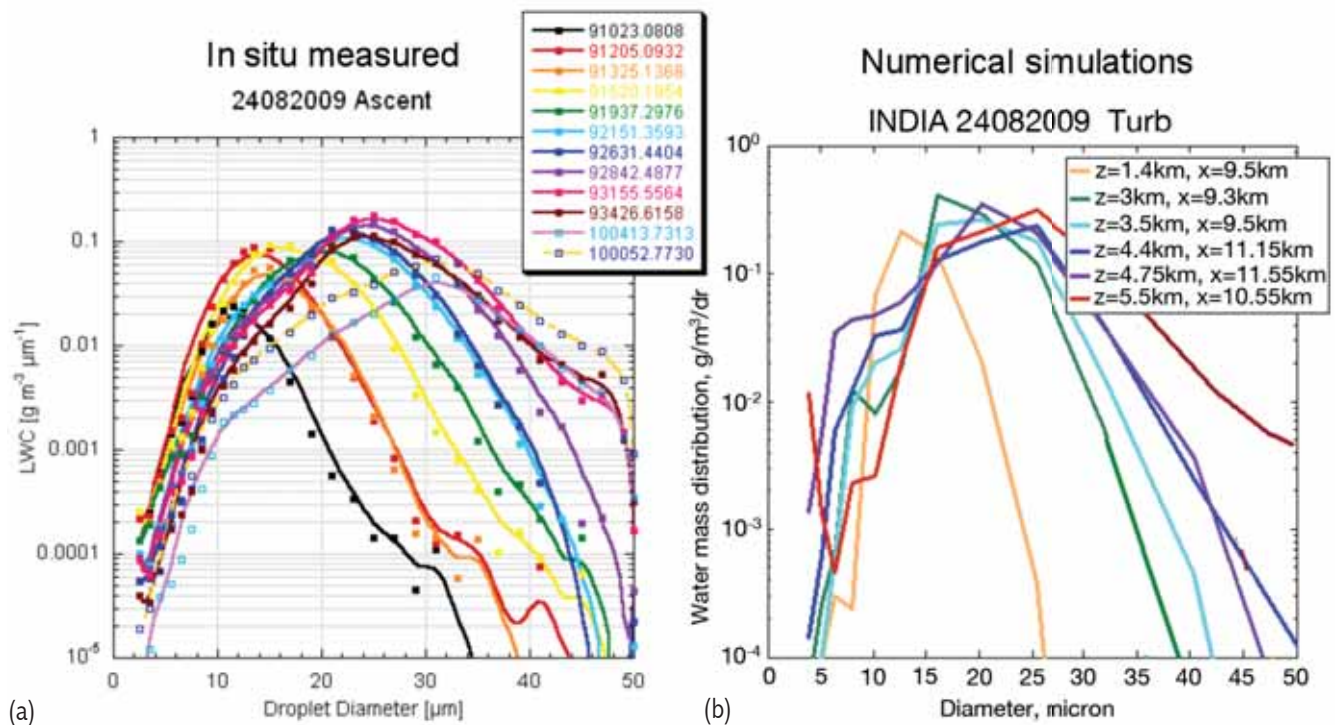


Figure 3.2 Droplet size distributions at different levels

Measured in situ (left panel) and simulated by the model (right panel).

mation is caused by the huge CCN concentration. Results of the first simulations are presented in Fig. 3.2 showing droplet size distributions at different levels measured in situ (left panel) and simulated by the model (right panel).

Comparison of the simulated size distributions with the distributions measured in situ indicates a good agreement. For instance in both measurements and simulations the size distributions are narrow and centered at diameters of about 26  $\mu\text{m}$ . In both measurements and simulations maxima, the droplet diameter reaches 50  $\mu\text{m}$  at a level of about 4.8 km. Formation of raindrops begins at  $\sim 5.5$  km (formation of large drops) in real clouds and is simulated properly by the model. In all simulations updraft velocities were several m/s higher in clouds developing in a polluted atmosphere.

These results show that a) the SBM model used accurately reproduces the observed cloud structure and b) indicate significant invigoration of clouds when the concentration of small CCNs is increased.

### 3.3 Development of a Unique Model for Investigation of Spray Effects

The effects of spray on atmosphere-ocean interactions in regions of strong wind (hurricanes) has attracted increased attention during the past decade after observational results showing that wind speed near the surface exceeds the value predicted by the classical theory of the BL.

Most existing models used for investigation of spray effects are 1-D models of the surface in which advection of spray by non-turbulent (large eddies) with scales of hundred meters was not taken into account. At the same time vertical velocities related to such vortices can reach 1-2 m/s. The existence of such vortices (rolls) is typical of the zone of strong wind in hurricanes (Ginis et al. 2004). The effect of advective transport of spray may be quite important on the vertical distribution of spray. Note that spray ingested into clouds can efficiently affect microphysics and precipitation formation in clouds. Accordingly, it is quite important to describe adequately the vertical distribution of spray mass as well as the

size distribution of spray droplets at different levels, including those close to cloud base.

A second specific feature of the existing spray models is utilization of quite simplified microphysics (if any). At the same time processes of spray evaporation/condensation as well as collisions between droplets may be extremely important to determine humidity and temperature changes in the BL.

The goals of the investigations were:

1. To calculate the vertical distribution of spray mass and concentration, taking into account spray advection by vortices in the BL with scales up to several hundred meters;
2. To evaluate the changes in surface heat and moisture fluxes caused by these changes in temperature and humidity.

As a basic model we used the Lagrangian model of the BL in which  $\sim 1500$  adjacent and interacting parcels move within a turbulent like flow (Pinsky et al. 2008; Magaritz et al. 2009). This model was used for simulation of microphysical and thermodynamical structure of the cloud-topped BL, for simulation of droplet size distribution (DSD) and drizzle formation in stratiform clouds.

New improvements related to turbulent mixing between parcels, calculation of surface fluxes as well as spray formation are implemented. The spray evolution is calculated within the computational area of 300 m in horizontal and 400 m in vertical. The height of the area of 400 m was chosen to avoid formation of clouds within the area. The velocity field is represented as a sum of a large number of harmonics with random amplitudes. The velocity field obeys turbulent laws and the model parameters are calculated to agree with the correlation properties of the measured velocity field. At  $t = 0$  min the Lagrangian air parcels, having a linear scale of about 8 m, are assumed equal and are distributed uniformly over the entire area. The parcels transport potential temperature and mixing ratio as well as aerosol/droplet size distributions. As a result of microphysical processes within the parcels and parcel motion, the vertical profiles of temperature and mixing ratio, DSD and AP size distribution change in each parcel. Corresponding

changes in the BL are calculated by averaging over the parcels.

The microphysics of a single Lagrangian parcel includes the diffusion growth/evaporation equation used for wetted aerosols and water droplets, the equation for super saturation and the stochastic collision equation describing collisions between droplets. The size distribution of cloud particles (both non-activated nuclei and droplets) is calculated on a single mass grid containing 500 bins within the 0.01  $\mu\text{m}$  to 1000  $\mu\text{m}$  radius range. The mass of each bin changes with time in each parcel according to the

equation for diffusion growth. A small 0.01s time step is used to simulate adequately the growth of the smallest AP, so that the separation between non-activated nuclei attaining equilibrium (haze particles) and the growing droplets is simulated explicitly, without any parameterization. The collision droplet growth is calculated using a collision efficiency table with a high 1  $\mu\text{m}$  resolution in droplet radii. Particle collisions are calculated with a one-second time interval. Total droplet evaporation leads to the formation of wet AP. A specific feature of spray particles is their high salinity. High salinity dramatically

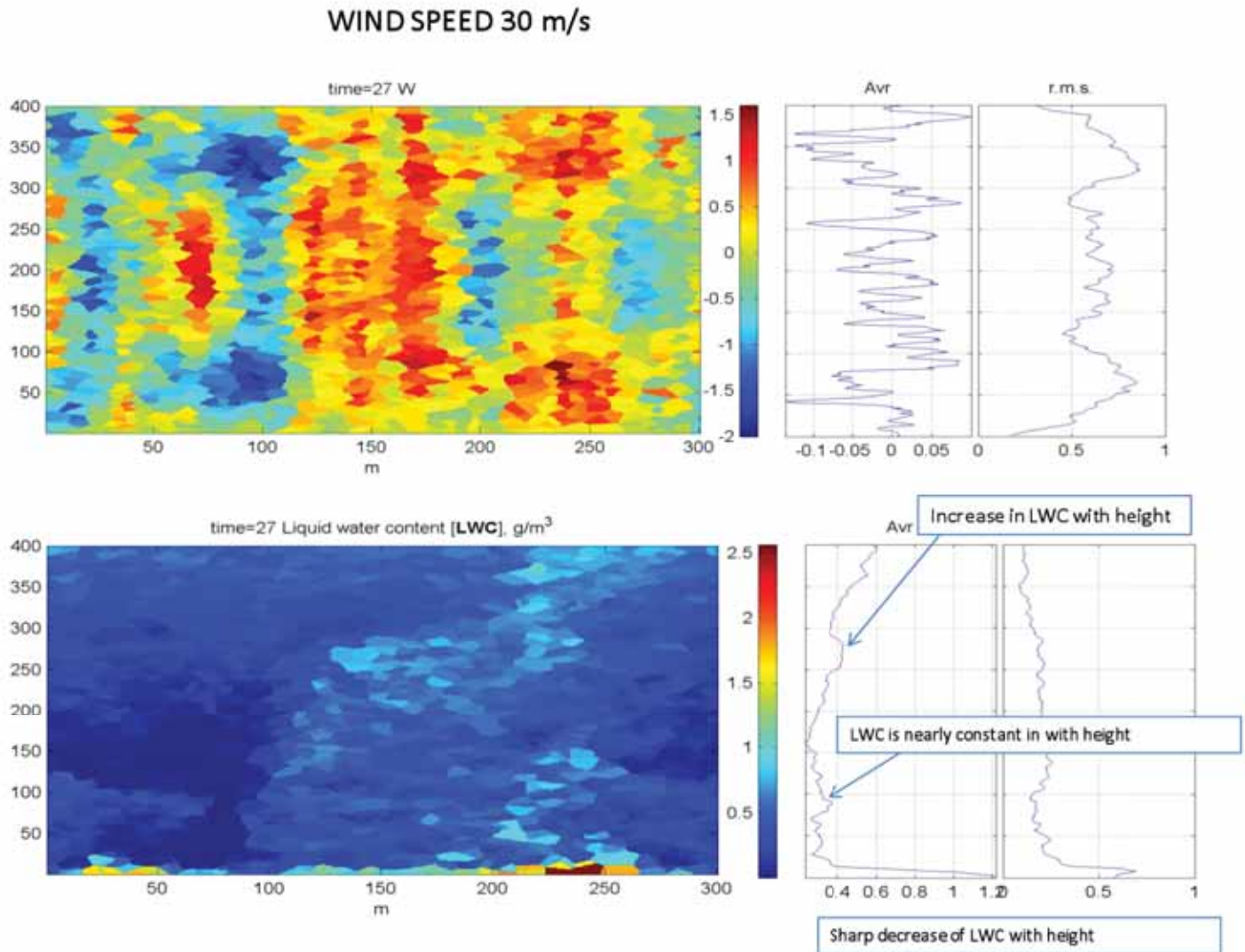


Figure 3.3 Fields of vertical velocity and liquid water content

In the control experiment at  $t=135$  min.

affects particle behavior. For instance, salty particles may grow in under saturation conditions.

The size distributions and amount of spray depends on wind speed. The size range of spray is wide: from  $0.01 \mu\text{m}$  to  $\sim 500 \mu\text{m}$ . Typically, in spray models only large particles with diameters exceeding  $10 \mu\text{m}$  are considered. This is because the main spray effect considered in these models is the creation of a vertical profile of loading that increases the stability of the surface layer. From a microphysical point of view, however, the particles of smaller size can also be important, because they can ascend to high levels and create a large amount of giant CCN affecting cloud microphysics and rain formation. That is why we match the spray source of large and small particles. A spray source function showing the rate of spray droplet production was used during model integration to change the size distributions in parcels adjacent to the surface. The changes of the size distributions were performed according to the vertical profile of the source.

Several preliminary simulations have been performed in which the background wind was set equal to  $20 \text{ m/s}$ . The preliminary results are presented in Figures 3.3 through 3.7. Fig. 3.3 shows fields of ver-

tical velocity and liquid water content in the control experiment at  $t=135 \text{ min}$ .

One can see that updraft velocities in large eddies reach  $1.5 \text{ m/s}$ . In the zone of updraft there is enhanced liquid water content (total spray mass). Horizontally averaged vertical profile  $\text{LWC}(z)$  indicates 3 zones: a) the lowest zone of sharp decrease of LWC with height. This zone arises because of sedimentation of the largest spray; b) zone of nearly constant LWC. In this zone there is a budget between sedimentation and evaporation on one hand and by upward transport, on another hand; and c) where diffusion growth of spray dominates over sedimentation. Note that 1-D models simulate actually only zone 1 with a strong exponential decrease in LWC with height. Zones b and c were not simulated in the 1-D models. Fig. 3.4 shows a field of rainflux at  $t=135 \text{ min}$ .

One can see that diffusion growth and collisions of spray lead to formation of raindrops (drops with radius exceeding  $\sim 50 \mu\text{m}$ ) and rainflux. Spray induced rain begins at a height of about  $300 \text{ m}$ . Note that maxima rainflux are located in downdrafts, when fall drop velocity is superimposed with downdraft velocity. Formation of rain consisting of drops forming by spray collisions was not simulated by earlier

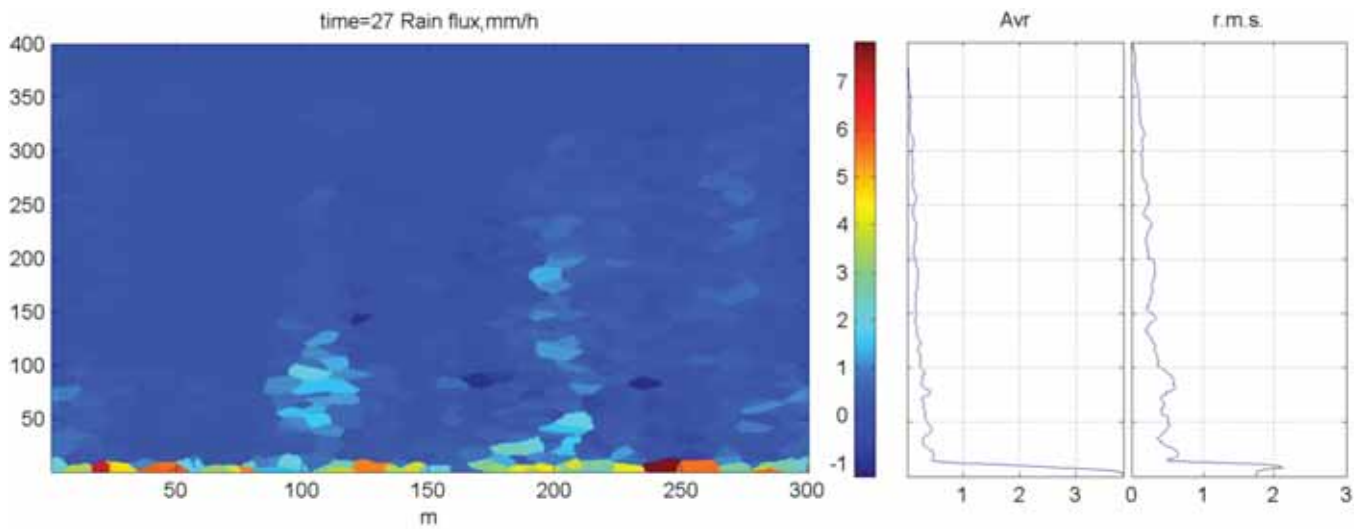


Figure 3.4 Field of rainflux at  $t=135 \text{ min}$ .

models because both collisions and advection of spray by air velocity were not taken into account.

Fig. 3.5 shows size distributions of wet particles (blue) and “dry” aerosols (red) within them in parcels located at different levels. Spectra near the surface actually represent size distributions of spray drops formed near the surface. The mass spectrum is centered at a radius of 100  $\mu\text{m}$ . The maximum spray size is about 400  $\mu\text{m}$  in radius. The part of the spectrum with  $r > 10 \mu\text{m}$  corresponds to the size distribution of large spray typically used in the 1-D models. Wet particles within the range  $5 \cdot 10^{-2}$  to 10  $\mu\text{m}$  are small wet particles forming at natural APs and in smallest spray. The maximum size of dry AP in the largest spray is  $\sim 100 \mu\text{m}$ . Fig. 3.5 shows also distributions in parcels located at 280 and 300 m. One can see that DSD in these parcels are quite different. A parcel located at 280 m contains giant “dry” aerosols with radii up to 10  $\mu\text{m}$ . Raindrops growing on these APs exceed 100  $\mu\text{m}$  in radius. The mass distribution depicts a pronounced maximum in the raindrop size. This spectrum shows that even large spray (with large AP size) reach levels of a few hundred meters ascending in the convective –scale updrafts. The DSD in parcel located at 300m contains relatively small “dry” APs. However, the DSD growing on the aerosols are quite large, and reach 100  $\mu\text{m}$  in radius.

Thus, it is shown that large eddies transport large spray to high levels toward cloud base. Moreover, spray drops form clouds with cloud base of  $\sim 200$  m, which precipitate. Thus, the effects of spray of cloud microphysics should be extremely important.

Figures 3.6 shows vertical profiles of absolute humidity (a) and potential temperature (b) in simulations when the effects of large eddies were taken into account (solid lines) and when large eddies were switched off (dashed lines). The dashed lines mimic the results simulated by the current 1D models of BL with spray. One can see the dramatic effect of large eddies. They lead to formation of nearly constant absolute humidity and potential temperature, which is a typical feature of a well mixed BL observed in the TC BLs. At the same time, the profiles obtained in

1D models (formed by turbulent diffusion) are not realistic.

The differences in the vertical profiles lead to dramatic differences in the surface fluxes in NO\_LE (no large eddies), and LE (large eddies included) simulations (Fig. 3.7).

One can see that taking into account the mixing of the BL by large eddies increases surface fluxes by factors as high as 1.5-2. Some decrease of the fluxes with time is related to the fact that the current model design has no sink of humidity and temperature except for precipitation fall to the surface. In a real TC advection of heat and dry air by the background flow can serve as a “sink” of humidity.

So, large eddies combined with those of spray dramatically change the thermodynamics and microphysics of the BL. The effects of large eddies should be taken into account in parameterization of spray effects in TC models.

### **3.4 Development of the Model of the BL That Resolves Large Eddies**

In collaboration with Ginis, we are developing a model of the BL in TC to better describe the interaction of the atmosphere and the ocean at strong winds. The results are presented in Chapter 4 of this report by Ginis.

### **3.5 Simulation of Aerosol Effects on the Intensity of a Land-Falling TC (Khain et al. 2008a, 2010)**

#### *3.5.1 Introduction*

Tropical cyclones (TCs) are known for their destructive power, particularly as they make land-fall. The prediction of TC intensity represents a difficult task. Well known factors affecting TC intensity are heat and moisture surface fluxes and wind shear. Implementation of TC-ocean coupling into prognostic TC models led to a significant improvement of forecast of TC intensity. These mechanisms represent thermodynamic factors affecting the convective intensity. During the past decade it was found that

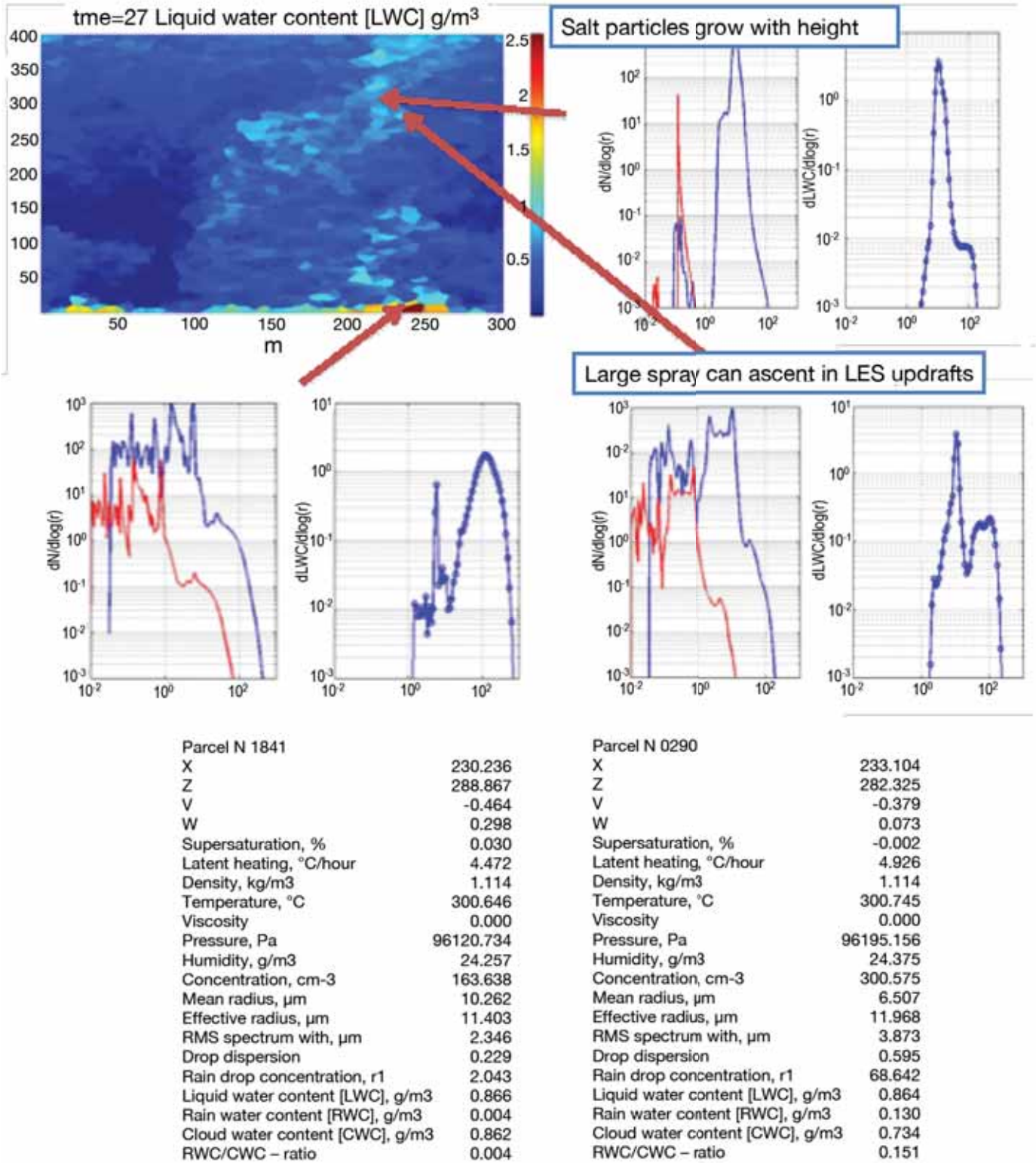


Figure 3.5 Number and mass distributions of drops (blue) and aerosols inside of droplets (red)

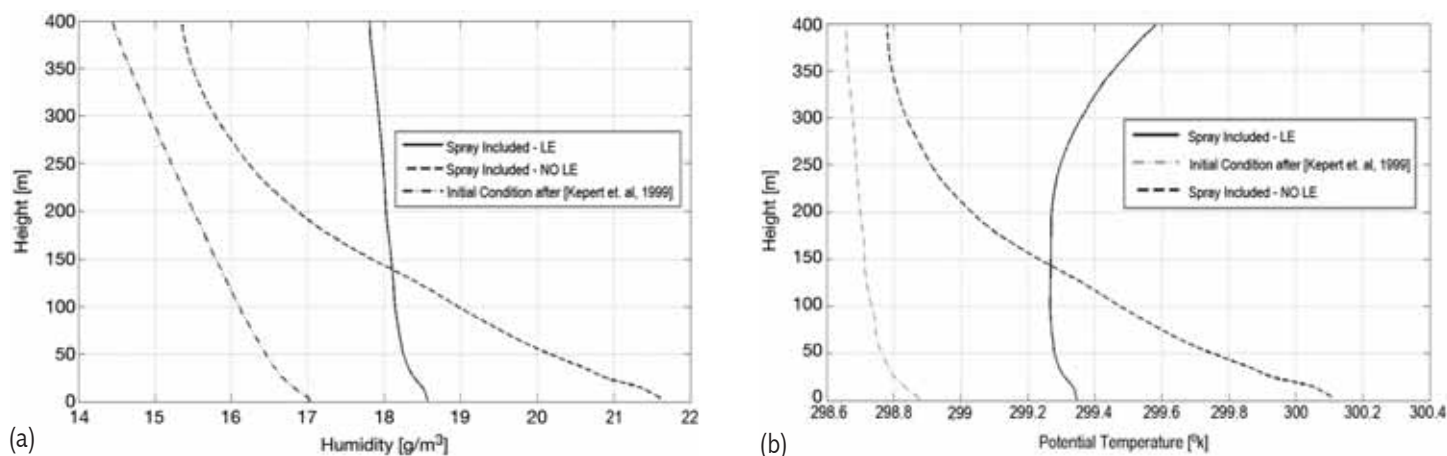


Figure 3.6 Vertical profiles of horizontally averaged absolute humidity (a) and potential temperature (b)

In NO LE (no large eddies-dashed lines), and LE (large eddies included-solid lines) simulations. The simulation time is 180 [Min]. The initial profiles of humidity and potential temperature are also presented (dash-dotted).

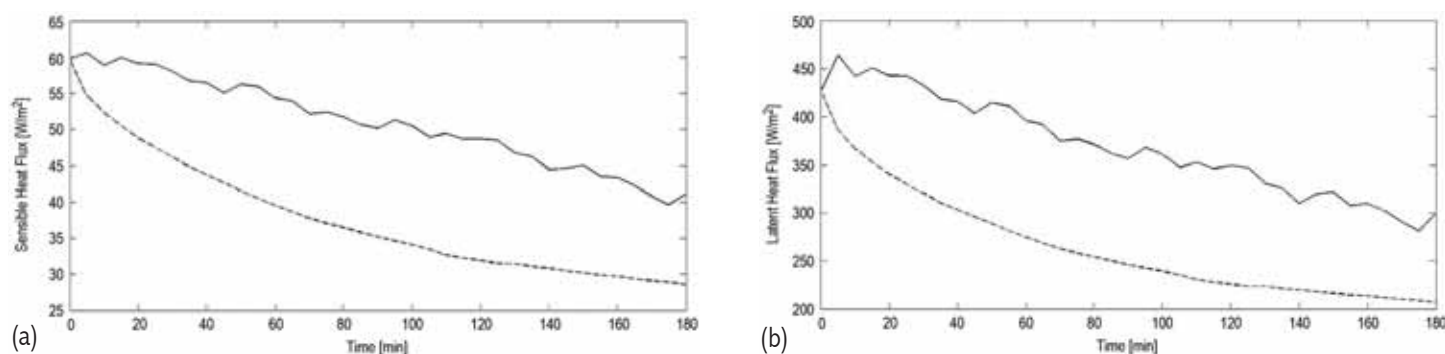


Figure 3.7 Time dependences of sensible (a) and latent (b) fluxes in the LE (solid) and No\_LE (dashed curve) runs.

aerosols (including anthropogenic ones) substantially affect cloud microphysics and consequently the rate of latent heat release, the dynamics and the precipitation (see, overviews by Levin and Cotton 2009; Khain et al. 2009; Rosenfeld et al. 2008). In particular, it was found that small aerosols invigorate tropical convection, increasing vertical velocities and cloud top heights of deep convective clouds (Khain et al. 2004, 2005, 2008b; Koren et al. 2005; Lynn et al. 2005a,b, Wang 2005, Lee et al. 2008; Khain 2009). Thus, aerosols affect cloud microphysics and dynamics.

Indirect evidence of aerosol effects on TC intensity can be derived from enhanced lightning at the periphery of land falling TCs (Khain et al. 2008a). They showed that the ingestion of continental aerosols by clouds at the TC periphery and their subsequent invigoration is the mechanism contributing substantially to lightning formation at the TC periphery. An increase in the concentration of small aerosols increases droplet concentrations and decreases droplet sizes. The net effect is a decrease in the collision rate, delaying raindrop formation and warm rain production. As a result, small droplets ascend in cloud updrafts and continue growing by condensation.

It leads to an increase in SC water content, which intensifies the riming, i.e. ice-water collisions accompanied by freezing of liquid water. Both processes are accompanied by extra latent heat release, leading to an increase in cloud updrafts and sometime to an increase in cloud top height (Khain 2009). Aerosol-induced increase in SC cloud water content (CWC) and vertical velocities foster lightning formation, when collisions of ice crystals and graupel take place in the presence of SC droplets. Khain et al. (2008a) simulated the evolution of hurricane Katrina (August 2005) during its movement in the Gulf of Mexico using a two nested grid Weather Research Model (WRF, NCAR version) with the Thompson et al. (2006) one-moment bulk-parameterization. Effects of continental aerosols were simulated by shutting off the drop-drop collisions only at the hurricane periphery. A similar approach was used by Rosenfeld et al. (2007). It was also shown that aerosols, invigorating clouds at 250-300 km from the TC center, decrease the convection intensity in the TC eye wall leading to some TC weakening. Similar results were reported by Rosenfeld et al. (2007), who proposed a method of TC mitigation by seeding of clouds at the TC periphery near their cloud base with small aerosol particles of 0.05  $\mu\text{m}$  to 0.1  $\mu\text{m}$  in radius. Also, simulations of the evolution of an idealized TC using the Regional Atmospheric Meteorological System (RAMS) (Zhang et al. 2007) supported the conclusion that aerosols (for instance, Saharan dust) can substantially affect the intensity of TCs.

To take into account microphysical factors (such as aerosols) properly, advanced microphysical schemes are required. The problem of the adequate description of convection in TC models remains one of the most difficult problems in TC modeling. The current operational TC forecast model developed at the Geophysical Fluid Dynamics Laboratory used large scale convective parameterizations till 2006 (Kurihara 1973, Arakawa and Schubert 1974). Since 2006 this model used a simplified Arakawa-Schubert scheme for cumulus parameterization and a simplified version of the Ferrier bulk-parameterization (Ferrier 2005) for large-scale condensation in cases when supersaturation at grid points is reached (Bender et

al. 2007). The simplified bulk scheme treats only the sum of the hydrometeor classes (referred as the total condensate) in the advection in both horizontal and vertical directions. Both schemes are insensitive to aerosols.

The development of one and two-moment bulk parameterization schemes was an important step toward the improvement in the description of convective processes and precipitation in numerical models. The comparatively small number of prognostic equations makes the schemes computationally efficient, so they are widely utilized in simulating different cloud-related phenomena such as supercell storms, squall lines, etc. These schemes were used recently for simulation of TCs (e.g., Zhang et al. 2007; Fierro et al. 2007).

Note that the bulk-parameterization schemes have significant limitations in describing microphysical processes affecting the shape of size distributions (Khain 2009). The second approach to simulate microphysical processes is the utilization of SBM, in which a system of kinetic equations for size distributions of particles of different classes is solved. The equation system solves the equations for advection, settling, collisions, freezing, melting, etc. for each mass bin (each particle size). This method is much more accurate than the bulk-parameterization as regards its ability to simulate cloud dynamics and microphysics and precipitation [see comparisons of SBM vs. bulk schemes in Lynn et al. 2005b, Lynn and Khain 2007, Li et al. 2009a,b, Iguchi et al. 2008; Khain and Lynn 2009; Khain et al. 2009].

In this study the evolution of hurricane Katrina over the Gulf of Mexico is simulated with WRF, in which cloud microphysics is described using a computationally efficient spectral bin microphysics scheme, in which all microphysical processes are described explicitly.

### *3.5.2 Model and Experimental Design*

#### **Spectral Bin Microphysics Scheme**

The SBM scheme implemented into the WRF (Skamarock et al. 2005, version 3) has been described

by Khain et al. (2004) and Lynn et al. (2007). The original scheme is based on solving the kinetic equation system for the size distributions of seven classes of hydrometeors: water drops, three types of crystals (columnar, plate- and branch-type), aggregates (snow), graupel and hail. Each hydrometeor class is described by a size distribution function defined on the grid of mass (size) containing 33 doubling mass bins. The minimum particle mass corresponds to that of the 2  $\mu\text{m}$  radius droplet. Aerosol particles are also described by a size distribution function containing 33 size bins. The size distributions are calculated in the course of the model integration. Using the values of supersaturation, the critical size of aerosol particles to be activated to drops is calculated. Aerosol particles exceeding the critical size are activated and the corresponding mass bins in the aerosol size distribution become empty. The SBM also takes into account possible droplet nucleation during dry air entrainment through the lateral cloud boundaries. An efficient and accurate method of solving the stochastic kinetic equation for collisions (Bott, 1998) was extended to a system of stochastic kinetic equations calculating water-ice and ice-ice collisions. The collision kernels for each pair of particles are calculated using an accurate superposition method (Pinsky et al. 2001, Khain et al. 2001) and used in the form of lookup tables. The ice nuclei activation is described using an empirical expression suggested by Meyers et al. (1992) and applying a semi-lagrangian approach (Khain et al. 2000) to allow the utilization of the proposed diagnostic formulas in a time dependent framework. Secondary ice generation is described according to Hallett and Mossop (1974). The rate of drop freezing follows the observations of immersion nuclei by Vali (1974, 1975), and homogeneous freezing according to Pruppacher (1995). Breakup of raindrops is described following Seifert et al. (2006).

The SBM model does not require any tuning of the scheme parameters and was successfully used without any changes for simulation of deep maritime convection (Khain et al. 2004, 2008b), continental clouds, including pyro-clouds (Khain et al. 2008b), squall lines (Lynn et al. 2005a,b; Tao et al. 2007; Li et al. 2009a,b; Khain et al. 2009), supercell storms

(Khain and Lynn 2009) and arctic stratiform clouds (Fan et al. 2009).

Since the treatment of 8 size distributions requires significant computer time, a Fast-SBM has been developed in which all ice crystals and snow (aggregates) are calculated on one mass grid (one distribution function). The ice particles with sizes below 150  $\mu\text{m}$  are assumed to be crystals, while the larger ones are assigned to aggregates (snow). Similarly, high-density particles (graupel and hail) are also combined into one size distribution (graupel). As a result, the number of size distributions decreases from 8 to 4 (aerosols, water drops, low density ice, high density ice). Note that Fast-SBM keeps the main advantages of SBM: a kinetic equation system is solved using the non-parameterized basic equations, particles of each size have their own settling velocity, particles depending on their mass have different densities, etc. The test simulations showed that Fast-SBM requires less than 20% of the time of the full SBM, which makes it possible to use the Fast-SBM on standard PC-clusters. The comparison of results obtained by the Exact and Fast SBM in simulation of tropical cloud systems (Khain et al. 2009) shows that the Fast SBM produces microphysical and dynamical structure as well as accumulated rain at the surface quite similar to those simulated with Exact SBM.

## Experimental Design

A set of simulations were used to study possible aerosol effects on the evolution of Hurricane Katrina (August 2005) in the Gulf of Mexico during about three days (beginning with 27 August 00z) prior to landfall (on about 12z 29 August). A two nested gridded WRF (version 3.1) was used, and the nest moved using a cyclone-following algorithm. The resolution of the finest and the outer grid was 3 km and 9 km, respectively. The number of the vertical levels was 31, with the distances between the levels increasing with height. The SBM is applied at the finest grid of 400 x 400 km sizes. The initial fields were taken from the Global Forecast System Reanalysis data. The lateral boundary conditions were updated every six hours using the data as well. The Gulf of Mexico surface

water temperatures were initialized on 27 August 00 z , and were not updated during the experiments. According to the reanalysis data the sea surface temperature (SST) taken along the TC track reached its maximum near the shore (the place of the TC landfall).

Cloud droplets arise on AP playing the role of Cloud Condensation nuclei (CCN). The initial (at  $t=0$ ) CCN size distribution is calculated using the empirical dependence of concentration of activated CCN  $N_{ccn}$  on super saturation with respect to water  $S_w$  (in %)  $N_{ccn} = N_o S_w^k$  as described by Khain et al. (2000).  $N_o$  and  $k$  are the measured constants for determining the AP concentration and shape of the AP size distribution. At  $t>0$  the equation for the size distribution of non-activated AP is solved. The initial AP concentration was assumed constant within the lowest 2 km layer and decreased exponentially with height with characteristic scale of 2 km. Aerosols were transported over the entire computational area similarly to other scalars like the mixing ratio.

To investigate aerosol effects on the microphysics and dynamics of the TC two simulations were carried out: a) in the first “MAR” simulation

was set equal to  $100 \text{ cm}^{-3}$ , typical of the maritime atmosphere over the whole computational area b) in the second, semi-continental MAR\_CON case the initial CCN concentration over the land  $N_o$  was set equal to  $1500 \text{ cm}^{-3}$  typical of continents under not very polluted conditions. Initially, over the sea  $N_o$  was set equal to  $100 \text{ cm}^{-3}$  in all simulations. In all simulations the slope parameter  $k$  was set equal to 0.5. When the TC enters the Gulf of Mexico, its circulation transports aerosols from the land to the sea, so that some continental aerosols penetrate clouds within the TC and affect their microphysics and dynamics. In all simulations the maximum size of dry AP is equal to  $2 \text{ }\mu\text{m}$ , which give rise to droplets of radius  $8 \text{ }\mu\text{m}$  at cloud base. No giant CCNs that could arise at high winds as a result of spray formation were assumed in the simulations.

### 3.5.3 Results of Simulations

Fig. 3.8 shows the time dependence of minimum pressure in all simulations for Katrina. One can see that the model TC has lower intensity during

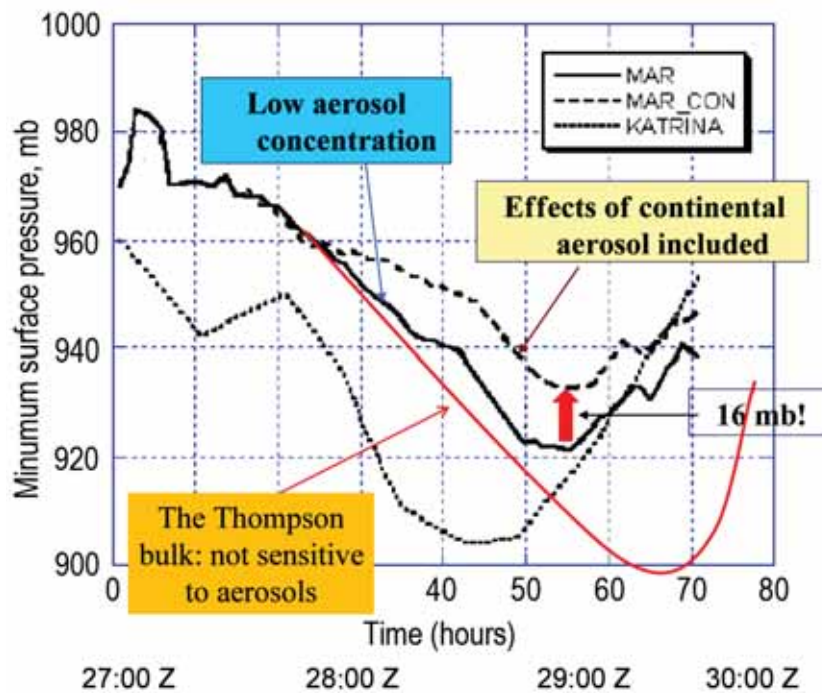


Figure 3.8 Time dependence of minimum pressure in numerical experiments and hurricane Katrina (August 2005)

the first ~50 h of simulations as compared to that of Katrina. Note in this connection that the WRF initialization used was not a TC forecast initial condition, so that no specific adjustment procedures were used to adapt the TC structure derived from the crude resolution (100 km) reanalysis data to the intensity of the real TC at  $t=0$  (27 Aug 00z). Hence, some relaxation period was required to get the model TC intensity close to the observed one. Yet, the accurate prediction of Katrina's intensity was not the primary purpose of the study. The main purpose of the simulations was to compare the TC intensity and structure in the simulations with and without aerosol effects on the TC clouds in a strong hurricane, which is able to involve aerosols from the continent. Fig. 3.8 shows that TC in the "MAR\_CON run turned out substantially weaker, so that at the time instances when the TC reached its maximum intensity the minimum pressure in its center was about ~16 mb higher than in the MAR run. Note that lower (as compared to Katrina) intensity of the model TC leads likely to an under-estimation of aerosol effects, because of a weaker TC involves lower AP amounts into the TC circulation.

Results shown in Fig. 3.8 indicate the existence of an important factor affecting the TC intensity, namely atmospheric aerosols. Note that SBM predicts correctly the TC weakening well before landfall. At the same time the bulk-parameterization schemes (for instance, the Thompson scheme) predicts the maximum TC intensity just during landfall (which does not agree with the observations).

In the analysis of the aerosol fields we addressed two main questions. The first one was: whether a significant aerosol concentration can enter the TC periphery when it is located at comparatively large distance from coastal line, and second, whether aerosols can penetrate the TC eye. Aerosol fields simulated in the MAR run (not shown) indicate very uniform distribution of AP concentration (which is very low) because the AP concentration over land was assumed equal to that over the sea.

Fig. 3.9 compares the fields of the column-maximum droplet concentrations (upper row) and cloud water mass content (CWC) (clouds with radii below 40  $\mu\text{m}$ ) in clouds in simulations MAR (left) and

MAR-CON (right) on August 28th 22z on the fine grid (46h, Fig. 3.8). One can see that in the MAR run droplet concentration does not exceed 50-100  $\text{cm}^{-3}$ , which is typical droplet concentration in clouds arising in clean maritime air. Zones of maximum droplet concentration in the MAR run at the TC periphery indicate zones of higher vertical velocities in rain bands. In MAR-CON, the penetration of continental aerosols led to an increase in droplet concentration at the TC periphery in the zone of high aerosol concentration, as well as in the eye wall. In the MAR-CON run the maximum droplet concentration reached 500  $\text{cm}^{-3}$  (especially high concentrations are at TC periphery), which is substantially higher than those in typical maritime clouds. An increase in droplet concentration within the eye wall in the MAR-CON run indicated that aerosols penetrated to the TC eye wall in the simulations.

The CWC dramatically increases (mainly SC water content) as a result of aerosol penetration: while the maximum CWC reached 0.6  $\text{gm}^{-3}$  in the MAR run, the CWC in the MAR-CON run exceeded 1.6  $\text{gm}^{-3}$ . The CWC increased largely at the TC periphery where the concentration of aerosols is higher.

The aerosol-induced changes in warm microphysics resulted in corresponding changes in ice microphysics. The penetration of larger amount of drops above the freezing level led to an increase in graupel and snow (aggregates) contents at the TC periphery (Fig. 3.10).

Note that convective invigoration of clouds at the TC periphery weakened the updrafts in the eye wall, which immediately resulted in the decrease and even disappearance of graupel and snow in the eye wall. Extra latent heat release caused by droplet condensation and freezing at the periphery causes an increase in vertical updrafts velocities and cloud top height (not shown). The values of maximum vertical velocities exceed 10 m/s, which are rare for maritime TC clouds (Jorgensen et al., 1985). At the same time such high velocities are required to form lightning. The increase in cloud top height within polluted air was observed from satellites (Koren et al. 2005) and simulated in many recent studies dedicated to aerosol effects on cloud dynamics (Khain 2009).

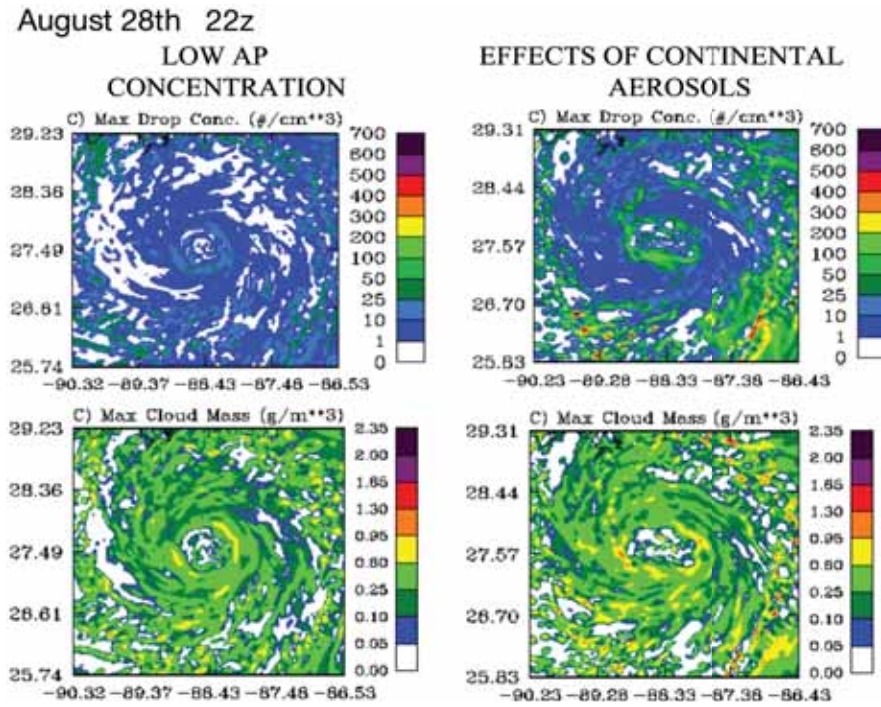


Figure 3.9 Droplet concentrations and CWC in MAR and CAR-CON simulations

Fields of the maximum droplet concentrations (upper row) and the CWC in simulations MAR (left) and MAR-CON (right) on August 28th 22z at the fine grid.

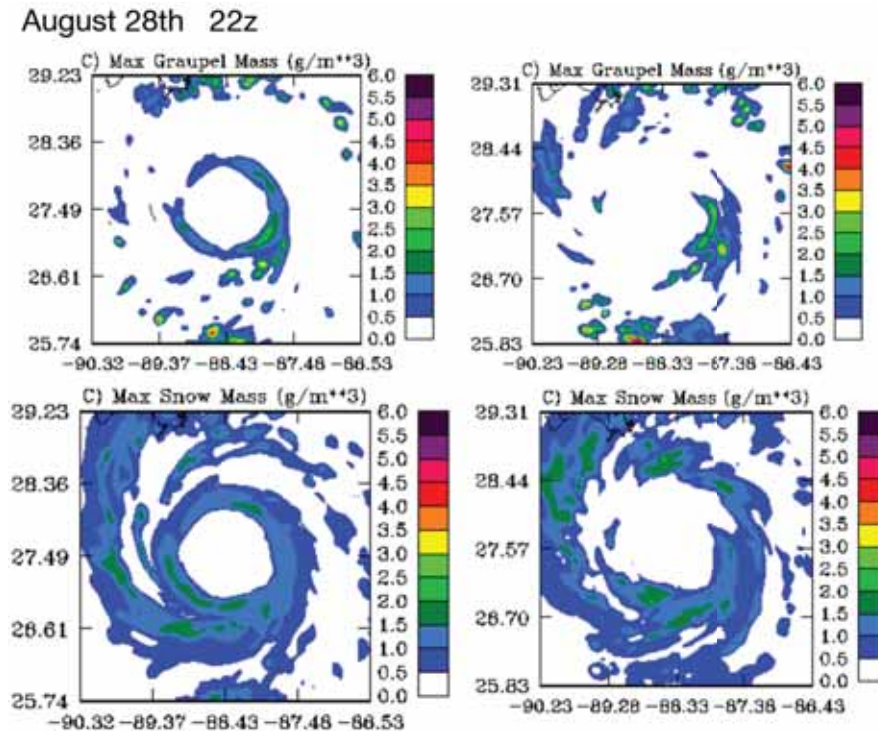


Figure 3.10 Graupel and snow concentrations in MAR and CAR-CON simulations

Fields of graupel (upper row) and snow (lower row) in MAR (left) and MAR-CON (right) on August 28th 22z at the fine grid.

As it was discussed above, Khain et al. (2008a) suggested that the evolution of lightning within a TC approaching the land results from the ingestion of continental aerosols into the TC periphery. The present study strongly supports this finding (not shown).

Fig. 3.11 shows the fields of maximum wind speed 28 Aug. 21 z (upper panels), and 22 z in runs MAR and MAR\_CON. One can see a significant decrease in the maximum wind speed up to 15 m/s, i.e. by 20-25%. This decrease is substantially stronger than was reported by Khain et al. (2008a). One of the reasons is that Khain et al. (2008a) used the bulk-parameterization scheme that is not sensitive to aerosols, as well as the fact that an artificial approach to parameterize aerosol effects by warm rain preventing was performed within the frame of this scheme.

Khain et al. (2008a) suggested that the evolution of lightning within a TC approaching the land results from the ingestion of continental aerosols into the TC periphery. The present study strongly supports this finding. For instance, Fig. 3.12 presents the fields of lightning potential index (LPI) on 28 Aug. 20 z, and 22 z (t=44 and 46 h). The LPI was introduced by Lynn and Yair (2009). The LPI is the volume integral

of the total mass flux of ice and liquid water within the “charging zone” (0 to -20°C) of the cloud. The LPI has the same meaning as the lightning probability parameter introduced by Khain et al. (2008a).

Fig. 3.12 shows also lightning in Katrina (2005) at two different times (Shao et al. 2005). The squares show the location of the fine grid approximately corresponding to these times. One can see that while in the MAR run the LPI is the highest in the eye wall all the time. Note that simulations of lightning in the TC using bulk-parameterization scheme (Fierro et al. 2007) (in which aerosol effects were not taken into account) also indicate that lightning was concentrated in the TC central area independently of the stage of TC evolution.

Fig. 3.12 shows the time instance of the dissipation of the internal lightning ring in the course of intensification of convection and lightning at the TC periphery. One can see that the disappearance of lightning in the eye wall in the MAR-CON run agrees well with the behavior of lightning in Katrina. The disappearance of lightning in the eye wall in the MAR-CON takes place about 5-6 hours before the TC weakening.

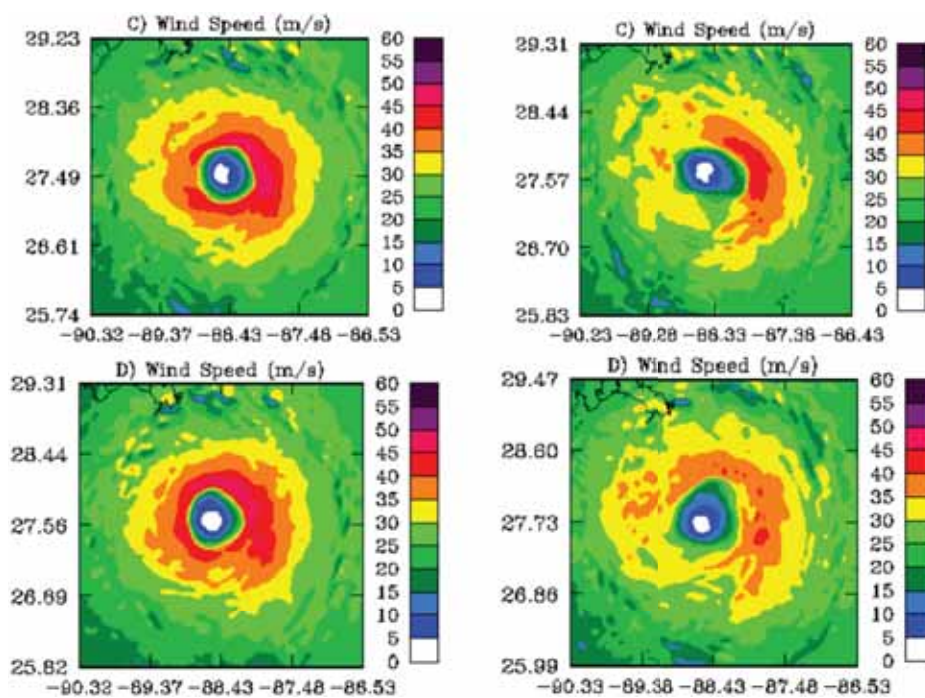


Figure 3.11 The fields of maximum wind speed 28 Aug. 21 z (upper panels), and 22 z. in runs MAR (left) and MAR\_CON (right)

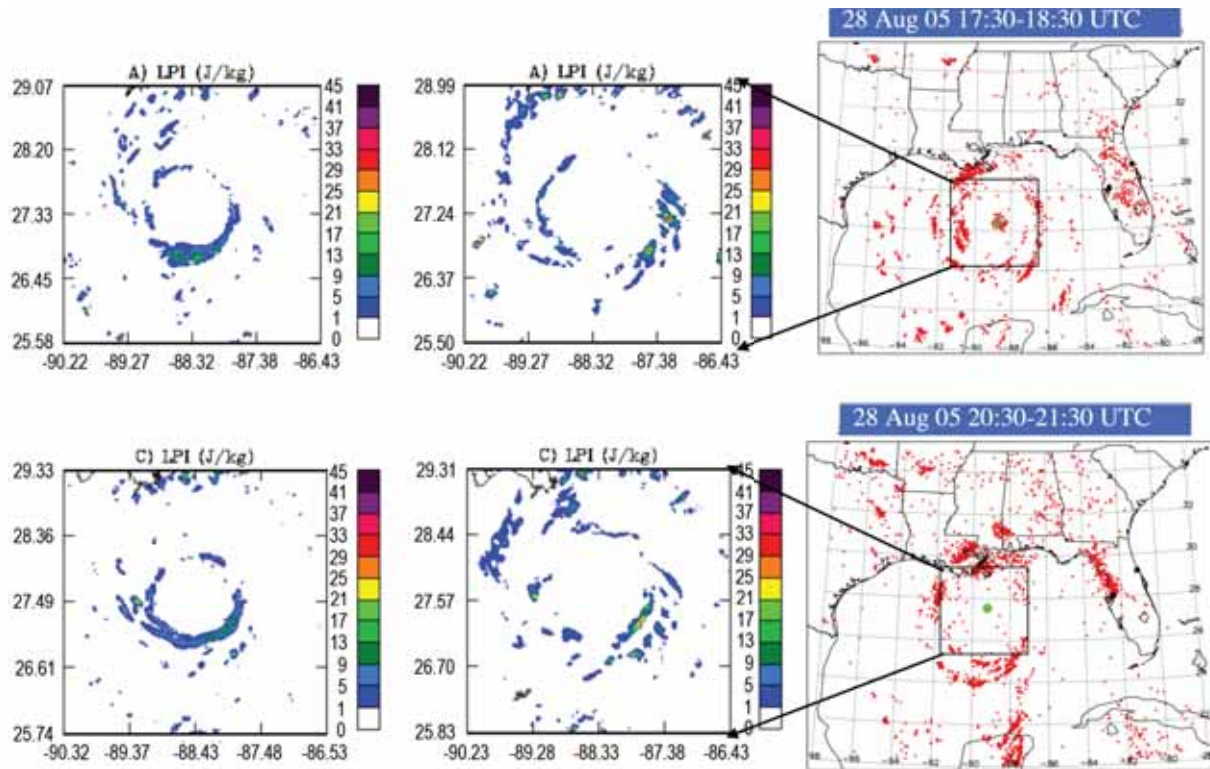


Figure 3.12 Fields of Lightning Potential Index (LPI) calculated in MAR (left) and MAR-CON (right)

Runs on 28 Aug. 20 z (top), and 22 z (bottom). The lightning in Katrina (2005) is also presented (after Shao et al. 2005). Zones of lightning are marked by red dots; the TC eye is marked green. The square shows the location of the fine grid corresponding to these time instances.

### 3.5.4 Discussion and Conclusions

For the first time, TC evolution has been calculated using explicit SBM. Simulations with resolution of 3 km were made with the WRF/SBM. The evolution of Katrina was simulated during 72 hours beginning after it had just bypassed Florida to 12 hours after landfall. In these simulations the effects of continental aerosols ingested into its circulation TC on the TC structure and intensity were investigated. It is shown that continental aerosols invigorate convection (largely at the TC periphery), which leads to TC weakening. Maximum TC weakening took place  $\sim 20$  h before landfall, when the TC intensity had reached its maximum. The minimum pressure increased by  $\sim 16$  mb, and the maximum velocity decreased by about 15 m/s. The difference in the intensities remains significant even during the TC landfall. Thus,

the results indicate that there is another (in addition to decrease in the surface fluxes) mechanism of weakening of TCs approaching the land. This mechanism is related to effects of continental aerosols ingested into the TC circulation. Note that the weakening and the inner core collapsing was simulated in spite of the fact that the SST maximum was located near the coastal line, and no TC-ocean interaction was taken into account.

Aerosols affect the intensity of deep convective clouds and foster formation of lightning in TC clouds. Penetration of aerosols into the TC periphery leads to the increase in the lightning activity at the TC periphery. Thus, intensification of lightning at the TC periphery of land falling hurricanes can serve as precursor of the TC weakening.

The application of the TC model with the spectral bin microphysics opens the way to improve

prediction of TC intensity, wind and precipitation and lightning of land-falling hurricanes.

The TC model with the spectral bin microphysics predicts the evolution of land-falling TC better than the bulk schemes. For instance, SBM predicts weakening of Katrina well before landfall, while the bulk schemes predicted TC intensification till landfall. The TC models with the SBM can be used for calibration and improvement of current TC forecasting models with bulk-parameterization of clouds. The results support the HAMP hypothesis about the possibility of weakening a TC by small soluble aerosol particle ingested to clouds at its periphery, mainly via cloud base.

### 3.6 Simulation of Aerosol Effects on TC Genesis

#### 3.6.1 Aerosol Effects on the TD Intensity

The WRF model with spectral bin microphysics was used for investigation of aerosols (including Saharan dust) in TD genesis via their effects on cloud microphysics. Simulation of TD Debbie (August 2006) was performed. The track of this TD and the geometry of the model meshes are presented in Fig. 3.13.

The depression initially moved west-northwestward to the south of the subtropical ridge. Around 1200 GMT 22 August, the center of the cyclone passed about 100 n mi to the southwest of the southernmost Cape Verde Islands, bringing thunderstorms and gusty winds to the southern islands of Fogo and Brava. The depression strengthened as it moved away from the islands, becoming a tropical storm around 0000 GMT 23 August. By 1200 GMT that day Debbie's sustained winds had reached 45 knots, and there was little or no change in strength for the next two days as the cyclone moved between west-northwest and northwest at 15-20 Knots over the open waters of the eastern Atlantic. Intensification during this period appeared to be limited by a dry and stable air mass surrounding the cyclone, along with marginal sea-surface temperatures. On 25 August, southerly shear began to increase in association with an upper-level trough, displacing the deep convection to the north of the center. Debbie started to weaken, and became a depression around 0600 UTC 26 August.

To investigate the possible aerosol effects on the microphysics and the dynamics of the TC, two simulations were carried out: a) in the first simulation  $N_o$  was set equal to  $100 \text{ cm}^{-3}$  typical of the maritime atmosphere over the whole computational area (hereafter, referred to as "MAR"); b) in the second, the initial

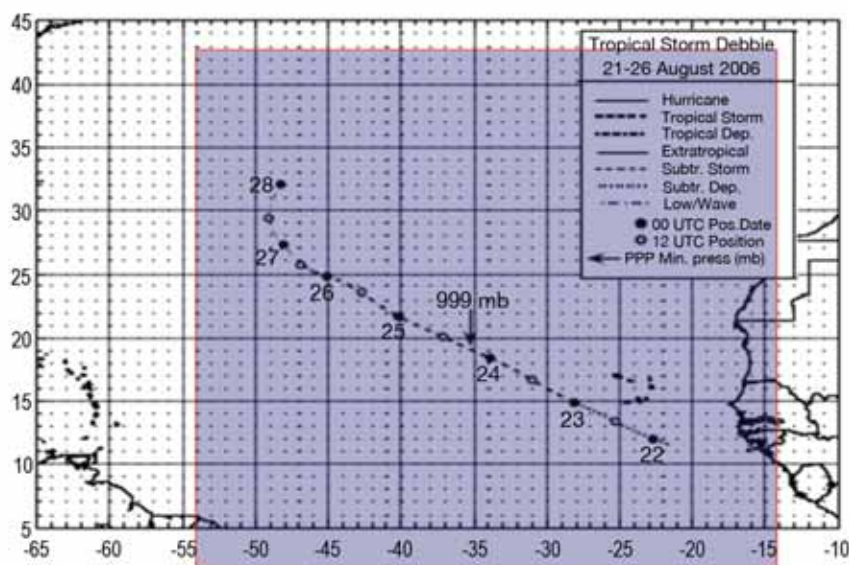


Figure 3.13 The track of TD Debbie and the geometry of the model meshes

CCN concentration over the land  $N_o$  was set equal to  $3000 \text{ cm}^{-3}$ , typical of continents under polluted conditions (in zone of Saharan dust). Initially, over the sea  $N_o$  was set equal to  $100 \text{ cm}^{-3}$  in all simulations. The second run is referred to as “MAR\_CON”.

Similar procedure was applied to simulate TD evolution using 12 bulk parameterization schemes available in WRF including the Double-Moment 6-class (WDM6) Microphysics scheme (Lim and Hong 2009).

Fig. 3.14 shows the time dependence of minimum pressure obtained in runs with 10 different bulk parameterization schemes. The observed  $P(t)$  dependence is presented as well.

One can see that both SBM simulations reproduce the observed changes in surface pressure in good agreement with observations. Toward 72 hr of simulation time, the errors in the prediction of minimum pressure and maximum velocity were very low

in both simulations when compared to the observed values. The simulation MAR-CON shows, however, better agreement with the observations, especially after 50 hours of simulation time.

One can see that the widely used bulk schemes failed to reproduce the evolution of TD Debbie. Paradoxically, the best agreement was obtained using the simplest scheme proposed by Kessler, which does not include ice microphysics at all.

In addition to runs with 10 different bulk-parameterization schemes the simulations with two-moment bulk parameterization were also performed. This scheme allows one to use design of simulations somehow similar to that of SBM (for instance, to separate simulations into that with low AP concentration, as with initially high AP concentration over the land. The comparison of time dependencies of minimum pressure for these simulations is presented in Fig. 3.15.

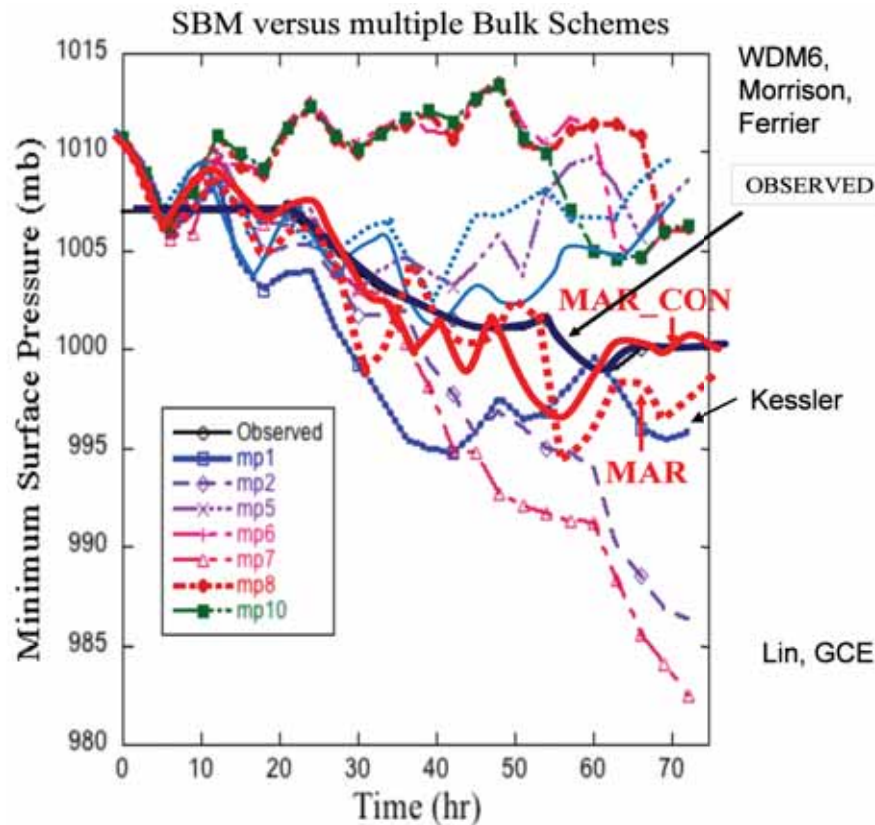


Figure 3.14 Time dependencies of minimum pressure in simulations of TD Debbie

Using 10 different bulk-parameterization schemes. Observed time dependence of the minimum pressure is also shown.

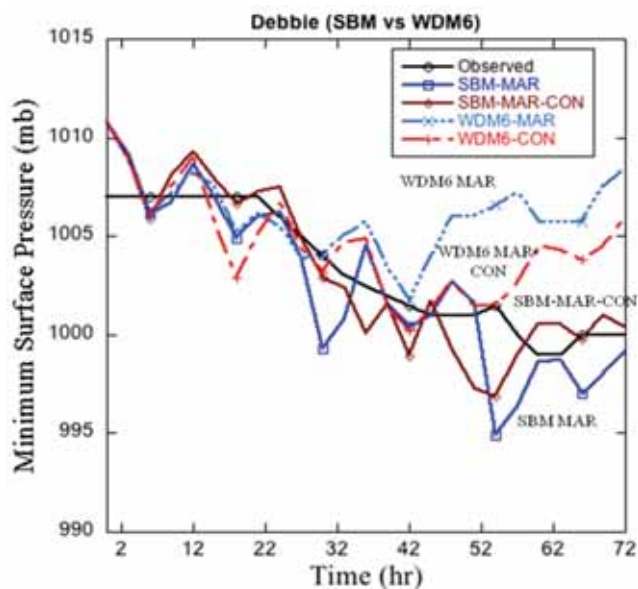


Figure 3.15 Time dependence of minimum pressure in observations and simulations

With SBM (SBM-MAR and SBM MAR\_CON) as well as in Bulk parameterization WDM6-MAR and WDM6-Mar-CON.

One can see that parameterization WDM6 predicts the evolution of Debbie better than the other bulk schemes tested (in spite of the fact that the WDM6 forecasts were not good after 42 hours). WRF\_SBM predicts the evolution of the TD much more accurately than the 2-moment 6 species bulk parameterization. TD is SBM\_MAR\_CON (where effects of dust are taken into account) TD is weaker than in case of MAR. This difference is especially pronounced when the fields of maximum velocity are analyzed (Fig. 3.16).

### 3.6.2 Simulation of Structure and Microphysics of Developing TD

Fig. 3.17 shows that droplet concentration and cloud water contents in CON\_MAR are substantially larger than in MAR in agreement with both observations and simulations of maritime clouds developing in clean and polluted air.

Fig. 3.18 shows the fields of total liquid water content (QC+QR) in the north-east –south-west vertical diagonal cross –section at  $t=72$  h in MAR

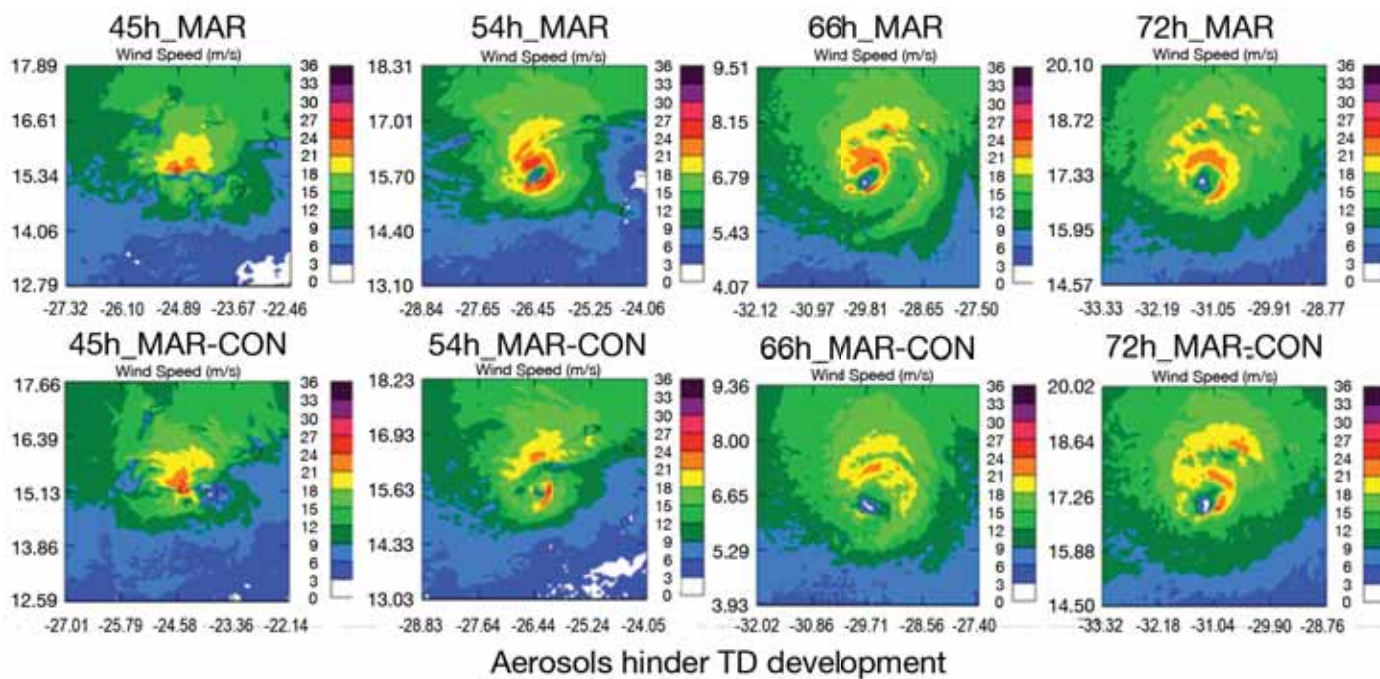


Figure 3.16 Fields of maximum winds in simulations

With low AP concentration [upper row] and in the case when effects of aerosols on cloud microphysics were taken into account [lower row].

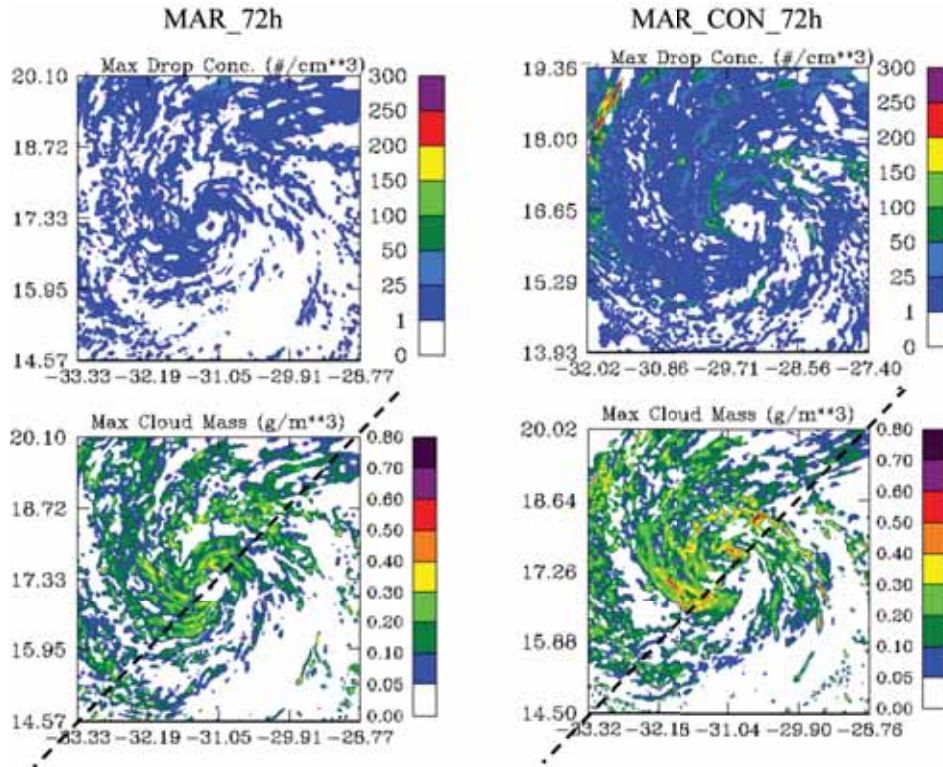


Figure 3.17 Fields of maximum values of droplet concentration and CWC in simulations MAR (a) and MAR-CON (b) at  $t=72$  h.

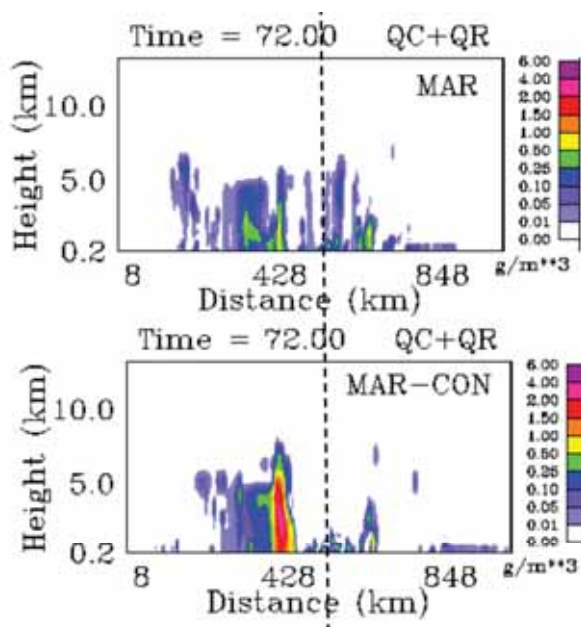


Figure 3.18 Fields of total liquid water content

(QC+QR) in the north-east-south-west vertical diagonal cross-section at  $t=72$  h in MAR (top) and MAR-CON (bottom) (the line showing the cross-section is shown in Fig. 3.17 by dashed lines).

and MAR-CON (the line showing the cross-section is shown in Fig. 3.17 by dashed lines). One can see the dramatic effect of APs on the microphysics and structure of cloudiness. Droplets in MAR-CON are smaller than in MAR and ascend to higher levels producing SC rain drops at  $\sim 5$  km. While in MAR, the spatial distribution of convection is more or less symmetric with respect to the TD center, it is highly asymmetric in MAR-CON. In MAR-CON droplets penetrate to higher levels and produce stronger SC rain that starts at height of 6-7 km.

Fig. 3.19 shows fields depicting the maximum updrafts. Prior to the penetration of aerosols into the storm, convection was concentrated in the storm central region in both simulations (not shown). Later the differences in the W fields became significant: W are lower in MAR, but elevated values are more strongly concentrated with respect to the TS center. In MAR\_CON, the vertical velocities are higher (up to 7 m/s), but zones with high updrafts are located more than 100 km from the TS center. Convection at

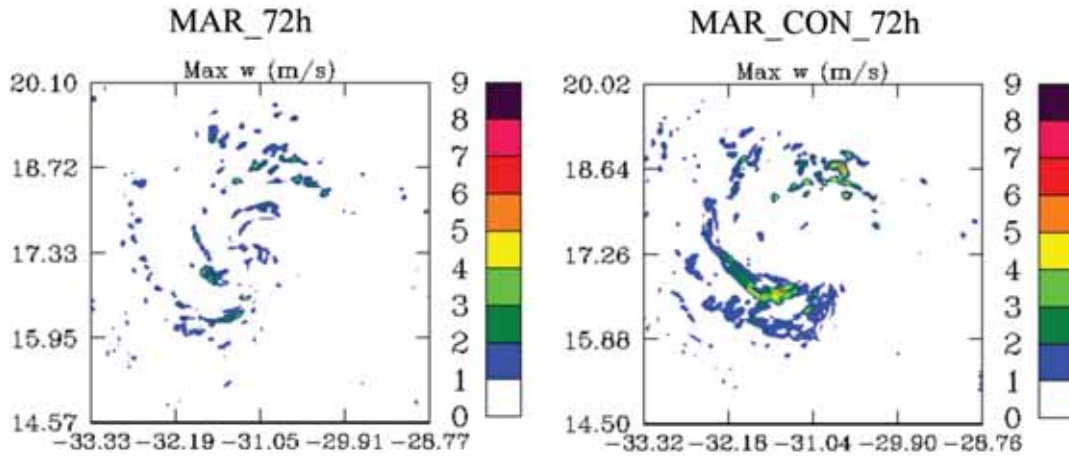


Figure 3.19 Fields depicting the maximum updrafts

In MAR (left) and MAR\_CON (right) at t=72 h.

the TC periphery is stronger in MAR-CON. A comparison of the two sets of maps reveals the aerosol-induced convection invigoration reported earlier in many observational and numerical studies (see Khain 2009 for detail) and discussed above in Sections 3.1 and 3.2.

Differences in warm microphysics and updrafts of clouds in MAR and MAR-CON lead to dramatic difference in ice microphysics. Fig. 3.20 show fields of maximum values of snow and graupel in MAR and MAR\_CON at t=72 h.

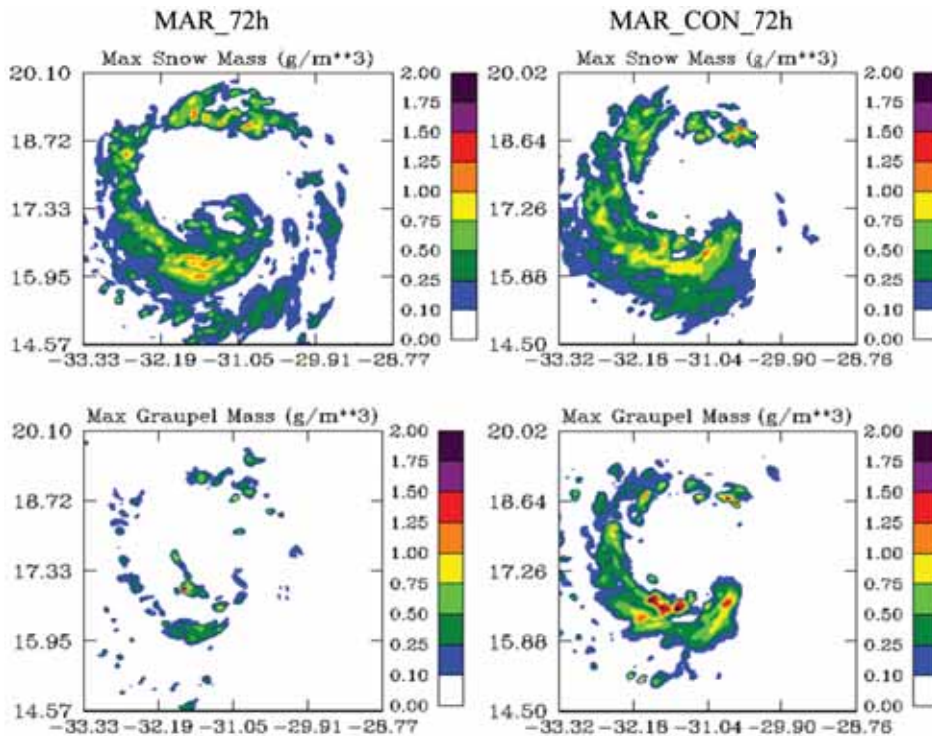


Figure 3.20 Fields of maximum values of snow and graupel In MAR (left) and MAR\_CON (right) at t=72 h.

Graupel is the dominating solid hydrometeor in MAR-CON, while snow dominates in MAR. The difference in the snow and graupel contents can be attributed to the fact that in MAR-CON SC CWC is higher than in MAR that leads to more intense riming of snow, which converts it to graupel. In the MAR experiment there is very little SC water and snow does not transfer to graupel as rapidly as in MAR-CON. The maximum graupel mass content in MAR-CON is of  $2\text{--}3\text{ gm}^{-3}$ , and snow mass content is of  $1\text{ gm}^{-3}$ . Again one can see that convection is stronger in the TS center in MAR, while it is stronger in MAR-CON at the TS periphery. Note that according to insitu observations (Zipser et al. 2009), graupel was dominating in Debbie, which corresponds well with the measurements of significant concentrations of AP in the surrounding cloud bands of this TC. As regards to rain mass content, no significant difference in area averaged values was found.

Radar reflectivity calculated in the same cross-section with the observed one (see Fig. 7 in Zipser et al. 2009) agrees well with observations: the structure of convection is substantially asymmetric with the maximum of convection within the south-east quadrant; the maximum radar reflectivity of 55-60 dBZ is reached within the layer from 3 to 5 km.

### 3.6.3 Comparison of Microphysical Structure of TD Simulated by the SBM and Bulk Parameterization Schemes

As was discussed above, none of the 10 bulk-parameterization schemes was able to reproduce the evolution of TD Debbie. Recall that all simulations were performed within the same dynamical framework and the same initial conditions. The only difference between the simulations was the utilization of different schemes to describe convection.

A more detailed comparison was performed between the results of the SBM simulations and those using a two-moment bulk-parameterization scheme WDM6 (Hong et al. 2010). This scheme is one of the most advanced bulk schemes and predicted the evolution of the TD better than most of the other bulk schemes. Aerosol are advected and scavenged in

WDM6 like in SBM. Corresponding simulations with the bulk scheme will be referred to as WDM6\_MAR and WDM6\_MAR\_CON, respectively. Fig. 3.21 shows time dependencies of maximum wind speed in Debbie, as well as in simulations using SBM and WDM6. One can see that wind speed in simulations with WDM6 rapidly reaches about 20 m/s and then remains nearly constant. Effects of aerosols as it simulated by WDM6 turns out to be opposite to that in SBM, namely, in WDM6 the increase in the aerosol concentration leads to intensification of the TD.

Figures 3.22 and 3.23 compare the fields of maximum of cloud and rainwater contents (RWC) in simulations with SBM and WDM6.

Comparison of the CWC and RWC shows substantial differences between the fields simulated by SBM and WDM6. In simulations using WDM6, the maximum values of CWC and RWC are larger than in the SBM simulations. SBM reveals higher sensitivity of microphysics to aerosols as compared to WDM6. In WDM6 maximum values of CWC are similar in clean and polluted air. This result seems to underestimate the effects of aerosols on maritime clouds. In WDM6 both the CWC and RWC fields have a spotted structure characterized by very intense clouds

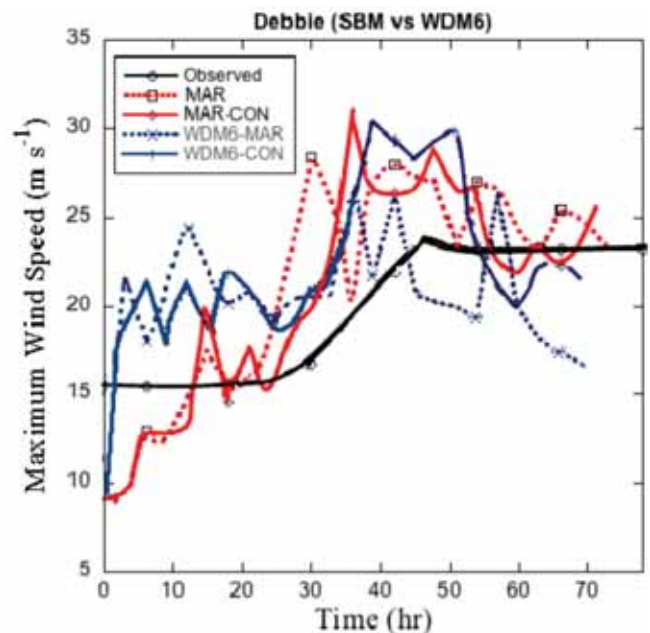


Figure 3.21 Time dependencies of maximum wind speed in Debbie Observed as well in simulations using SBM and WDM6.

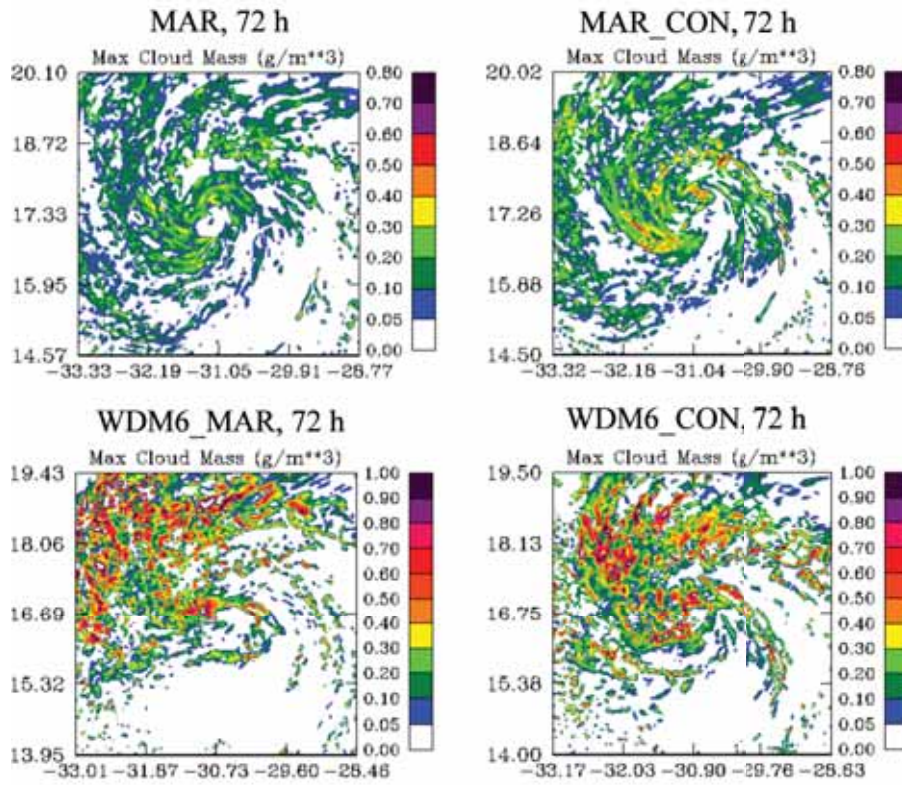


Figure 3.22 Fields of the maximum of cloud water contents in simulations with SBM and WDM6 at  $t=72$  h.

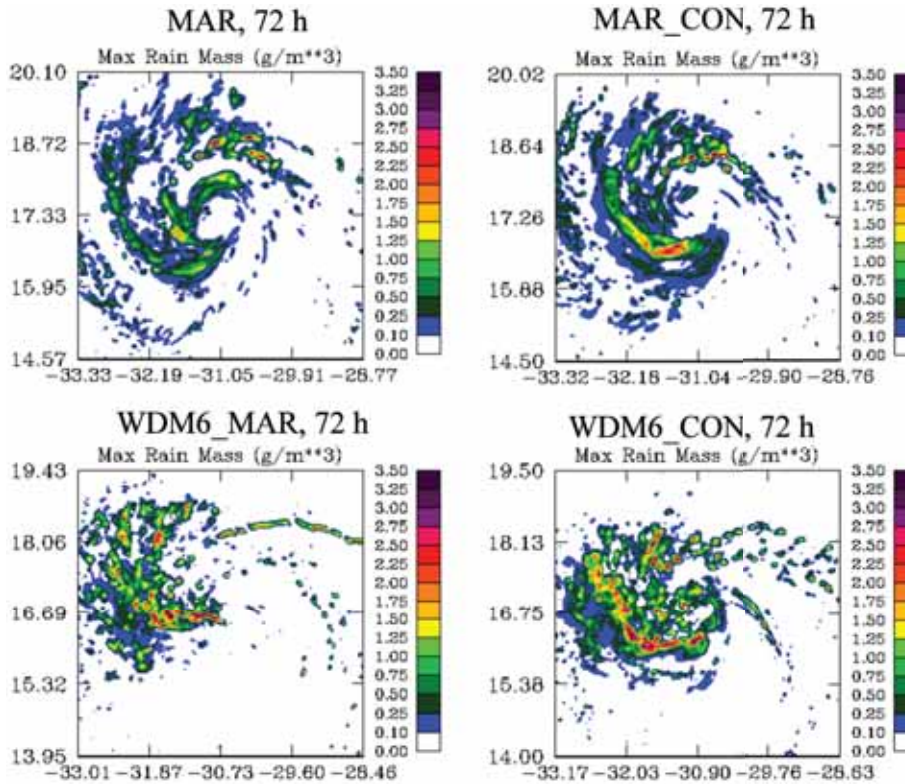


Figure 3.23 Fields of the maximum of rain water contents in simulations with SBM and WDM6 at  $t=72$  h.

with strong precipitation. In contrast the SBM simulations simulate a wide range of CWC and precipitation gradations. The underestimation of low rate precipitation and overestimation of the rate of strong convective precipitation is the typical feature of the bulk schemes. Lastly, the structure of CWC and RWC in the SBM simulations indicates the formation of a TC vortex more clearly than that simulated using WDM6. Fig. 3.24 shows fields of maximum snow and graupel contents in the WDM6 simulations.

Comparison of the microphysical fields of ice hydrometeors simulated using WDM6 with those simulated with the SBM (compare Figures 3.20 and 3.24) shows even larger differences than those found between the fields of CWC and RWC. First, the maximum values of these important ice hydrometeors in the WDM6 are substantially lower than those simulated by the SBM. Thus, the WDM6 indicates much stronger warm rain processes (larger CWC and RWC) and at the same time much weaker ice processes (lower values of snow and graupel contents) as compared to the SBM. Owing to the intense lightning observed in Debbie (that forms due to ice-graupel

collisions in the presence of SC water) the results obtained using the SBM seem to be more realistic.

In the WDM6 both graupel and snow contents are larger in the polluted case. In contrast, the SBM predicts lower snow content in the polluted atmosphere. As was discussed above, smaller amounts of snow can be attributed to more intense riming in polluted clouds containing more SC water.

An analysis of the reasons for such behavior of the WDM6 scheme is beyond the scope of the report. The purpose of this comparison was to show the substantial advantages of SBM in reproduction of microphysics and dynamics of a developing storm even in comparison with the advanced two moment bulk-parameterization schemes.

As regards other bulk-parameterizations tested, the microphysical fields produced by these schemes are quite unrealistic, so no comparison is presented here.

These results indicate that a) SBM model reproduced TC genesis (pressure and wind fields) much more precisely than the bulk schemes, b) SBM model simulates more realistic microphysical cloud struc-

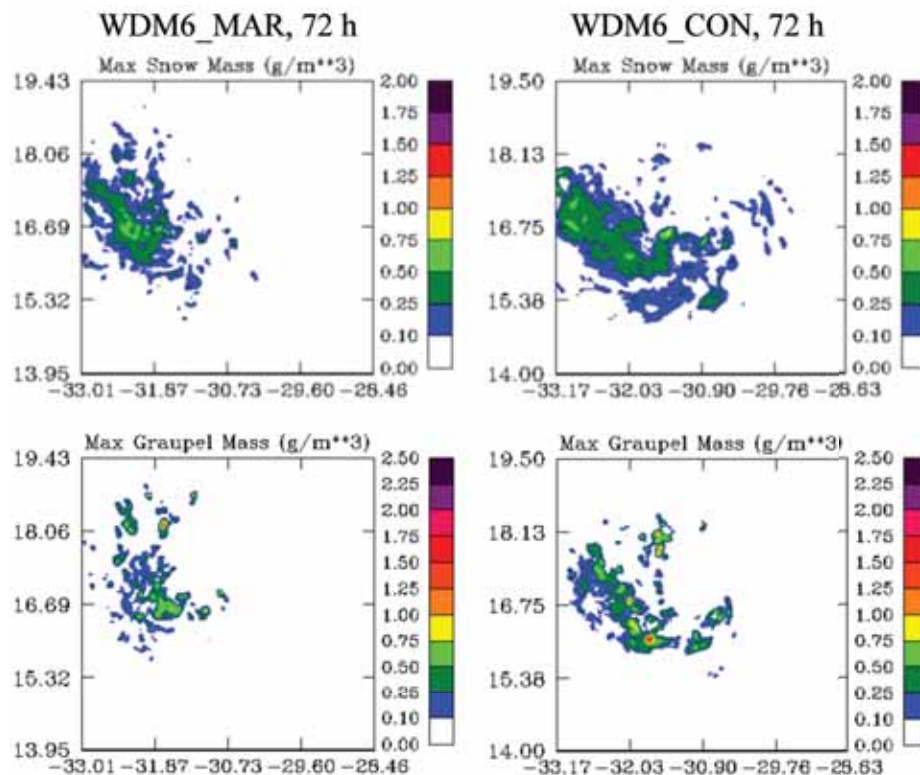


Figure 3.24 Fields of maximum snow (upper) and graupel contents (lower) in the WDM6 simulations at  $t=72$  h

ture; and c) that dust hinders TC development, invigorating convection at the TC periphery. Again, we see one of the important applications of the WRF/SBM is an improvement of TC forecasts by calibration of existent bulk-parameterization schemes.

In summary, the development of WRF model with the novel spectral bin microphysics opens the new generation of TC models with advanced microphysics that are sensitive to atmospheric aerosols.

Implementation of accurate parameterization of the BL processes including spray effects will significantly improve the description of TC-ocean interaction and calculation of surface fluxes. We believe that these two improvements, taken together, will lead to dramatic improvement of understanding of TC physics and prediction of TC intensity.

### **3.7 Conclusions and Recommendations for the Future**

During the first year, the HAMP project has taken a significant step toward creation of a new TC model with an advanced microphysics. A new microphysical scheme based on the first principles (spectral bin microphysics) has been modified and tested using insitu observations in deep convective clouds. Dramatic sensitivity of maritime convective clouds to aerosols was obtained. A good agreement of simulated size distributions and other parameters with observations justifies the ability of the microphysical scheme to simulate effects of aerosols on clouds.

The SBM has been implemented into WRF. As a result, the first TC model with spectral bin microphysics was developed. The new WRF/SBM model was used to simulate land falling hurricane Katrina and TD Debbie. It was shown that SBM reproduces the evolution of land falling TC and the TC genesis much more accurately than the existent bulk-parameterization schemes.

The high sensitivity of TC intensity to natural aerosols has been demonstrated. It was shown that increase in the AP concentration at the TC periphery leads to intensification of convection at the TC periphery and to the TC weakening. These results show that a) effects of aerosols should be taken into

account in the prediction of TC intensity, and b) the results support the HAMP hypothesis about the possibility of weakening a TC by small soluble aerosol particle ingested to clouds at its periphery, mainly via cloud base.

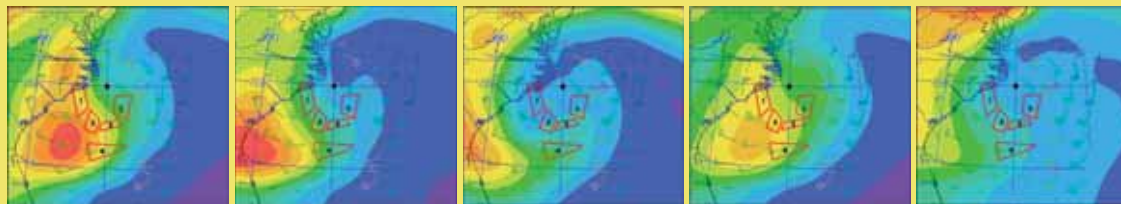
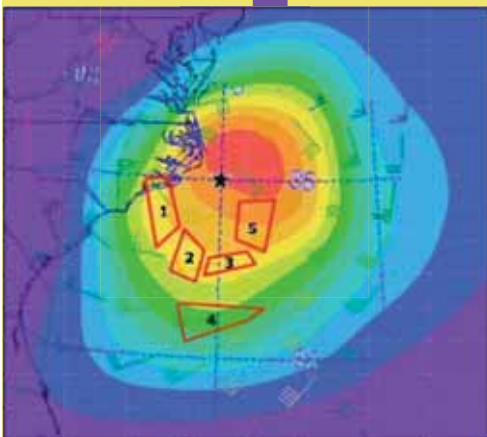
A novel model for investigation of spray effects has also been developed. It is shown that large eddies always existing in the BL dramatically affect spray transport in the BL lowering the cloud base to  $\sim 200$  m and producing precipitation from spray. These results will be used for parameterization of the spray effects in TC.

Future research based on these accomplishments should include:

1. Further development of spray model; Creation of lookup tables describing the relationship of surface fluxes and wind conditions and taking into account spray effects.
2. Further modification of the microphysical scheme; simulations of single clouds measured in situ; and detailed comparison with observations are needed.
3. Simulations of different TC using the advanced WRF/SBM model. Investigation of aerosol effects on intensity of hurricanes and on TC genesis under different environmental conditions.
4. Modification of the SBM codes (development and implementation of a new parallelization method) to significantly decrease of the computer time needed for WRF/SBM simulations.
5. Update of the model output to include different practically important quantities such as radar reflectivity, effective radii, precipitation rate, etc.
6. Simulation of ingestion of soluble by clouds at the TC periphery. Estimation of the effect of varying amounts of seed material and varying particle size on changes in storm intensity.
7. Collaboration with different TC groups and participation in calibration of bulk-parameterization schemes.



# 4



## Development and Implementation of Innovative Physics Packages for New-Generation, High-Resolution, Coupled Hurricane-Wave-Ocean Models<sup>4</sup>

### 4.1 Introduction

The new generation, high-resolution TC models are now capable of simulating the hurricane structure in great detail. Yet some critical aspects of the TC physical processes, such as cloud microphysics, BL parameterization, and the air-sea fluxes must be improved before reliable forecasts of hurricane intensity can be achieved with the help of numerical TC models. Future improvements in hurricane prediction must be based on novel theoretical concepts and high-resolution coupled atmosphere-wave-ocean numerical models tested against high-quality observations.

The main focus of our effort has been a) to implement the Hebrew University bin microphysics package into high-resolution coupled hurricane-wave-ocean models combined with b) explicit simulations of sea spray and c) new strategies for wind-wave-current interactions. The coupled models are built based on two NOAA operational TC prediction models. The first model is the GFDL/University of Rhode Island (URI) tropical prediction system that has been operational at NOAA's National Centers for Environmental Prediction (NCEP) since 1995 and at the U.S. Navy Fleet Numerical Meteorology and Oceanography Center (FNMOC) since 1996.

---

4. Principal Author: Prof. Dr. Isaac Ginis, University of Rhode Island, Rhode Island, USA; With contributions from: Dr. Biju Thomas and Dr. Yalin Fan; Graduate Student: Mr. Zhitao Yu in collaboration with Prof. Dr. Alexander Khain.

The URI group has made major contributions to the improvements of this model over the years since it became operational (Bender et al. 2007). The second coupled model is the WRF model, a non-hydrostatic mesoscale model. There are two versions of WRF available to the research community: Hurricane WRF (HWRF) developed at NCEP (Surgu 2007) and Advanced Hurricane WRF developed at NCEP (Davis and Holland 2007). Both WRF versions are designed for simulation and prediction of fine-scale atmospheric phenomena, capable of utilizing horizontal grid lengths of a few kilometers or less.

The research conducted on the implementation of bin microphysics is described in Chapter 3. Here we describe the URI group's work on the development of a new air-sea interface module and sea spray parameterization.

### 4.2 Sea State Dependence of Momentum Flux

Proper evaluation of the sea state dependence of air-sea fluxes requires modeling the wave BL (atmospheric BL that is affected by surface waves) and the equilibrium range of wave spectra. Moon et al. (2004a, b, and c) developed a coupled wave-wind model to predict the air-sea momentum fluxes over any given surface wave fields including TCs. The model is based on the NOAA WAVEWATCH III wave model, the equilibrium wave spectrum model by Hara and Belcher (2002) and the conservation of momentum and energy (Hara and Belcher 2004) by

explicitly resolving the form drag due to non-breaking waves. Their results have shown that the drag coefficient is spatially variable and is generally reduced at very high wind speeds under TCs, being consistent with recent observations. Based on the work we developed a new parameterization of the drag coefficient that depends on two parameters – wind speed and input wave age – regardless of the complexity of the wave field. Here, the input wave age is a measure of the development stage of locally wind forced waves, excluding the effects of long swell and waves that are misaligned with the local wind. The new parameterization takes into account the impact of air-flow separation due to breaking waves on the wave BL Kukulka and Hara (2008a and b). The predicted Charnock coefficient (normalized roughness length) is consistent with laboratory data and available field observations and includes both breaking and non-breaking wave effects.

### 4.3 Air-Sea Flux Budget

Traditionally, the momentum fluxes from wind to waves are assumed to be identical to the fluxes into subsurface currents due to wave breaking based on the assumption that no net momentum is gained (or lost) by surface waves. This assumption, however, is invalid when the surface wave field is not fully developed. Especially under TC conditions, the surface wave field is complex and fast varying in space and time and may significantly affect the air-sea flux budget.

We extended the wave-wind model of Moon et al. (2004a, b, c) to incorporate an air-sea flux budget model, which estimates the momentum flux into currents under growing seas and tropical cyclones (Fan et al. 2009a,b). Numerical experiments were performed to investigate the momentum flux budget across the air-sea interface under both uniform and idealized TC winds. The wave fields are simulated using the NOAA WAVEWATCH III wave model. The difference between the momentum flux from wind and the flux into currents is estimated using an air-sea momentum flux budget model. In many of our experiments the momentum flux into currents is

significantly reduced relative to the flux from wind. The spatial variation of the hurricane-induced surface waves plays an important role in reducing the momentum into subsurface currents in the rear-right quadrant of the hurricane. The percentage of this reduction depends on the choice of the drag coefficient parameterization and can be as large as 25%. For the TC cases, the reduction is mainly in the right-rear quadrant of the hurricane, and the percentage of the flux reduction is insensitive to the changes of the storm size and the asymmetry in the wind field, but varies with the TC translation speed and the storm intensity. The results of this study suggest that it is important to explicitly resolve the effect of surface waves for accurate estimations of the momentum flux into currents under TCs.

### 4.4 Wave-Current Interaction

By incorporating an ocean model with the coupled wave-wind model and the air-sea flux budget model we have developed a coupled wind-wave-ocean model, which accounts for sea state dependence, air-sea flux budget and wave-current interaction Fan et al. (2009c). Using this model, we investigated the effects of wave-current interaction on the ocean and surface gravity wave responses to hurricanes. The wave-current interaction together with the air-sea flux budget tends to reduce the momentum flux into subsurface currents. This reduction is the largest in the rear-right quadrant of the hurricane. In an idealized Category 3 tropical cyclone moving with a forward speed of  $5 \text{ m s}^{-1}$ , this reduction can be up to 14% relative to the flux from wind. The reduction in momentum flux into the ocean due to the variation of the surface gravity wave field (both in time and space) and wave-current interaction consequently reduces the magnitude of subsurface current and SST cooling to the right of the storm track and lessens mixed layer deepening in the wake of a TC.

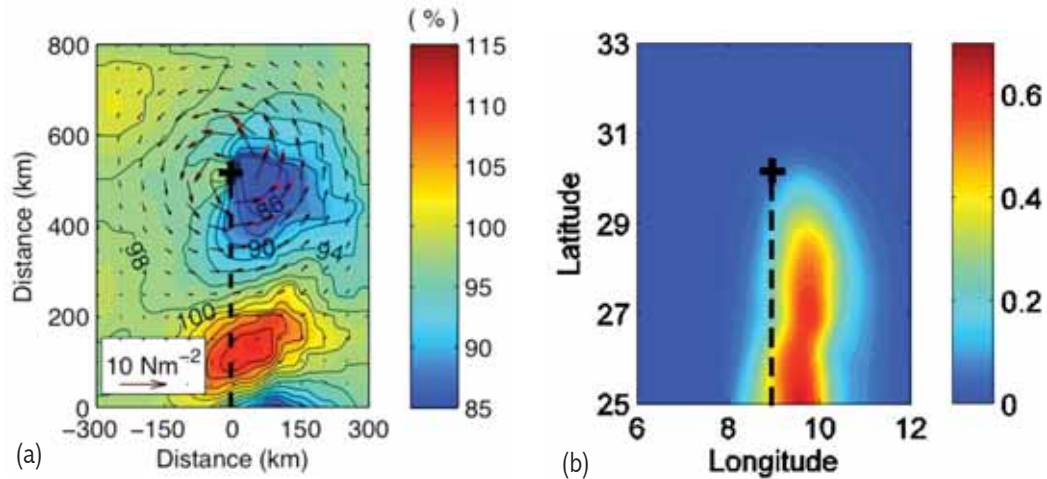


Figure 4.1 Flux and SST Adopted from Fan et al. 2009c

(a) Percentage of the magnitude of momentum flux into currents relative to the magnitude of momentum flux from air; (b) SST anomaly from the coupled wind-wave-ocean model minus SST anomaly from the ocean model without the effect of wave-current interaction.

## 4.5 Implementation of Sea Spray Parameterization into Coupled Hurricane-Wave-Ocean Models

In hurricane conditions, a large amount of sea spray is produced by bursting air bubbles in whitecaps and by tearing spume from the wave crests. Consequently, both turbulence and sea spray provide routes by which moisture, heat and momentum cross the air-sea interface. Although the question as to whether or how sea spray affects the evolution of hurricanes has been around for a long time, the answer has remained elusive. All the modeling attempts to study the impact of sea spray evaporation on hurricanes have so far relied on simplified bulk parameterizations of the spray-mediated fluxes. There are several complex and not well understood aspects of sea spray dynamics in TC conditions that cannot be investigated without realistic incorporation of full marine boundary layer (MBL)-scale physics and explicit wind-wave-current coupling. One of critical components of the parameterization of sea spray is accurate specification of the droplet source function. In all existing sea spray models the source function is related to the wind speed. In reality, sea spray is generated by wave

breaking and thus depends on the sea state. In the current NOAA/ESRL air-sea heat flux parameterization scheme (Fairall et al. 2009) sea spray generation explicitly depends on two key wave parameters, namely, the total energy dissipation rate due to surface wave breaking, and the height of the droplet sources (i.e., the height of dominant breaking wave crests). These wave parameters are uniquely related to the wind speed if wave fields are fully developed. However, with young and complex wave fields under TCs these parameters are highly variable in space and time (Fan et al. 2009). Therefore, a coupled TC-wave model is required to accurately simulate the sea spray generation and its impacts on TC forecasts.

We have developed a new approach in which the new URI air-sea interface model is used to explicitly calculate the sea state and wave breaking statistics and estimate the two key parameters for the sea spray model: the droplet source function and source height. The droplet source height is determined not from the significant wave height but from the input wave age (wave age of the wind forced part of the spectrum) and the wind stress. We have implemented the NOAA/ESRL sea spray model (Fairall et al. 2009) into the URI ASIM. The ASIM, shown in Fig. 4.2, consists of 1) the coupled wind-wave BL model of Moon

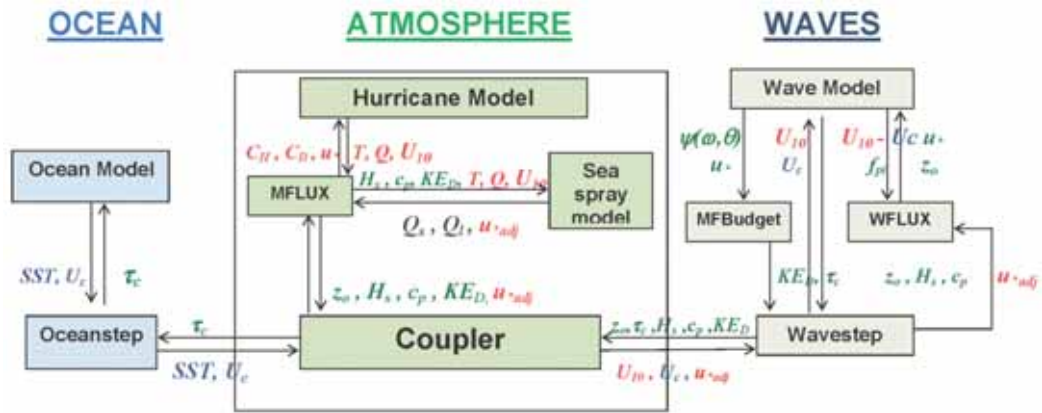


Figure 4.2 A schematic of the coupled wind-wave-current modeling system and the URI air-sea interface module (ASIM)

Represented by the following components: MFLUX, Sea spray model, MFBudget, and WFLUX. The arrows indicate the prognostic variables that are passed between the model components.

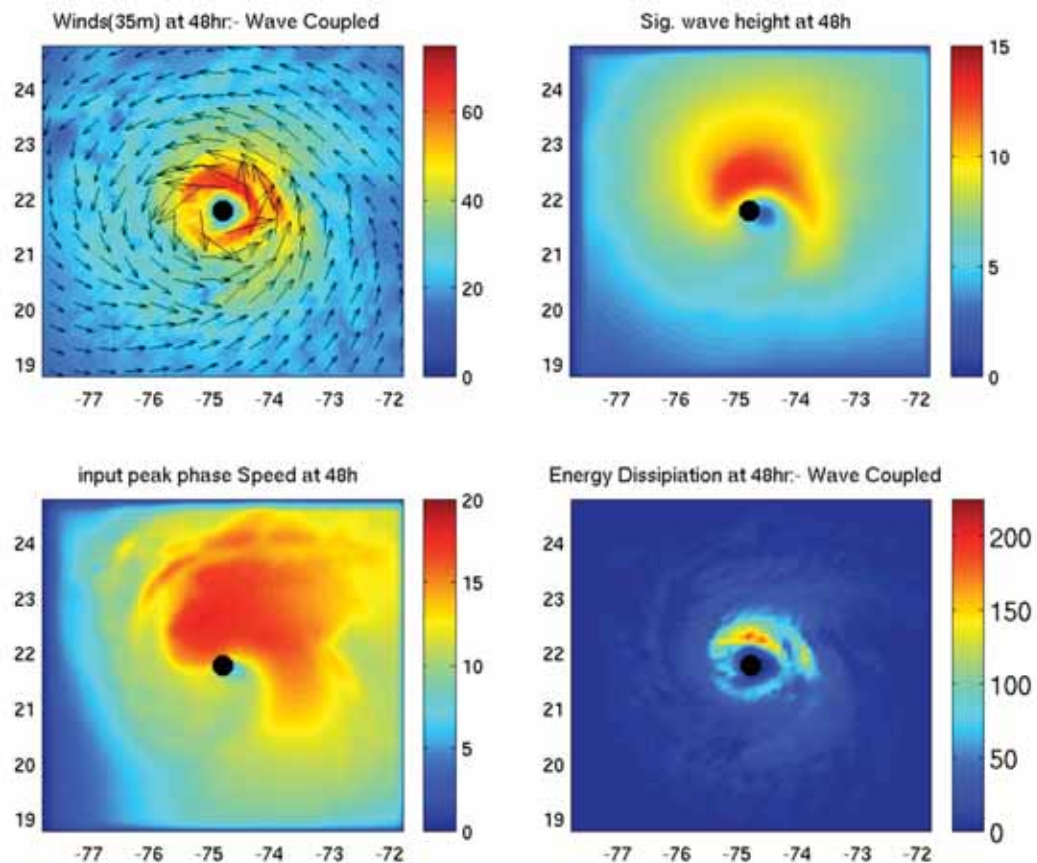


Figure 4.3 Surface wind vector, significant wave height, phase speed of dominant wind-forced waves, and wave energy dissipation

Calculated in an idealized experiment using the GFDL coupled hurricane-wave-ocean coupled model. These parameters are used as the input of the ESRL sea spray model.

et al. (2004a,b) (sub-module “MFLUX” in Fig. 1) and Fig. 2) the air-sea energy and momentum flux budget model of Fan et al. (2009, 2010) (sub-modules “MF-Budget” and “WFlux” in Fig. 1).

Our approach to the parameterization of the air-sea processes is based on the following two mechanisms associated with surface waves. The first mechanism is the modification of the turbulence field in the wave BL due to surface waves, which affects both sensible and latent heat fluxes. The second and more important mechanism is the generation of sea spray due to breaking waves. One of the novel features implemented in ASIM is the method of coupling between breaking waves and the NOAA/ESRL sea spray generation model. In the present NOAA/ESRL sea-spray model, the source function is parameterized in terms of energy lost to the wave breaking process,  $EF_c$ , which is simply related to the wind speed. The effective droplet source height  $h$  is related to the significant wave height. Within the framework of ASIM, the total energy lost to breaking ( $EF_c$ ) is accurately estimated by explicitly accounting for the sea state dependence and the air-sea flux budget (Fan et al. 2010). The source height  $h$  is determined not from the significant wave height but from the input wave age (wave age of the wind-forced part of the spectrum) and the wind stress. This modification is important under tropical cyclones because the dominant scale of breaking waves is related to the scale of the actively wind-forced waves – not related to the scale of swell generated elsewhere. Examples of the wind and wave parameters provided to the ESRL sea spray model is are shown in Fig. 4.3.

More recently, we have focused on the implementation of the improved NOAA/ESRL parameterization scheme of sea-spray mediated fluxes improved by taking into account the feedback effects on the momentum flux across the air-sea interface. The improvement was made based on an improved understanding of the dynamical aspects of the sea-spray feedback effects via the balance of turbulent kinetic energy (TKE) and enthalpy in the spray-laden surface layer and the impact of the spray-mediated thermal and momentum fluxes on the wave atmospheric BL dynamics. We are in the process of implementing

the new theoretically and experimentally derived formulation of spume droplet production and dispersion to estimate the sea spray source function and the relationship between the implied source strength and forcing parameters such as wind speed, surface turbulent stress, and wave properties. The new sea spray parameterization has been implemented into the GFDL hurricane-wave-ocean research model. Examples of the impact of sea spray on the drag coefficient are shown in Fig. 4.4.

During this project the sea spray source functions estimated by the URI ASIM model was coupled with the sea-spray dynamics model based on the bin spectral microphysics developed by Khain and his team (see their report for details). In collaboration with Khain, we reviewed available sea spray algorithms. At present, all the spray-mediated flux schemes utilize very simple diagnostic relations to provide the wave-characteristic information based on the wind information only.

Over the past few years, the feedback effects of sea spray on the mean wind, temperature and moisture profiles in the atmospheric surface BL associ-

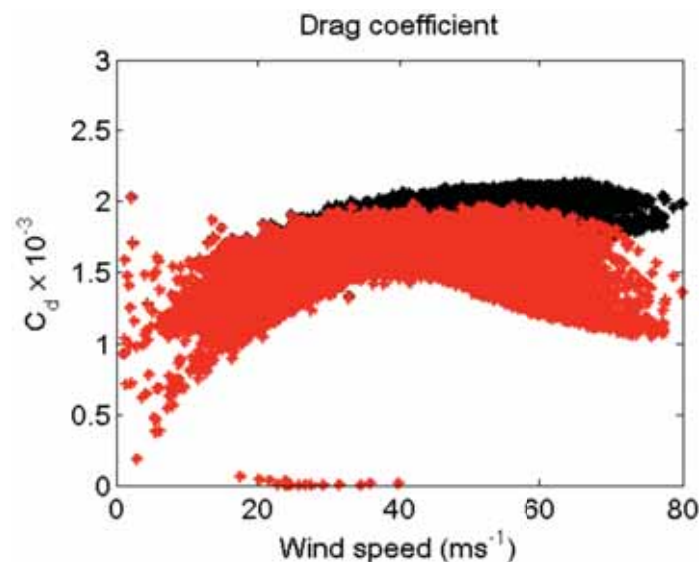


Figure 4.4 Drag coefficient vs. surface wind speed

In the GFDL coupled hurricane-wave-ocean model with (red) and without (black) sea spray parameterization.

ated with tropical cyclones have been investigated at NOAA/ESRL using a 1-D coupled sea-spray and surface BL model. This model is capable of simulating the microphysical aspects of evaporation of saline water droplets of various sizes and their dynamic and thermal interaction with the turbulence mixing that is simulated by the Mellor-Yamada 1.5-order closure scheme. After careful evaluation, we have identified some limitations in the present ESRL sea spray model and have decided to develop a new 1-D coupled sea spray and near surface model based on the spectral bin microphysics framework developed by the HUJI group and the wave coupling framework developed by the URI group.

#### **4.6 Development of a Boundary Layer Model with Explicit Resolution of Large Eddies**

A number of recent observational, numerical and theoretical papers have conclusively demonstrated that linearly organized coherent structures are prevalent in hurricane boundary layers (HBLs). The observational studies include analyses of satellite synthetic aperture radar (SAR) imagery (Katsaros et al. 2002; Zhang et al. 2008), land-based Doppler radar studies (Morrison et al. 2005; Lorsolo and Schroeder 2006; Wurman and Winslow, 1998; Wurman et al. 2006) and aircraft penetrations into the BL of hurricane Isidore (2002, Zhang et al. 2008). Numerical studies include two-scale BL models (Ginis et al. 2004) and linearized stability analyses of axisymmetric swirling BLs modeled after tropical cyclones (Nolan 2005). Theoretical studies include Nolan (2005) and Foster (2005).

These linear features are the result of embedded secondary circulations in the HBL that consists of an overturning “roll” circulation in the plane roughly perpendicular to the mean flow direction. These rolls are spatially periodic with wavelengths that range from 100’s of meters to several km. The typical vertical and cross-roll velocities are  $>\sim 3$  to  $5 \text{ m s}^{-1}$  and the along-mean-wind perturbation velocities are  $>\sim 7$  to  $10 \text{ m s}^{-1}$ .

When rolls are present, the direct transfer of momentum (and presumably heat and water vapor as well) by these structures across the HBL represents a potentially important contribution to the overall transport of momentum and enthalpy that is not currently included in hurricane models. Zhang et al. (2008) found that for cross-wind flight legs in the BL of Isidore, half of the  $\langle uw \rangle$  covariance was contained in the roll wavelength band as estimated from SAR imagery. Morrison et al. (2005) estimate that the roll contribution to the momentum flux is about a factor of two larger than what would be calculated using standard turbulence models. These estimates are supported by the theory of Foster (2005; 2006) and similar results are found in the two-scale BL model of Ginis et al. (2004).

The lack of roll-induced fluxes in existing HBL parameterizations has potentially major implications for forecasting hurricane intensity. Since hurricanes are heat engines whose fuel source is the water evaporated from the sea surface and since numerical models are very sensitive to surface flux parameterizations and secondarily to differences in existing HBL parameterizations (Braun and Tao 2002) the identification of an unparameterized mechanism that may have the potential to make first-order changes in the HBL flux parameterizations cannot be ignored in a program that is dedicated to improving intensity forecasts.

Under HAMP funding the URI research group in collaboration with Khain has developed an efficient 2-D LES model that explicitly simulates roll vortices and their interaction with the 3-D mean flow in the marine BL. This model is based on an approach that has been originally developed by Khain et al. (1986) and Ginis et al. (2004) for an atmospheric BL model in non-rotating fluid. The equation system of the model is deduced based on the results of a scale analysis allowing separation of the 3-D equation system into two coupled sub-systems: 2-D equations that resolve roll vortices explicitly (2-D LES model), imbedded into the 3-D equations of the large-scale atmospheric flow.

In the following sections we briefly describe the main results concerning the new BL model develop-

ment and investigation of the physical process controlling the formation and evolution of rolls vortices in the marine BL in high wind conditions. We will also discuss a proposed methodology for explicit representation of roll vortices in hurricane models.

#### 4.6.1 The New BL Model Development and Validation

The exact process that leads to the formation of horizontal convective rolls is not well understood, but most formation theories involve a combination of thermal (buoyancy) or convective instability and dynamic instability (inflection-point instability). The main limitation of the most previous theoretical and numerical studies is that they did not consider the interaction between the mean, large-scale flow and convective motions in the BL. Although high-resolution 3D LES models would be the best tools for studying such interaction, but they are not practical at present because of computer limitations. It is known (Emanuel, 1994) that rolls tend to be elongated along the mean wind direction within the BL. Utilization of the assumption of 2D structure of roll convection allows one to simplify the problem and dramatically decrease the computation time. Khain et al. (1986) and Khain and Ingel (1988) were first to introduce the idea of solving two coupled models: a large-scale model and a model of convective motions. Assuming the 2D roll structure within the BL, they separated the 3D equation systems typically used in LES models into two interacting subsystems describing the motions of different horizontal scales: the large scale mean flow and the convective motions. Not much research has been done under the high wind conditions resembling those of TC. Even for the weak and moderate wind conditions, the previous research mostly focused on the formation and characteristics of the roll vortices, but not on their impact on the mean flow.

Ginis et al. (2004) applied the same method as Khain et al. (1986) and successfully simulated roll vortices under different wind speeds. The model results showed that mean flow-convection interaction dramatically intensifies with increasing of wind speed

and increase the near surface wind of the background flow. They pointed out that neglecting the adequate consideration of large eddy effects might be one of the reasons for the underestimation of wind speed and surface fluxes in hurricane models.

In this study, we apply the modeling approach introduced by Khain et al. (1986) and Ginis et al. (2004). A new feature introduced in this study, is the inclusion of Coriolis effects that takes into account the influence of Earth rotation on the background wind. It is known (Emanuel 1994) that direct effect of the Coriolis force on cellular convection in the atmosphere is negligible because of the small scales of convective motions. However, this study focuses on the effect of the Coriolis force on convection through the background flow. The Coriolis force changes the background flow velocity components that may affect the roll structure. Details of the model equations are presented in Yu et al. (2010a).

The BL model was validated through simulations of the classical Rayleigh-Benard convection (Rayleigh 1916) between two horizontal plates, which have constant temperatures; warmer below and cooler above. Previous study revealed that a critical unstable temperature gradient has to be exceeded before the convection begins and fully grows to a stationary state (Emanuel 1994). The dimensionless parameter that determines the stability of the fluid between two parallel plates is the Rayleigh number,

$$Ra = -\frac{g}{\theta_0} \frac{\partial \bar{\theta}}{\partial z} \frac{h^4}{\nu k}, \quad (1)$$

where  $\theta_0$  is the reference potential temperature,  $h$  is the height between the two horizontal plates,  $k$  is the momentum viscosity, and  $\nu$  is the thermal viscosity. The Rayleigh number represents the amount of potential energy being applied to the fluid. The ratio of viscosity and thermal diffusivity is defined as Prandtl number,  $Pr = k/\nu$ . Clearly, the Prandtl number is a function of the characteristics of the fluid only. Previous laboratory experiments show that Benard convection is a steady 2D flow with Rayleigh number range between the critical Rayleigh number and 13 times the critical Rayleigh number (Krishnamurti 1970).

Previous theoretical studies show that the critical Rayleigh number for both freeslip boundary conditions at the top and bottom boundary is 657.5, and the aspect ratio associated with this critical Rayleigh number is 2.84 (Rayleigh 1916, Emanuel 1994). We first use this critical Rayleigh number in our model experiment. It takes more than 1000 hours for the model to reach to a steady state. At the steady state, the aspect ratio is 2.91, which is very close to the theoretical number. The vertical velocity is very weak (in the order of  $\mu\text{m/s}$ ) and the mean temperature profile has not changed in this case. When the Rayleigh number is slightly increased to 700, the aspect ratio is still 2.91 at steady state but the maximum vertical velocity is increased to about 2.5 cm/s (Fig. 4.5). These model results have validated that the critical Rayleigh number is around 657.5.

The model was run with different Rayleigh numbers varied from 1.5 to 7 times the critical Rayleigh number as shown in Fig. 4.6. The mean potential temperature profiles at the steady state for all these runs compare very well with Kuo (1961). We can see that the initial linear potential tempera-

ture profile has a S-shape at the steady state, forming two BLs near the top and bottom with a much higher potential temperature gradient than the initial profile. The potential temperature profile in the interior has less, no, or even reversed temperature gradient.

#### 4.6.2 Comparison with 3D Large Eddy Simulation (LES) Model

Glendening (1996, 2000) used a Large Eddy Simulation (LES) model to investigate the lineal structures generated by roll vortices for dry convection (with no clouds). To compare the performances of the 2D and 3D LES models, we ran the 2D BL model using the same initial BL conditions as in Glendening's (1996), in particular, the mean potential temperature profiles, mean velocity profiles, and the total (roll-induced + sub-grid scale turbulence) momentum flux profiles.

The 2D model had the same grid resolution, vertical domain size, geostrophic wind (15 m/s), and 10 K/km strong inversion layer above the BL as the LES model in Glendening (1996).

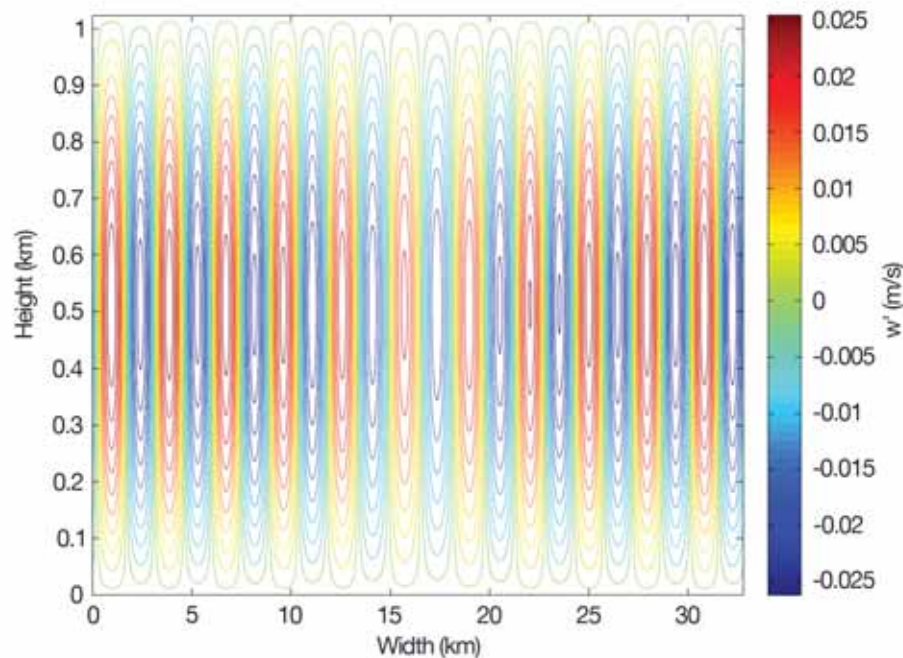


Figure 4.5 Contour plot of vertical velocity

At the final steady state for Rayleigh-Benard convection with  $Ra=700$ .

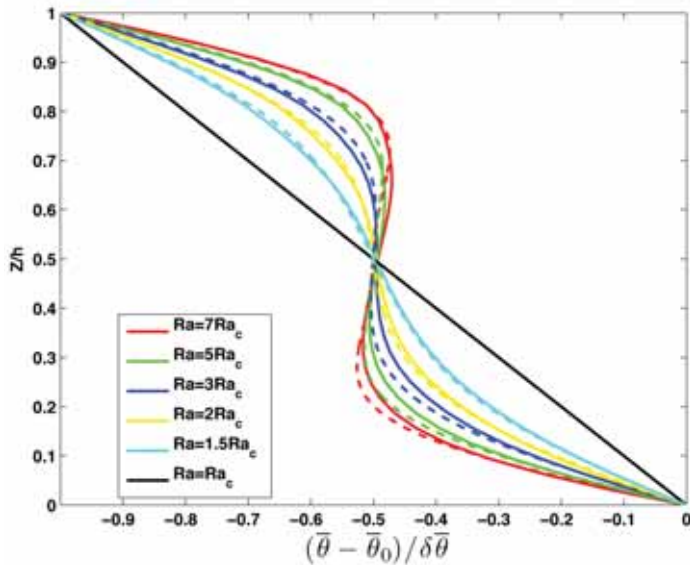


Figure 4.6 Mean potential temperature profile

At steady state with different Rayleigh numbers. Solid lines represent model simulations and dashed lines represent the theory (Kuo 1961). Dashed lines were digitized from Kuo (1961).

We found that the differences in the calculated surface momentum, sensible, and latent heat fluxes between the 2D model and the 3D LES are less than 10%. The angle between the mean BL wind and the geostrophic wind in the 2D model varies between 9 and 16 degrees, which agrees well with Glendening (1996) results. The mean profiles generated by the 2D model show typical strongly mixed BL characteristics (Fig. 4.7). Both temperature and humidity profiles [Fig. 4.7(a)] are well mixed within the BL. The along-roll mean velocity [Fig. 4.7(b)] is well mixed over most of the BL with strong velocity shear close to the bottom and top of the BL. These mean profiles are very similar to Glendening (1996) results (dashed lines in Fig. 4.7).

The total along-roll momentum flux

$$\left( \overline{w'v'} - \kappa \frac{\partial \bar{v}}{\partial z} \right)$$

profile is quasi-linear in the BL and the total

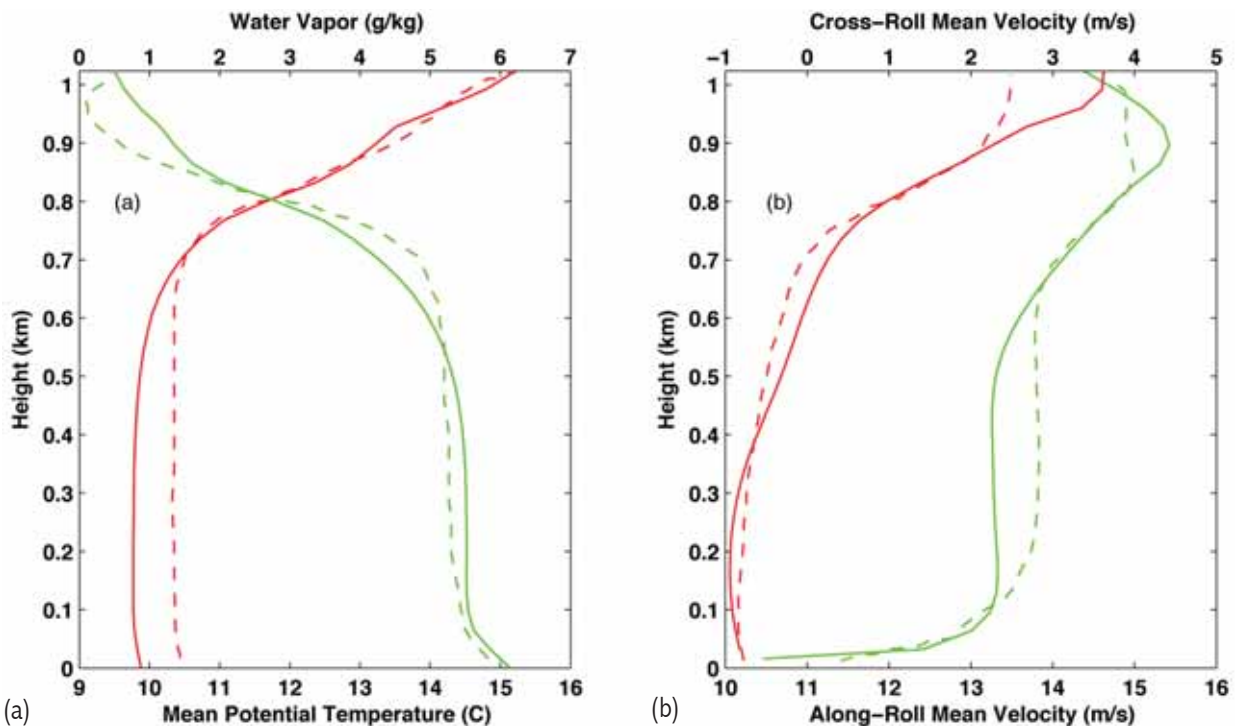


Figure 4.7 Mean profile comparison of potential temperature, vapor mixing ratio, and along-roll velocity, and cross-roll velocity

(a) potential temperature (red) and vapor mixing ratio (green), and (b) along-roll velocity (green) and cross-roll velocity (red) between 2D model results (solid) and LES results (dashed) at boundary layer depth of 720 m with roll vortices. Dashed lines were digitized from Glendening (1996).

cross-roll momentum flux

$$\left( \overline{w'u'} - \kappa \frac{\partial \bar{u}}{\partial z} \right)$$

profile is relatively small, positive near the surface and then changes to a negative value (Fig. 4.8). This also agrees well with the LES model results (Glendening 1996).

We can conclude the 2D model is capable of simulating the main characteristics of the temperature, velocity and momentum fluxes induced by BL roll vortices.

#### 4.6.3 The Effect of Coriolis Force on Marine Boundary Layer Roll Vortices

Numerical simulations were conducted to investigate the effect of the Coriolis force on BL roll vortices. The model was run with and without the Coriolis force while keeping all other conditions the same. The initial temperature profile was set to be 295 K below 320 m and then linearly increased towards the top boundary with a 10 K/km vertical gradient. The air-sea temperature difference was held constant as -1.5 K for both cases. In both simulations, the pres-

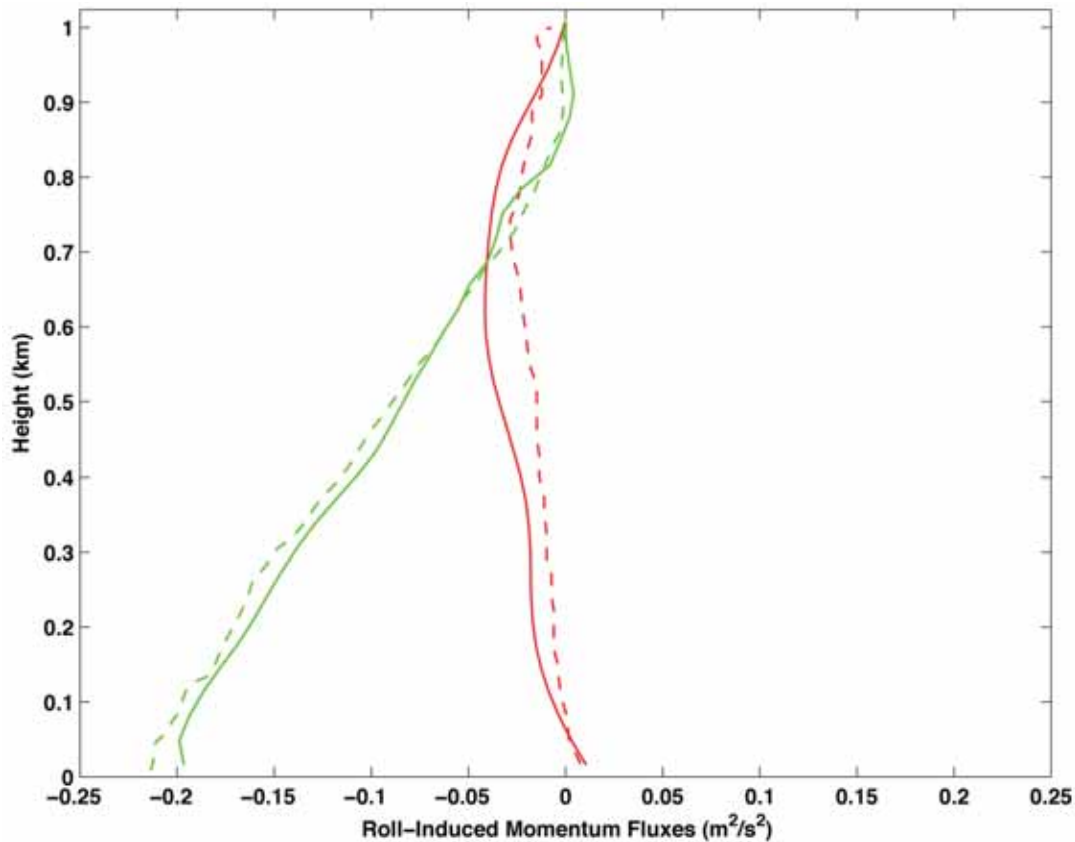


Figure 4.8 Total momentum flux profiles comparison

Between 2D model (solid lines) and LES (Glendening 1996) results (dashed lines). Green lines show the total along-roll momentum flux

$\left( \overline{w'v'} - \kappa \frac{\partial \bar{v}}{\partial z} \right)$  and red lines show the total cross-roll momentum fluxes

$\left( \overline{w'u'} - \kappa \frac{\partial \bar{u}}{\partial z} \right)$ . Dashed lines were digitized from Glendening (1996).

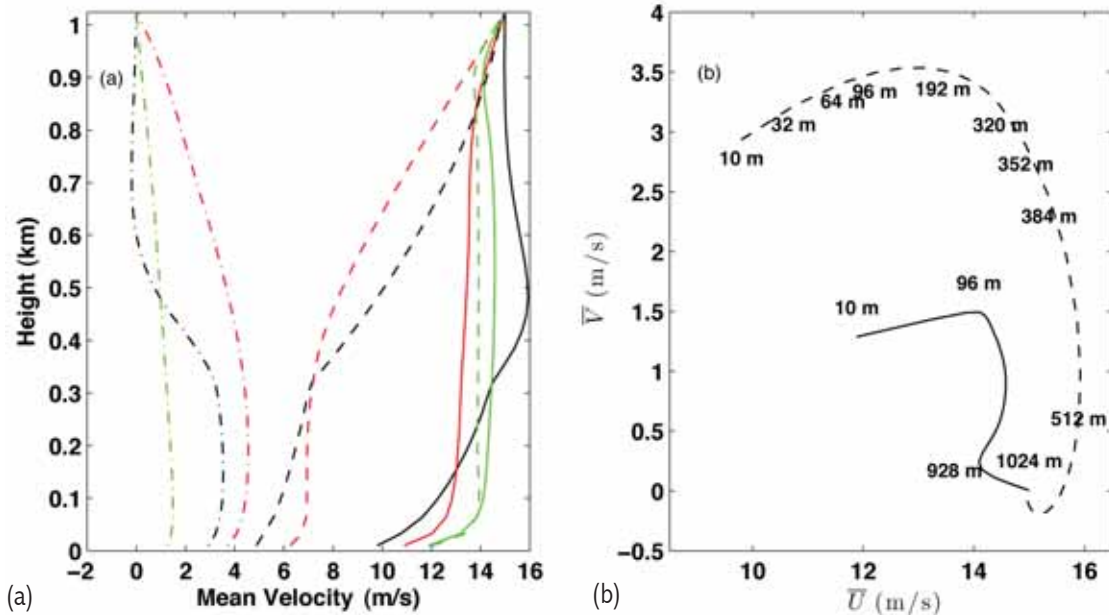


Figure 4.9 Mean velocity profiles

(a) with (solid and dash-dotted lines) and without (dashed lines) Coriolis force. With Coriolis force, solid lines show mean velocity component along geostrophic wind direction and dash-dotted lines show mean velocity component perpendicular to geostrophic wind direction. Black lines show mean velocity at the quasi-steady state without rolls; red lines show mean velocity at 18 hours after turning on convective motion; and green lines show mean velocity at the quasi-steady state with simulation of rolls. (b) Ekman spiral at the quasi-steady state without rolls (dashed) and with rolls (solid).

sure gradient at the top boundary was set to generate a mean wind geostrophic velocity of 15 m/s.

With the Coriolis force, the wind forms an Ekman spiral in the BL [dashed line in Fig. 4.9(b)]. The dynamic balance in this case is between the pressure gradient force, friction, and Coriolis force. Far away from the surface, the geostrophic wind is perpendicular to the pressure gradient. The wind rotates to the left from top to the bottom due to the bottom friction [Fig. 4.9(b)]. The surface wind forms an angle of about 13 degrees to the left of the geostrophic wind. This angle differs from the classical Ekman solution of 45 degrees because of different boundary conditions at the surface (Monin-Obukhov similarity theory) and variable turbulent viscosity. We found that the surface wind is much stronger with the Coriolis force (10 m/s) than without it (5 m/s) [Fig. 4.9(a)].

At  $T = 5$  hours after convection is switched on, roll vortices extend to about 400 meters in the case without Coriolis force [Fig. 4.10(a)], while they occupy the entire vertical domain in the case with Coriolis

force [Fig. 4.10(b)]. The magnitudes of the maximum vertical velocity of roll vortices in the case with Coriolis force are larger than that in the case without Coriolis force. At the quasi-steady state (Fig. 4.11), there are less numbers of roll vortices than at the earlier stage and the rolls are stronger in magnitude and taller in vertical. In both cases, the rolls occupy the whole vertical domain and have symmetrical updraft/downdraft pairs. While the magnitudes of the vertical velocity maxima in both cases are about the same, the rolls aspect ratio in the case with Coriolis force (6.4) is significantly larger than in the case without Coriolis force (2.7). This finding implies that the Coriolis force is one of the important factors that affect the aspect ratio of roll vortices in the BL. Further analysis shows that Coriolis force increases the aspect ratio of rolls through the internal gravity waves in the stable inversion layer. We will discuss the interaction between internal gravity waves and BL roll vortices in the following section.

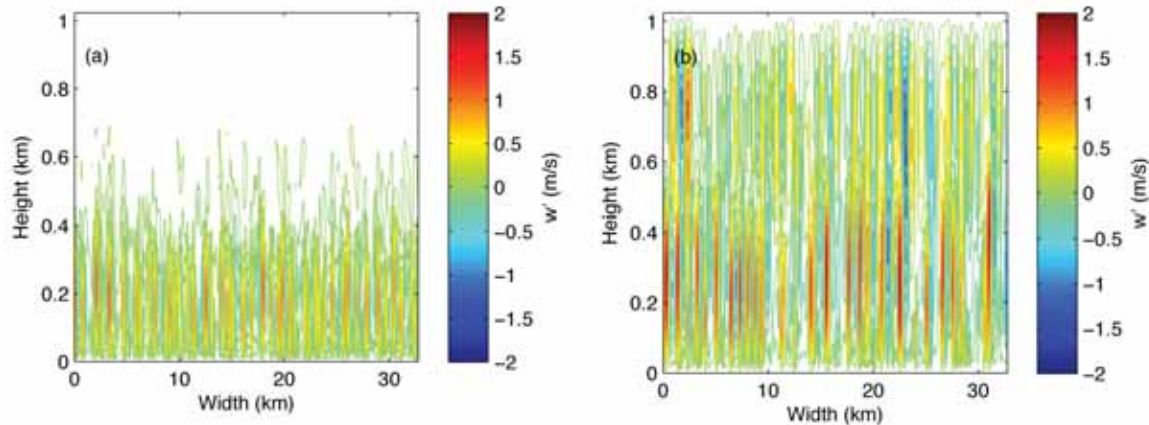


Figure 4.10 Vertical velocity at 5 hours after turning on convection for the experiments Without (a) and with Coriolis force (b).

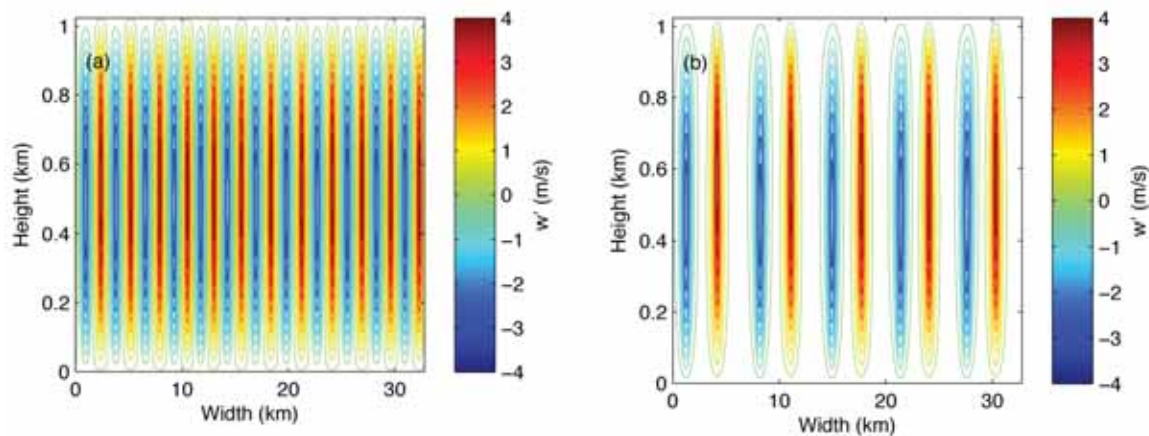


Figure 4.11 Vertical velocity at a quasi-steady state for the experiments Without (a) and with Coriolis force (b).

#### 4.6.4 Interaction of the BL Roll Vortices and Internal Gravity Waves

The classical Rayleigh convection theory that considers a thin layer of liquid between two solid plates heated from below predicts the aspect ratio of the convective cells typically smaller than those observed in nature. Several mechanisms were proposed to explain such discrepancy: anisotropy of turbulence in the horizontal and vertical directions (Priestley 1962; Sheu et al. 1980; Ray 1986), non-linear interaction between roll vortices (Rothermel and Agee 1986), and the formation of elevated heat sources

during cloud formation (Khain 1976a, 1976b, 1976c; Ivanov and Khain 1976).

With the existence of a stable inversion layer above the convective BL, convection penetrates and overshoots a short distance upward from the top of the convective BL to the stable region and then sinks back to the convective layer (Stull 1976) to trigger internal gravity waves. Internal gravity waves can interact with the convection within the BL, affecting the parameters of convective cells. In many previous numerical studies, simulations of roll vortices were conducted using computational areas with the vertical extent of  $\sim 1$  km or smaller and the upper model boundaries often associated with the base of the

inversion layer. They, thus, neglected the interaction between BL roll vortices and internal gravity waves. The effect of this interaction on the mean flow and surface fluxes remains unknown, especially under strong wind condition resembling those of tropical cyclones.

In this study we extended the vertical domain in our 2D model to 3 km to allow the interaction between roll vortices and internal gravity waves. In our approach we assume that the roll vortices are elongated along the vertical-averaged mean flow direction in the convective BL. Due to the wind rotation induced by the Coriolis force internal gravity waves in the stable inversion layer can be triggered by convection in the cross-roll direction. For this study, the model

was configured to simulate the BL roll vortices and the internal gravity waves excited by BL roll vortices under strong wind conditions ( $U_g = 45 \text{ m/s}$ ).

We conducted two experiments, C1 and C2 that had the same initial and boundary conditions and were run to a quasi-steady state. The difference between the two experiments is that the mean cross-roll advection terms from convective equations were set to zero in experiment C2. The removal of the mean cross-roll advection terms from convective equations disables the generation of internal gravity waves. The formations of roll vortices and internal gravity waves in these experiments are illustrated in Fig. 4.12. The internal gravity waves in experiment C1 are initially triggered by BL roll vortices. The

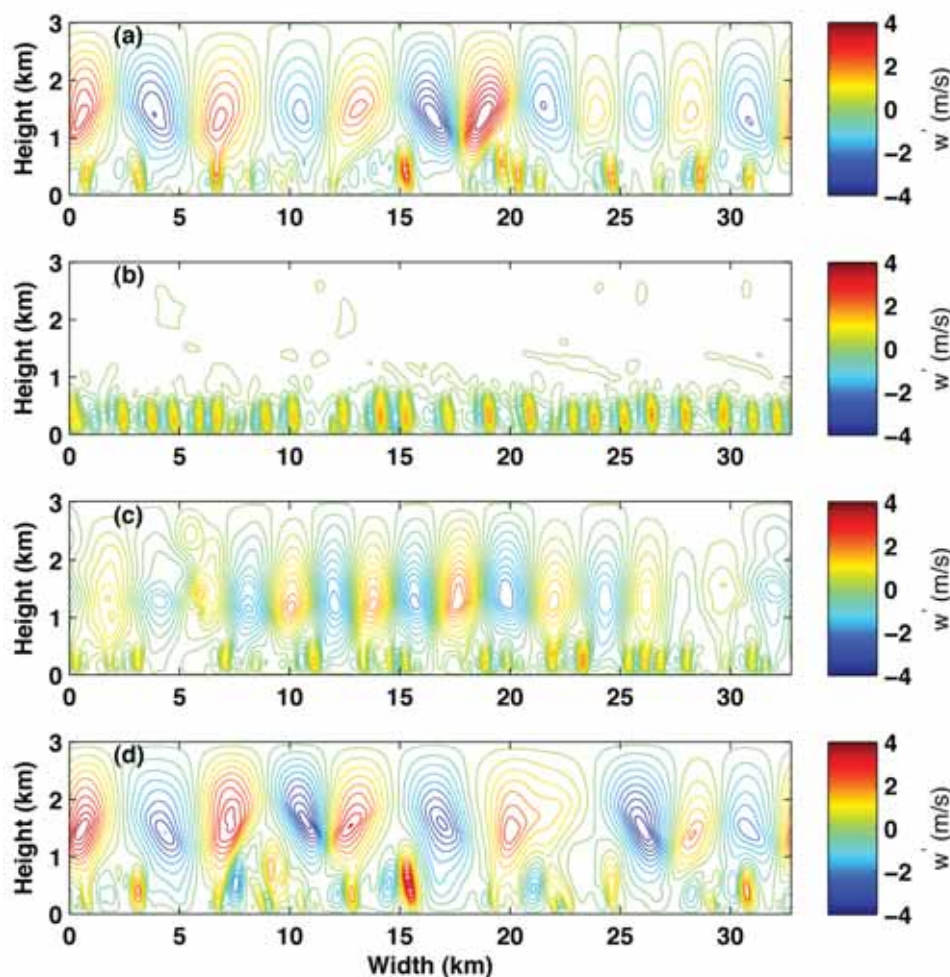


Figure 4.12 Contour plots of vertical convective velocity from experiment C1

(a) experiment C2, (b) experiment S1, (c) and experiment S2, (d) at  $T = 10 \text{ hr}$

subsequent interaction between the gravity waves and rolls leads to an increase of roll's aspect ratio compared to experiment C2. Another important finding is that the interaction between internal gravity waves and roll vortices tends to decrease the roll-induced momentum and heat fluxes in the convective BL (not shown). This implies that the internal gravity waves weaken the roll-induced mixing in the BL.

Additional experiments, S1 and S2, were designed to investigate the impact of the temperature slope in the stable inversion layer on the internal gravity waves characteristics. Experiment S1 (S2) has a more (less) stable inversion layer than that in experiment C1. Fig. 4.12 shows that the characteristics of internal gravity waves and BL roll vortices are modulated by the temperature profile in the stable inversion layer. This implies that the interaction between internal gravity waves and roll vortices must be taken into account for proper simulations of convective motions in the BL.

The current study was designed to simulate 'dry' convection; there was no latent heat release in the model. We assumed relatively low humidity for which the water vapor mixing ratio never reaches the saturation level. Effects of latent heat release on the structure of the waves and rolls in the BL are discussed in the following section.

#### *4.6.5 Effect of BL Convection with Latent Heat Release on Large Scale Mean Flow*

Ginis et al. (2004) focused on the effect of moist convection (with cloud condensation process) on the mean flow under strong winds from typical tropical cyclones. They showed that presence of roll vortices causes an increase of the surface mean wind and latent heat fluxes. However, Ginis et al. (2004) did not include the effect of Coriolis force. This study focuses on the impact of dry and moist convection on the mean flow and surface fluxes under strong wind (45 m/s geostrophic wind) conditions. Two numerical experiments were conducted; S1 is a 'dry' case without cloud condensation process and experiment S2 is a 'moist' case with cloud condensation.

The vertical velocity, liquid water content, perturbations in potential temperature and water vapor mixing ratio in experiment S2 at  $T=2.5$  and  $T=4.0$  hrs are shown in Figures 4.13 and 4.14.

Around  $T = 2.5$  hours, three relatively weak and small clouds disappear and five large and strong clouds develop due to cloud interaction [Fig. 4.13(c)]. The maximum liquid water content is around 2 g/kg and the cloud top reaches to  $Z = 2$  km. The black lines in Figures 4.13(b), 4.13(d), and 4.13(e) show the location of clouds, defined by the contours lines of 0.01 g/kg of the liquid water content. Convective motions generated by clouds are strong enough to skew the shapes of gravity waves [Fig. 4.13(b)] at this time.

At  $T = 4$  hours, there are three large clouds with maximum liquid water content around 3 g/kg [Fig. 4.14(c)]. The height of cloud top of the largest cloud is 2.6 km. The maximum vertical velocity in the largest cloud is 3 m/s with updraft in the center and downdraft along the two edges from the cloud top. The internal gravity waves are greatly damped by cloud-induced convective motions [Fig. 4.14(b)].

Figures 4.13 and 4.14 illustrate very interesting interactions between the clouds, roll vortices, and internal gravity waves. The BL roll vortices supply the clouds with moisture within the updrafts on the upwind side of the clouds. In the presence of strong internal gravity waves, distance between clouds is determined by the wave's wavelengths. The updrafts (downdrafts) of gravity waves always occur on the upwind (downwind) sides of the clouds. The positive (negative) temperature perturbations near the cloud bases (top) are due to cloud condensation (evaporation) [Figures 4.13(d) and 4.14(d)].

The dominant effect of cloud condensation and associated moist convection is the suppression of the internal gravity waves in the inversion layer. As a result, the height of the mixed layer increases along with the rising clouds. In the current study we simulated non-precipitating clouds. The effect of cloud precipitation on the mean flow and BL structures will be studied in the future.

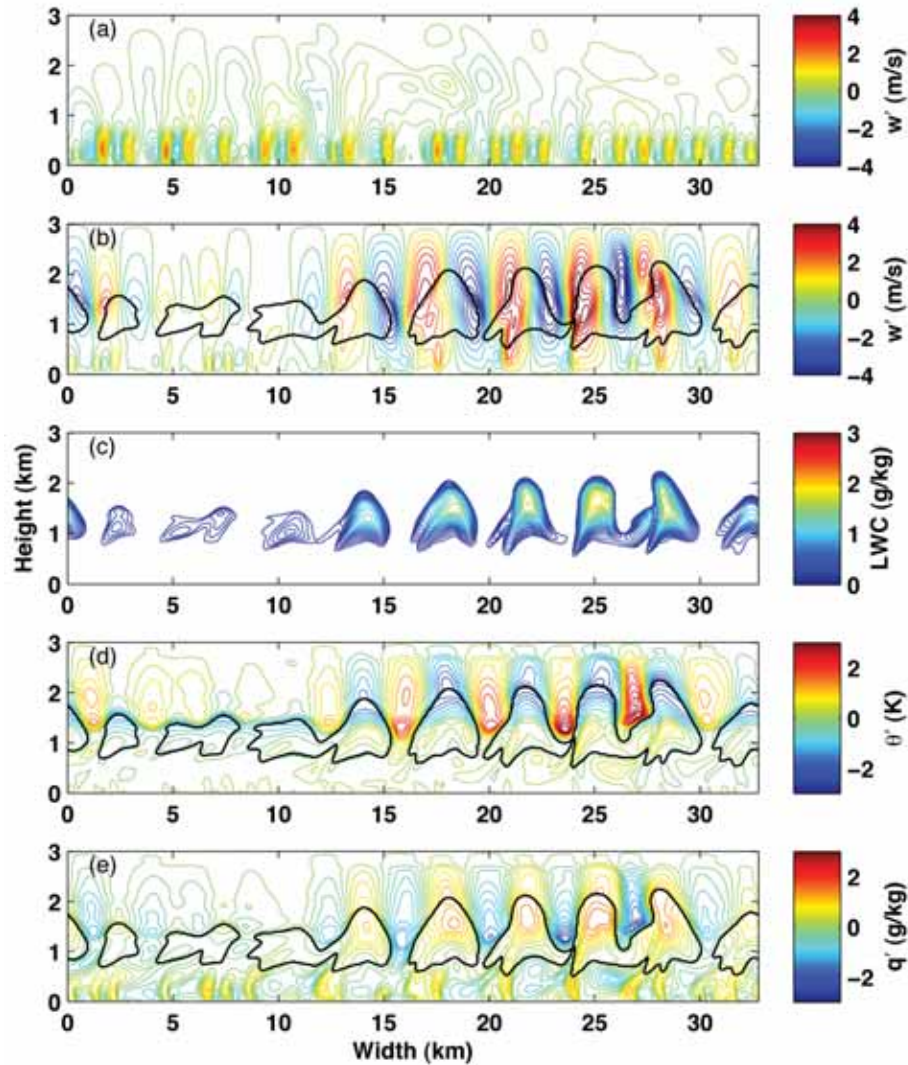


Figure 4.13 Experiment S2 T=2.5 hours

(a) Vertical velocity structure at  $T = 2.5$  hours in experiment S2; (b) vertical velocity; (c) liquid water content; (d) perturbations of potential temperature; and (e) water vapor mixing ratio at  $T = 2.5$  hours in experiment S2. The black solid lines in (b), (d), and (e) show cloud locations identified as 0.01 g/kg of liquid water content.

## 4.7 Proposed Methodology to Explicitly Represent Roll Vortices and Sea Spray Dynamics

Our proposed approach to parameterization of roll vortices in a TC model resembles a recently emerging approach of “super-parameterization” of the cloud physics processes in general circulation models (Grabowski 2001; Randall et al. 2003). Super-

parameterization consists of a cloud resolving 2-D model embedded into a general circulation model, allowing explicit cloud simulations. This approach is ideally suited for parallel computers and can operate with one to two orders of magnitude fewer computations than a 3-D cloud-resolving large-scale model. Similarly, our proposed methodology can be called super-parameterization of the MBL that includes a roll vortices resolving 2-D LES model embedded into the 3-D equation system representing a TC model.

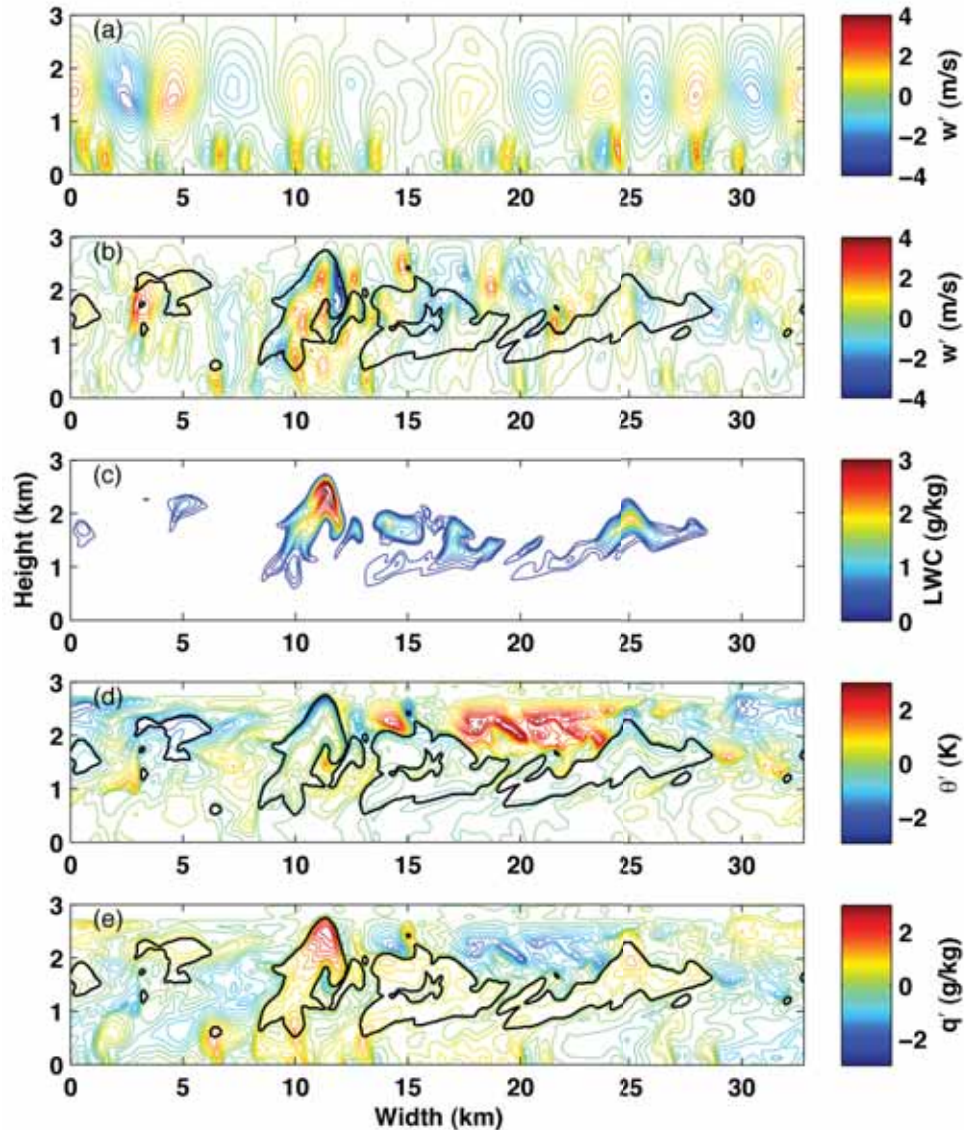


Figure 4.14 Experiment S2 T=4 hours

(a) Vertical velocity structure at  $T = 4$  hours in experiment S2; (b) vertical velocity; (c) liquid water content; (d) perturbations of potential temperature; and (e) water vapor mixing ratio at  $T = 4$  hours in experiment S2. The black solid lines in (b), (d), and (e) show cloud locations identified as 0.01 g/kg of liquid water content.

The decomposition of a 3-D equation system into two coupled equation systems for the mean flow and convective scale motions (roll vortices) is described in detail by Ginis et al. (2004) for an idealized 2-D mean flow. We have proposed to extend this procedure for a general case of a 3-D TC model. In addition, we introduce explicit equations for sea spray dynamics and its feedback to the temperature and

humidity by generalizing the one-dimensional model of Keppert et al. (1999) to three dimensions in the TC model and two dimensions in the LES model. The new model will explicitly resolve (1) vertical diffusion of droplets, (2) droplet evaporation microphysics, and (3) feedback effects. Below we provide some details of our methodology.

Let us assume that the TC model is formulated in the (X, Y, Z) coordinate system. The 2-D LES model is formulated in a local Cartesian coordinates (x, y, z) embedded in each column of the TC model so that the y-axis is directed along the roll vortices, which are typically at a small angle to the mean flow within the MBL. The x-axis is perpendicular to this direction. According to observations, the length of roll vortices can reach several tens of kilometers, while the distance between neighboring rolls can vary from hundreds of meters to a few kilometers (Morrisson et al. 2005). Glendening (1996), using a 3-D LES model, found that the characteristic along-axis length of roll vortices is about 5 times of that in the cross-axis direction. These differences in the characteristic spatial scales allow for splitting the full 3-D system of equations into two subsystems for the mean flow variables and for the deviations, correspondingly. The decomposition is done by averaging of the 3-D system of equation system along the x-axis using the following averaging operator:

$$\langle a \rangle (X, Y, Z) = 1/L \int_{x-\frac{L}{2}}^{x+\frac{L}{2}} a(x, Y, z) dx$$

where L is width of one or several roll vortices in the x-direction. All variables are represented as sums  $a = \langle a \rangle + a'$ , the averaged values denoted as  $\langle a \rangle$  are referred to as mean variables, deviations denoted by  $a'$  are referred to as convective-scale (or simply convective) values. As an example of the splitting procedure, let's apply the above averaging operator to the continuity equation written as  $\text{div } \dot{V} = 0$ , where  $\dot{V} = (u, v, w)$  is the velocity vector. Assuming the periodic boundary conditions along the x-axis we can obtain

$$\frac{\partial \langle u \rangle}{\partial X} + \frac{\partial \langle v \rangle}{\partial Y} + \frac{\partial \langle w \rangle}{\partial Z} = 0$$

$$\frac{\partial u'}{\partial x} + \frac{\partial w'}{\partial z} = 0$$

Here are examples of the momentum and heat equations describing evolution of the mean flow after applying averaging along the x-axis:

$$\frac{D \langle v \rangle}{Dt} = -\frac{1}{\rho} \frac{\partial \langle P \rangle}{\partial Y} - f \langle u \rangle - \frac{\partial \langle u' w' \rangle}{\partial Z} + \langle T_v \rangle;$$

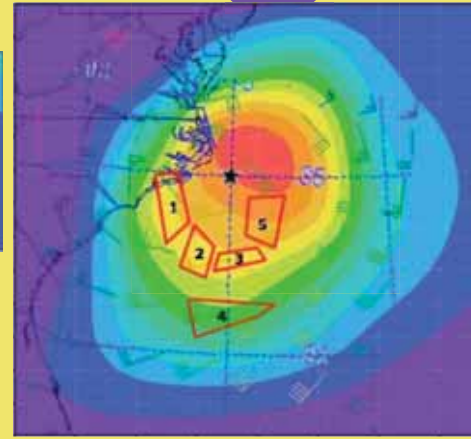
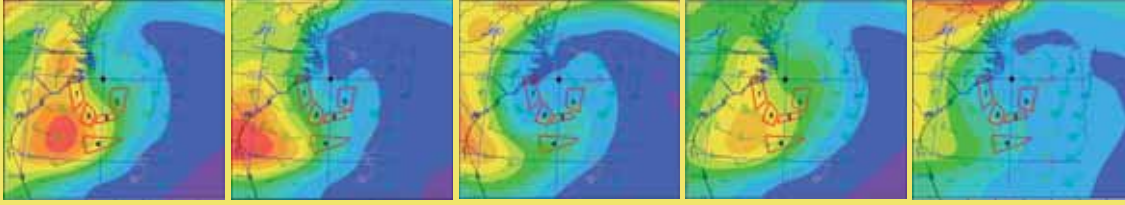
$$\frac{D \langle \theta \rangle}{Dt} = \frac{L}{c_p} \langle \phi \rangle + \frac{\langle q_s \rangle - \langle q_l \rangle}{\rho c_p} - \frac{\partial \langle \theta' w' \rangle}{\partial Z} + \langle T_\theta \rangle;$$

$$\frac{D \langle n \rangle}{Dt} = -w_{fall} \frac{\partial \langle n \rangle}{\partial Z} - \frac{\partial}{\partial r} \left( \frac{\partial r}{\partial t} \langle n \rangle \right) - \frac{\partial \langle n' w' \rangle}{\partial Z} + \langle T_n \rangle + \langle S \rangle$$

$$\frac{D}{Dt} = \frac{\partial}{\partial t} + \langle u \rangle \frac{\partial}{\partial X} + \langle v \rangle \frac{\partial}{\partial Y} + \langle w \rangle \frac{\partial}{\partial Z}$$

where  $\langle u \rangle$ ,  $\langle v \rangle$  and  $\langle w \rangle$  are the horizontal and vertical components of the mean flow velocity,  $\langle \theta \rangle$  is the mean potential temperature,  $\langle \phi \rangle$  is averaged rate of heating/cooling due to phase transition and radiation fluxes.  $\langle q_s \rangle$  and  $\langle q_l \rangle$  are the averaged source terms for the transfer of sensible and latent heat from the spray droplets to the atmosphere,  $\langle n \rangle$  is the averaged number-size distribution of droplets,  $w_{fall}$  is the fall velocity, r is the droplet radius, and  $\langle S \rangle$  is the mean source. Terms  $\langle T_v \rangle$ ,  $\langle T_\theta \rangle$  describe the effects of small scale turbulence mixing (diffusion) of momentum and heat, correspondingly. Terms  $\frac{\partial \langle v' w' \rangle}{\partial Z}$ ,  $\frac{\partial \langle \theta' w' \rangle}{\partial Z}$ ,  $\frac{\partial \langle n' w' \rangle}{\partial Z}$  describe the effects of roll vortices on the mean profiles of velocity, potentially temperature and droplet distribution, respectively. These terms are calculated explicitly from the LES model as described below. The complete system of equations of the TC model also includes the equations for  $\langle u \rangle$ , mixing ratio  $\langle q \rangle$  and cloud water content (CWC)  $\langle l \rangle$ , as well as the static equation. In addition, we will implement the equations describing the sea spray physics following Keppert et al. (1999): the equation for  $r$  and the equations to relate  $\langle q_s \rangle$  and  $\langle q_l \rangle$  with  $\langle n \rangle$ .

The 2-D LES grids with horizontal (across roll) resolution of  $\sim 50$  m will be implemented at each vertical column in the TC model. The vertical resolution will vary from several meters near the surface to several tens of meters near the top of the MBL. The width of the LES grids will be set equal to  $\sim 10$  km to resolve several rolls, and to obtain statistically grounded averaged fluxes of heat, moisture and momentum,  $\langle \theta' w' \rangle$ ,  $\langle q' w' \rangle$ ,  $\langle u' w' \rangle$ ,  $\langle v' w' \rangle$  and other terms determining effects of convective-scale motions on the large-scale flow in the TC MBL.



## Dissemination of Results and Developing Collaborations

### 5.1 Fostering Collaboration Between HAMP and Scientists at NOAA, the U.S. Navy, and NASA

In the course of the HAMP project we have made significant efforts to establish and foster collaborations with scientists at NOAA, NASA and the Navy. Here we briefly describe some of our activities in this area.

Khain and Ginis visited University of Florida and the Hurricane Research Center during the period 13 Sept-17 September 2009. Khain delivered a seminar about results of WRF with spectral bin microphysics and Ginis delivered a seminar on coupled hurricane-wave-ocean modeling.

Khain and Ginis had detailed discussions with HRD director Dr. Frank Marks and HRD scientists. HRD's modeling group led by Dr. Gopalakrishnan (Gopal) is developing a high resolution version of NOAA's operational hurricane model, HWRF. Khain and Ginis proposed to develop a benchmark model that will utilize the highest possible spatial and vertical grid resolutions and the most advanced physics packages. The model will include explicit simulations of some physical processes, such as spectral bin cloud microphysics, sea spray dynamics and thermodynamics, BL roll vortices, air-sea coupling. The development of major elements of this model aligns very well with the HAMP execution plan and NOAA's HFIP. Marks expressed interest in developing the benchmark TC model for both research purposes

and for calibration of the operational TC forecasting model(s). Marks instructed Gopal to prepare a working plan for the development of the benchmark TC model. Khain and Ginis prepared a first draft during the HRD visit and passed it to Gopal. The model will be based on a version of the HWRF model and will include the spectral microphysical package implemented into WRF (NCAR). This plan was discussed in detail during the joint meeting on September 16, 2009.

Ginis visited NCEP/EMC on October 13, 2009 and discussed the idea of the benchmark model with the EMC Director Steve Lord and Deputy Director, Bill Lapenta, as the pathway to improve the operational HWRF model. They both were also very receptive to this proposal.

Ginis met with HFIP program managers Fred Toepfler and Bob Gall on October 14, 2009 and discussed the idea of the benchmark model. Their initial response was very positive. It was discussed that a team of selected "experts" from different academic institutions and government organizations can lead this effort, including Khain and Ginis. Through HFIP significant computer resources can be made available.

Ginis and Woodley met with Dr. Scott Braun (NASA's Goddard Space Flight Center) during the Interdepartmental Hurricane Conference in Savannah, GA on March 1-4, 2010. They discussed the possibility of obtaining access to the data collected by the Cloud-Aerosol Lidar and Infrared Pathfinder Satellite Observation (CALIPSO). The CALIPSO provides information on the vertical distribution of aerosols

and clouds, cloud particle phase, and classification of aerosol size. They also discussed observations from the Tropical Rainfall Measuring Mission (TRMM) precipitation radar (PR) and microwave imager (TMI) to evaluate the cloud microphysical schemes. Braun expressed interest in collaborating with the HAMP group to study the effect of aerosols on hurricane formation and evolution and was willing to assist with obtaining the above satellite data.

Khain and Ginis visited NOAA's Geophysical Fluid Dynamics Laboratory in Princeton, NJ on Aug 12-13, 2010. They met with GFDL scientists and participated in a "roundtable" discussion about improving parameterizations of cloud microphysics and air-sea interaction in the high-resolution global models and tropical cyclone models being developed at GFDL. Khain also delivered a seminar on bin microphysics.

On September 3, 2010, Ginis spoke with Dr. Jim Doyle at the Naval Research Laboratory regarding future collaboration between HAMP and NRL's COAMPS-TC group. It was a follow-up conversation after the meeting held at the Office of Naval Research (ONR) by DHS program manager Wil Laska and ONR program managers including Dr. Ronald Ferek, Program Manager, Marine Meteorology and Atmospheric Effects. Here is a brief summary.

1. The Navy is accelerating development of COAMPS-TC with a planned operational implementation in two-three years. COAMPS-TC will be used operationally in all ocean basins where tropical cyclones occur.
2. The COAMPS-TC group is developing a fully coupled atmosphere-wave-ocean system and is presently ahead of NOAA in this process.
3. Improvements in the intensity prediction are the highest priority for COAMPS-TC.
4. Jim Doyle spoke highly about qualification of the HAMP scientists and expressed strong interest in collaboration.
5. ONR plans to support a major new initiative (~\$10 million for 5 years) on convective processes to start in 2013. They believe HAMP scientists can contribute greatly to the development of the science plan and participate in the program.

In conclusion, this presents an excellent opportunity for developing a strong joint research program with ONR and Navy scientists.

## 5.2 Dissemination of Results

In the course of HAMP project, the participating scientists have actively disseminated their work through peer-reviewed journals, conferences, and workshops. Here we briefly describe some of our activities in this area.

### *5.2.1 Participation in Scientific Projects, Meetings, and Conferences*

Rosenfeld provided scientific guidance to the CAIPEEX project, measuring the impacts of aerosols on clouds over India, conducting research flights from May to September 2009. The results were used to validate the Hebrew University Cloud Model. Rosenfeld and Woodley are continuing these measurements in a second phase in September and October 2010.

Khain also visited the University of Rhode Island several times (to collaborate with Ginis) and delivered seminars. Khain and Ginis visited the Hurricane Research Center in Miami during September 2009 and delivered seminars.

Two HAMP meetings were held in December 2009 and on 19 February 2010.

Khain and Ginis participated in a HFIP Hurricane Physics workshop on February 18-19, 2010. They made presentations and led the discussions on convection parameterization and air-sea interaction. The goal of the meeting was to provide recommendations for improving physical process representation in operational hurricane forecasts in the near term (1-2 years) and 3-5 years.

Khain participated in the meeting dedicated to the plans of new TC model development (Boulder, NCAR, February 2010) and in the ASR meeting (Bethesda, USA, April 2010) as an invited speaker.

Rosenfeld and Clavner made two oral presentations at the AMS Conference on Hurricanes and Tropical Meteorology, May 2010.

Rosenfeld presented results from HAMP and CAIPEEX as invited talks in the following scientific meetings:

- September 2009, Max Planck Institute for Atmospheric Chemistry, Mainz, Germany
- December 2009, The American Geophysical Union, San Francisco, USA.
- February 2010, CALTEC, Pasadena, California.
- February 2010, A series of lectures in Scripps Institute of Oceanography, La Jolla, California.
- March 2010, Yale University.
- April 2010, Haon, Israel, Kaplan International Workshop on climate and water.
- June 2010, Portland, Oregon, The International Conference for Cloud Physics.
- July 2010, Hyderabad, India, The annual meeting of the Asia and Oceania Geophysical Society.

Khain visited the Institute of Tropical meteorology (Pune, India) during May 2010. He delivered a course of lectures on numerical modeling of clouds and aerosol effects. He showed the results obtained during the HAMP project.

Several seminars were organized where the advantages of the SBM scheme, as well as results of simulations performed under the HAMP support were reported.

Khain was invited to GFDL in Aug. 2010 and delivered a set of seminars.

Khain and Ginis visited NOAA's Geophysical Fluid Dynamics Laboratory in Princeton, NJ on Aug 12-13, 2010. They met with GFDL scientists and participated in a "roundtable" discussion about improving parameterizations of cloud microphysics and air-sea interaction in the high-resolution global models and tropical cyclone models being developed at GFDL. Khain also delivered a seminar on bin microphysics.

On September 3, 2010, Ginis spoke with Jim Doyle at NRL regarding future collaboration between HAMP and NRL's COAMPS-TC group. It was

a follow-up conversation after the meeting held at ONR by DHS program manager Wil Laska and ONR program managers including Dr. Ronald Ferek.

### 5.2.2 Publications Resulting from this Work

The following papers have been published (or submitted) on topics related to the HAMP program:

Bell, T. L., D. Rosenfeld, and K.M. Kim, 2009: *Weekly cycle of lightning: Evidence of storm invigoration by pollution*. Geophys. Res. Lett., 36, L23805, doi:10.1029/2009GL040915

Carrió, G. G., and W. R. Cotton, 2010a: *Investigations of aerosol impacts on hurricanes: Virtual seeding flights*. Submitted to Atmos. Chem. Phys. doi:10.5194/acpd-10-22437-2010.

———, 2010b. *Study of the feasibility of the mitigation of the intensity of tropical cyclones by CCN seeding in the outer rainband region: A HAMP Project*. 29th Conf. on Hurricanes and Tropical Meteorology, Tucson, AZ, Amer Meteor. Soc.

———, 2010c. *Virtual flights modifying simulated hurricanes*. Weather Modification Assn. Annual Meeting, Santa Fe, NM, Weather Modification Assn.

Carrió, G. G., W. R. Cotton, and W.Y.Y. Cheng, 2010: *Urban growth and aerosol effects on convection over Houston. Part I, The August 2000 case*. Atmos. Res., 96, 560–574.

Drofa, A. S., V. N. Ivanov, D. Rosenfeld, and A. G. Shilin, 2010: *Studying an effect of salt powder seeding used for precipitation enhancement from convective clouds*. Atmos. Chem. Phys. Discuss., 10, 10741–10775

Fan, Y., I. Ginis, and T. Hara, 2009: *The effect of wind-wave-current interaction on air-sea momentum fluxes and ocean response in tropical cyclones*. J. Phys. Oceanogr., 39, 1019–1034.

Fan, Y., I. Ginis, and T. Hara, 2010: *Momentum flux budget across air-sea interface under uniform and tropical cyclones winds*. J. Phys. Oceanogr., in press.

Fan, Y., I. Ginis, T. Hara, C. W. Wright, and E. Walsh, 2009: *Numerical simulations and observations of surface wave fields under an extreme tropical cyclone*. J. Phys. Oceanogr., 39, 2097–2116.

- Khain A. P. 2009: *Effects of aerosols on precipitation: a review*. Environ. Res. Lett. 4 (2009) 015004.
- Khain, A., and B. Lynn, 2009: *Simulation of a supercell storm in clean and dirty atmosphere using weather research and forecast model with spectral bin microphysics*. J. Geophys. Res., 114, D19209. doi:10.1029/2009JD011827.
- , 2010b: *The effects of aerosols on the evolution of a tropical depression off the coast of Africa: As seen from simulations with the WRF model with spectral (bin) microphysics*. J. Atmos. Sci., in review.
- Khain, A. P., N. BenMoshe, and A. Pokrovsky, 2008: *Aerosol effects on microphysics and precipitation in convective clouds with a warm cloud base: An attempt of classification*. J. Atmos. Sci., 65, 1721–1748.
- , 2010: *Effects of small aerosols on microphysics and lightning in deep maritime convective clouds*. Submitted to J. Atmos. Sci.
- Khain, A., J. Shpund, and M. Pinsky, 2010: *Spray effects as seen from simulations by the Lagrangian microphysical model of the boundary layer*. Submitted to J. Atmos. Sci.
- Khain, A., N. Cohen, B. Lynn, and A. Pokrovsky, 2008: *Possible aerosol effects on lightning activity and structure of hurricanes*. J. Atmos. Sci., 65, 3652–3667.
- Khain, A. P., D. Rosenfeld, A. Pokrovsky, N. BenMoshe, J. R. Kulkarni, R. S. Maheshkumar, and T. Prabhakaran, 2010: *Microphysics of deep convective clouds over India: Simulations with a 50 m resolution spectral bin microphysics model*. Submitted to J. Geophys. Res.
- Khain, A. P., B. Lynn, and J. Dudhia, 2010: *Aerosol effects on intensity of landfalling hurricanes as seen from simulations with WRF model with spectral bin microphysics*. J. Atmos. Sci., 67, 365–384.
- Kolodny Y., R. Calvo, and D. Rosenfeld, 2009: *“Too low” d18O of paleo-meteoric, low latitude, water; do paleotropical cyclones explain it?* Paleogeog., Paleoclimatol., Paleoecol. 280, 387–395.
- Konwar, M., R. S. Maheshkumar, J. R. Kulkarni, E. Freud, B. N. Goswami, and D. Rosenfeld, 2010: *Suppression of warm rain by aerosols in rain-shadow areas of India*. Atmos. Chem. Phys. Discuss., 10, 17009–17027.
- Lensky, I. M., and D. Rosenfeld, 2008: *Clouds-Aerosols-Precipitation Satellite Analysis Tool (CAPSAT)*. Atmos. Chem. Phys., 8, 6739–6753.
- Lynn, B., R. Healy, and L. M. Druryan, 2009: *Investigation of Hurricane Katrina characteristics for future, warmer climates*. Clim. Res., 39, 75–86. doi:10.3354/cr00801.
- Lynn, B., and Y. Yair, 2009: *Prediction of lightning flash density with the WRF model*. Adv. Geosci., Adv. Geosci., 23, 11-16, doi:10.5194/adgeo-23-11-2010, 2010.
- Rosenfeld, D., M. Clavner and R. Nirel, 2010: *Pollution and dust aerosols modulating tropical cyclones intensities*. (Environmental Research Letters, submitted).
- Rosenfeld, D., M. Clavner, and R. Nirel, April, 2010: *Pollution and dust aerosols modulating hurricane intensities*, (Science, submitted).
- Ryzhkov A., M. Pinsky, A. Pokrovsky, and A. Khain, 2010: *Polarimetric radar observation operator for a cloud model with spectral microphysics*. J. Appl. Meteorol. & Climatol., in press.
- Shpund, J., M. Pinsky, and A. Khain, 2010: *Evolution of sea spray in the marine boundary layer as seen from simulations using spectral bin microphysics—2D Lagrangian Model. Part 1, Effect of large eddies*. Submitted to J. Geophys. Res.
- Yu, Z., I. Ginis, and A. P. Khain, 2010a: *Interaction of the boundary layer convection and internal gravity waves*. Submitted to J. Atmos. Sci.
- , 2010b: *Numerical modeling of boundary layer roll vortices in high wind conditions*. J. Atmos. Sci., in preparation.
- , 2010c: *Interaction of convective roll vortices and internal gravity waves: A numerical study*. J. Atmos. Sci., in preparation.
- Zhitao Yu, I. Ginis and A. Khain 2010: *Interaction of the Boundary Layer Convection and Internal Gravity Waves* (J. Atmos. Sci. Submitted)
- Zhang, H., G. M. McFarquhar, W. R. Cotton, and Y. Deng, 2009: *Direct and indirect impacts of Saharan dust acting as cloud condensation nuclei on tropical cyclone eyewall development*. Geophys. Res. Lett., 36, L06802. doi:10.1029/2009GL037276.

### 5.2.3 Presentations

The following are abstracts of presentations to the 29th Conference on Hurricanes and Tropical Meteorology, held May 10–14, 2010, in Tucson, AZ, sponsored by the American Meteorological Society and organized by the AMS Committee on Tropical Meteorology.

Ginis, I., Y. Fan, T. Hara, B. Thomas, J.-W. Bao, and L. Bianco, 2010: *Developing coupled wind-wave-current interaction framework with sea spray effects for hurricanes models*. 29th Conf. on Hurricanes and Tropical Meteorology, Tucson, AZ, Amer. Meteor. Soc. Lynn, B., J.-W. Bao, I. Ginis, A. P. Khain, and S. G. Gopalakrishnan, 2010: *Development of a tropical cyclone microphysical model*. 29th Conf. on Hurricanes and Tropical Meteorology, Tucson, AZ, Amer. Meteor. Soc.

Shpund, J., M. Pinsky, A. P. Khain, and I. Ginis, 2010: *Spray microphysics and effects on surface fluxes as seen from simulations using a Lagrangian model with spectral bin microphysics (the HAMP contribution)*. 29th Conf. on Hurricanes and Tropical Meteorology, Tucson, AZ, Amer. Meteor. Soc.

Yablonsky, R. M., and I. Ginis, 2010: *Numerical simulations of the hurricane intensity response to a warm ocean eddy*. 29th Conf. on Hurricanes and Tropical Meteorology, Tucson, AZ, Amer. Meteor. Soc.

Yu, Z., I. Ginis, and A. Khain, 2010: *Numerical modeling of boundary layer roll vortices in high wind conditions*. 29th Conf. on Hurricanes and Tropical Meteorology, Tucson, AZ, Amer. Meteor. Soc.

### 5.2.4 Conference Papers Submitted

Carrió, G. G., and W. R. Cotton, 2010a: *Virtual flights for modification of simulated hurricanes*. Weather Modification Assn. Annual Meeting, Santa Fe, NM, Weather Modification Assn.

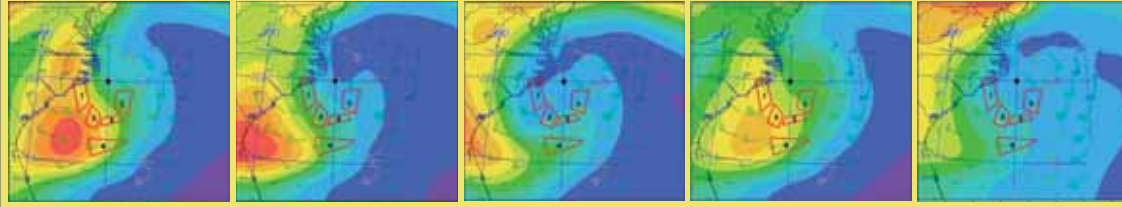
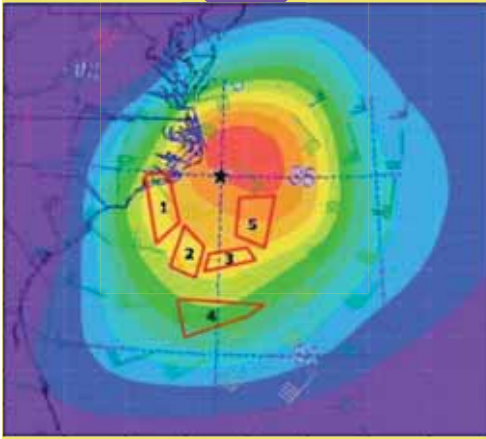
———, 2010b: *Study of the feasibility of the mitigation of the intensity of tropical cyclones by CCN seeding in the outer rainband region*: A HAMP Project. 29th Conf.

on Hurricanes and Tropical Meteorology, Tucson, AZ, Amer. Meteor. Soc.

Cotton, W. R., 2009: *Top-down versus bottom-up genesis of tornadoes and tropical cyclones*. 13th Conf. on Mesoscale Processes, Salt Lake City, UT. Amer. Meteor. Soc.

Cotton, W. R., G. G. Carrió, and S. R. Herbener, 2010: *Aerosol impacts on tropical cyclones*. 13th Conf. on Cloud Physics, Portland, OR, Amer. Meteor. Soc.

Herbener, S. R., and W. R. Cotton, 2009: *Microphysical-dynamical interactions in an idealized tropical cyclone simulation*. 13th Conf. on Mesoscale Processes, Salt Lake City, UT. Amer. Meteor. Soc.



## Conclusions and Recommendations for the Future

The HAMP team performed numerous simulation studies that, along with the previous work of others, support the hypothesis that CCN aerosols decrease the intensity of tropical cyclones. Our statistical analyses show that aerosols can explain part of the errors in predicting changes in storm intensity.

### 6.1 Rosenfeld's Conclusions and Recommendations

Observations presented by Rosenfeld reported in Chapter 1 support key links in the conceptual model that describes how aerosols might be affecting the intensity of the storms. The main observations were:

- Pollution aerosols reduced the cloud drop size and suppressed the warm rain forming processes in the external spiral cloud bands of the storms; adjacent unpolluted spiral bands had much larger cloud drops and produced readily warm rain.
- The polluted rain bands produced stronger precipitation radar reflectivities extending to greater heights; in the adjacent pristine rain bands, only moderate reflectivities were confined to below the freezing level. This supports the hypothesis that aerosols cause invigoration of the convection at the periphery of the storm.
- Frequent lightning flashes were observed in the polluted spiral cloud band, but none were observed anywhere else in the storm. This further supports the invigoration hypothesis.

- The cloud drop size in polluted clouds increased substantially when the clouds moved inward to the storm in the areas with higher winds over the sea surface. This supports the hypothesis that sea spray raised by high winds seeds the polluted clouds and restores the warm rain processes in them when they move inward to areas with high wind speeds.

In summary, this study provided observational support that added to simulation and statistical studies supporting the hypothesis that CCN aerosols reduce the intensity of tropical cyclones. To further substantiate and validate the remote sensing observations and inferences additional research is necessary involving in situ aircraft measurements in tropical cyclones that ingest heavy air pollution.

1. Aircraft observations in India demonstrated that heavy air pollution can suppress warm rain in deep tropical clouds up to and above the freezing level, as hypothesized. Aircraft measurements over the sea show that added giant CCN, apparently from sea spray, restore some of the rain in the polluted clouds.
2. These aircraft measurements validated the correctness of the microphysical representation of cloud-aerosol interactions and their impacts on rain forming processes in our model simulations.
3. Satellite measurements showed that similar processes occur when heavy air pollution inter-

acts with clouds that constitute the outer spiral bands of TCs.

4. An initial quantification of the impact of aerosols on hurricane maximum wind speed was obtained by comparing the observed intensities of TCs with their predicted intensities using models that do not account for the aerosols.

5. This quantification indicates that strongly absorbing aerosols such as black carbon have invigoration effects on hurricanes.

6. The observational and simulation effects are consistent with each other, and provide strong support to the hypothesis of aerosols impacts on hurricanes. These results show that a) effects of aerosols should be taken into account in the prediction of TC intensity, and b) the results support the HAMP hypothesis that small soluble aerosol particles ingested to clouds at the storm's periphery, mainly via the cloud base can reduce the intensity of TCs.

### **Recommended research includes:**

- Coordinate with NOAA on the incorporation of aerosols into the SHIPS statistical hurricane prediction model.
- Analyze existing data that are being measured in the present flights of the P3, which are not optimized for the HAMP objectives, and extract relevant information that might be found there.
- Coordinate with NOAA on the use of hurricane surveillance P3 airplanes for measuring aerosols, cloud microstructure, precipitation forming processes, and the impacts on cold-pools in hurricanes.
- Conduct a field campaign that will be coordinated with a simulation effort for validating the HAMP simulations.
- Validate further the satellite retrievals of cloud microstructure in hurricanes.
- Examine the microstructure of the low clouds and aerosols in the eye.

## **6.2 Cotton et al. Conclusions and Recommendations**

As reported in Chapter 2, Cotton et al. performed a series of multi-grid cloud-resolving simulations to examine the response of a simulated hurricane to the targeted insertion of CCN. The modeling framework included improved microphysical modules that included a bin-emulating treatment of rimming processes, sea-salt surface sources in three modes, sinks for cloud nucleating particles due to scavenging by precipitation, and a code that simulates the targeted insertion of CCN by aircraft.

The results of these numerical experiments clearly support the hypothesis that aerosols influence hurricane processes. Virtual flights cause a reduction of collision and coalescence, resulting in more SC liquid water to be transported aloft. This SC liquid water enhances latent heat of freezing, which produces higher updraft maxima at higher altitudes. Results also suggest that the higher evaporative cooling from enhanced rainfall rates in the outer rainbands produces stronger and more widespread cold-pools. These cold-pools covering larger areas interfere with the flow of enthalpy into the storm core and therefore weaken the storm. Reimer et al. (2010) also finds evidence that the invigoration of convective activity in the outer rainbands leads to a reduction in TC intensity. That study focused on the role of vertical wind shear on the TC inflow layer.

Given the long history in hurricane research that implicates strong vertical shear as being detrimental to storm intensity, we speculate that the aerosol signal we see in these idealized simulations is secondary to the more dominant role that environmental shear plays. Likewise, we suspect that variability in moisture content of the storm plays a more dominant role over aerosols in modulating cold-pools and hence storm intensity. Again, there is a rich history in hurricane research that suggests that rapid intensification of a storm coincides with moistening of the storm interior to almost saturation.

The increase in cold-pool spatial physical dimensions as well as the temperature difference with

respect to their surrounding environment was clearly linked to the enhanced aerosol concentrations, mainly due to the monotonic response they exhibited when increasing CCN concentrations up to  $8000 \text{ cm}^{-3}$ . A similar monotonic response was observed for the overall downward flux, the area covered with downdrafts as well as the buoyancy, rain mixing ratio, and (decreasing) raindrop size within the downdrafts associated with the largest cold-pools. Moreover, simulated reduction in frequencies of high surface winds behaved in a similar manner. Nonetheless, with the exception of raindrop sizes, all of the aforementioned quantities exhibited a different response when we considered concentrations above  $8000 \text{ cm}^{-3}$  along the flight trajectories. This change of behavior is consistent with the mechanism suggested by Carrió et al. (2010) and Carrió and Cotton (2010). Briefly, further enhancing CCN concentrations reduces the size of SC droplets, which reduces riming growth of ice particles, which results in the transport of a greater fraction of the ice-phase water mass to anvil levels as pristine ice crystals instead of being precipitated to the surface. In this way, the importance of the entire chain of processes leading to the eventual reduction of surface winds is reduced as the cold-pools are weakened.

In summary, the primary impact of aerosols on TC genesis and intensity is by altering the strength of cold-pools. The idea that cold-pools are an important modulator of TC intensity is consistent with observations that TC rapid intensification follows the formation of a nearly saturated core (results in weak cold-pools). It is also consistent with strong vertical wind shear as being a detriment to TCs (strong shear enhances entrainment of dry air increasing cold-pool strengths) as shown by Reimer et al. (2010). We speculate that during TC genesis vigorous cold-pools can lead to vertical decoupling between a mid-level MCV and low-level vorticities similar to what we find with tornadoes (Lerach et al. 2009). Furthermore, vigorous cold-pools in mature TCs can interfere with the flow of enthalpy into the storm core.

An implication from this research for hurricane intensity prediction is that greater attention has to be taken in cold-pool formation and monitoring. A re-

mote sensing method of TC cold-pools would be ideal to map cold-pool variability in TCs. Furthermore, in order to simulate and predict aerosol impacts on TCs, models need high enough resolution and microphysics to represent convective-scale dynamical responses to aerosols as well as environmental properties affecting cold-pools.

This research has clearly shown that aerosols can have an appreciable impact on tropical cyclone intensity. The results show that the aerosol impacts are greatest in the outer rainbands of a TC and that the mechanism is linked to the strength of cold-pools. These results are consistent with the findings of Reimer et al. (2010) who found that varying wind shear impacted TC intensity by varying the strength of cold-pools in the outer rainbands. The major impact of this research on hurricane intensity prediction is that it highlights the importance of low-level cold-pools, particularly in the outer rainbands on hurricane intensity. It means that methods for diagnosing cold-pool strength and area in real time need to be developed for hurricane intensity prediction. In addition, operational forecast models need to be implemented that can explicitly represent the variability of TC cold-pools due to variations in wind-shear, environmental moisture, and aerosols.

A natural question then is how responsive is a TC to varying CCN as vertical wind shear increases? Likewise, how responsive is a TC to varying aerosol and moisture amounts in the TC environment and the central core region? This is a natural question to ask as we expect that with higher amounts of moisture in the storm environment it will become increasingly difficult for aerosol to modulate storm intensity. These are questions that can be answered in the idealized storm studies that we have done so far.

Following that, we plan to investigate how actual mature case study storms vary in intensity with targeted insertion of CCN. We focus on the targeted insertion approach because it provides a more definitive representation of “cause and effect” without the confusing issues of did the aerosol enter outer rainband convection at the right time and place.

Because the recent statistical studies by Michal Clavner (an MS student under the supervision

of Rosenfeld) suggest that black carbon aerosols intensify hurricanes in contrast to Professor Gray's hypothesis, we also plan to investigate how black carbon aerosols introduced at low levels in a hurricane environment can impact TC intensity. We will also investigate how black carbon aerosols introduced above the anvils and over a large area extending beyond the storm impact its intensity. We anticipate that at the conclusion of this research we can state with some confidence how hurricane intensity is modulated both by hygroscopic aerosols and by light-absorbing black carbon aerosols.

### **6.3 Khain's Conclusions and Recommendations**

For the first time, as reported in Chapter 3, TC evolution has been calculated by Khain and his collaborators, using explicit spectral bin microphysics (SBM). Simulations with resolution of 3 km were made with the WRF/SBM. The evolution of Katrina was simulated during 72 hours beginning after it had just bypassed Florida to 12 hours after landfall. In these simulations the effects of continental aerosols ingested into its circulation TC on the TC structure and intensity were investigated. It is shown that continental aerosols invigorate convection (largely at the TC periphery), which leads to TC weakening. Maximum TC weakening took place  $\sim 20$  h before landfall, when the TC intensity had reached its maximum. The minimum pressure increased by  $\sim 16$  mb, and the maximum velocity decreased by about 15 m/s. The difference in the intensities remains significant even during the TC landfall. Thus, the results indicate that there is another (in addition to decrease in the surface fluxes) mechanism of weakening of TCs approaching the land. This mechanism is related to effects of continental aerosols ingested into the TC circulation. Note that the weakening and the inner core collapsing was simulated in spite of the fact that the SST maximum was located near the coastal line, and no TC-ocean interaction was taken into account.

Aerosols affect intensity of deep convective clouds and foster formation of lightning in TC clouds. Penetration of aerosols into the TC periphery leads to

the increase in the lightning activity at the TC periphery. Thus, intensification of lightning at the TC periphery of land falling hurricanes can serve as precursor of the TC weakening.

The application of the TC model with the spectral bin microphysics opens the way to improve prediction of TC intensity, wind and precipitation and lightning of land-falling hurricanes. The TC model with the spectral bin microphysics predicts the evolution of land-falling TC better than the bulk schemes. For instance, SBM predicts weakening of Katrina well before landfall, while the bulk schemes predicted TC intensification till landfall. The TC models with the SBM can be used for calibration and improvement of current TC forecasting models with bulk-parameterization of clouds.

The results also show that ingestion by tropical clouds of soluble aerosols at the TC boundary leads to invigoration of these clouds and to the intensification of latent heat releases in them. This effect of small aerosol particles at the TC periphery was discussed by Rosenfeld et al. (2007) and Khain et al. (2008a).

Khain's results indicate that a) SBM model reproduced TC genesis (pressure and wind fields) much more precisely than the bulk schemes, b) SBM model simulates more realistic microphysical cloud structure; and c) that dust hinders TC development, invigorating convection at the TC periphery.

Again, Khain sees one of the important applications of the WRF/SBM is an improvement of TC forecasts by calibration of existent bulk-parameterization schemes.

In summary, the development of WRF model with the novel spectral bin microphysics opens the new generation of TC models with advanced microphysics that are sensitive to atmospheric aerosols.

Implementation of accurate parameterization of the BL processes including spray effects will significantly improve the description of TC-ocean interaction and calculation of surface fluxes. Khain believes that these two improvements, taken together, will lead to dramatic improvement of understanding of TC physics and prediction of TC intensity.

The new generation high-resolution TC models are now capable of simulating the hurricane struc-

ture in great detail. Yet some critical aspects of the TC physical processes, such as cloud microphysics, BL parameterization and the air-sea fluxes must be improved before reliable forecasts of hurricane intensity can be achieved with the help of numerical TC models. Future improvements in hurricane prediction must be based on novel theoretical concepts and high resolution coupled atmosphere-wave-ocean numerical models tested against high-quality observations. The latter scientific effort has been the focus of the Ginis et al. (URI) group.

## **6.4 Ginis et al. Conclusions and Recommendations**

As reported in Chapter 4, the main focus of the Ginis et al. (URI) effort has been a) to implement the Hebrew University bin microphysics package into high-resolution coupled hurricane-wave-ocean models combined with b) explicit simulations of sea spray and c) new strategies for wind-wave-current interactions. The coupled models are built based on two NOAA operational TC prediction models. The first model is the GFDL/URI tropical prediction system that has been operational at NCEP since 1995 and at FNMOC since 1996. The URI group has made major contributions to the improvements of this model over the years since it became operational (Bender et al. 2007). The second coupled model is the WRF (WRF) model, a non-hydrostatic mesoscale model.

The research conducted on the implementation of bin microphysics is described in this final report by Khain in Chapter 3. In Chapter 4, the URI group's work on the development a new air-sea interface module and sea spray parameterization is described.

Ginis et al. summarize their work on the momentum fluxes and wind-wave-current interaction in hurricanes and their research on sea spray was also presented.

The lack of roll-induced fluxes in existing hurricane boundary layer parameterizations has potentially major implications for forecasting hurricane intensity. Since hurricanes are heat engines whose fuel source is the water evaporated from the sea surface and since numerical models are very sensitive to surface flux

parameterizations and secondarily to differences in existing BL parameterizations, the identification of an unparameterized mechanism that may have the potential to make first-order changes in the HBL flux parameterizations cannot be ignored in a program that is dedicated to improving intensity forecasts.

Ginis et al. in collaboration with Khain have developed an efficient 2-D large eddy simulation (LES) model that explicitly simulates roll vortices and their interaction with the 3-D mean flow in the marine BL. They used the new BL model to investigate the physical process controlling the formation and evolution of rolls vortices in the marine BL in high wind conditions and proposed a methodology for explicit representation of roll vortices in hurricane models.

## **6.5 Overall Conclusions and Recommendations**

The findings of this first phase of the HAMP research effort illustrate the importance of precipitation forming and evaporation processes in TC clouds. The work demonstrates the need to properly simulate these processes and the resultant cold pools to improve TC prediction models. Specifically, the HAMP work shows the following.

- a) The effects of aerosols should be taken into account in the prediction of TC intensity, and
- b) The HAMP hypothesis that the introduction of small aerosol particles into the clouds act as CCN and can weaken the storm intensity is supported.

For example, air pollution that comes from the land into a TC can substantially affect the cloud micro-structure and suppress the warm rain forming processes there. This can lead to invigoration of the affected clouds at the periphery of the storm. This invigoration is manifested by greater lightning activity and stronger precipitation reflectivities above the freezing level. The rain is restored further inside the storm by a possible combination of natural cloud seeding from sea spray and the washing down of the aerosols by rain.

The research reported here has made a significant contribution to the understanding of hurricane microphysics and our ability to improve some forecast models, but much more can be accomplished if we continue to build on the work completed in 2009/2010.

A second year of research funded for the HAMP team could address the following needs and improve forecasting of hurricane intensity through consideration of the effects of aerosols.

1. Refine inclusion of aerosols and explicit microphysics in the current HAMP models.

2. Provide for inclusion of aerosols and microphysics in the operational models used for hurricane intensity forecasting, e.g. the GFDL and SHIPS models.

3. Acquire NOAA P3 aircraft data on aerosols and microphysical parameters in Atlantic tropical systems, including hurricanes and use these data for selected cases to test/validate HAMP models and impacts of aerosols on hurricane intensity changes.

4. Develop a proper formulation of the effects of aerosols in the models requires additional research involving in situ measurements of aerosols and cloud properties to be conducted with the hurricane monitoring airplanes in storms ingesting air masses with various aerosols.

5. Further develop the spray model by creating advanced parameterization of spray effect on surface fluxes and on the structure of the BL.

6. Conduct simulations of different TC using WRF/SBM model. Investigation of aerosol effects on intensity of hurricanes and on TC genesis under different environmental conditions.

7. Modify the SBM codes (development and implementation of a new parallelization method) with the purpose of significant decrease of the computer time of WRF/SBM simulations.

8. Simulate the effects of introduction of CCN aerosols into clouds at the TC periphery. Estimate the impact of varying amounts of CCN aerosols and various particle sizes on the storm intensity.

9. Calibrate current two-moment bulk parameterizations to improve representation of convec-

tion and aerosol effects in current TC forecasting models in collaboration with HRC (of GFDL).

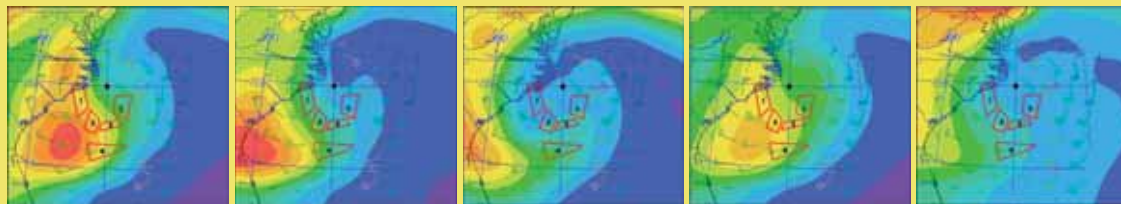
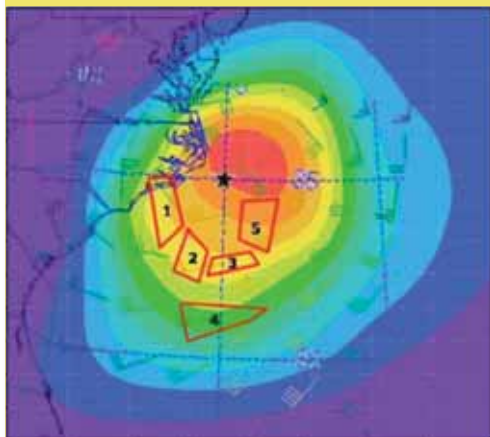
10. Examine impacts of aerosols on hurricane intensity change relative to other important factors, such as vertical wind shear, moisture, and sea-surface temperatures.

11. Investigate how black carbon aerosols introduced at low levels in a hurricane environment can impact TC intensity. Also investigate how black carbon aerosols introduced above the anvils and over a large area extending beyond the storm impact its intensity.

12. Continue to build coalitions with groups tasked with the improvement of TC intensity. For example, there is a good possibility if HAMP is continued of collaboration with the Navy's development of a new operational TC prediction model, Coupled Ocean and Atmosphere Mesoscale Prediction System (COAMPS)-TC at its facilities in Monterey. We plan to hold a joint HAMP/Navy Workshop in the Washington, DC area in early December, 2010 to explore such collaboration. The Navy has expressed interest in utilizing some of the new HAMP microphysical and aerosol expertise in its COAMPS model.

13. Apply the HAMP TC models to test new cases defined by the NHC Science Operations Officer, Dr. Landsea, as "problem cases" for current NHC operational hurricane intensity change models in the 2010 hurricane season.

If Phase 2 funding for HAMP is approved, these important activities will take place in 2011.



## References

- Albrecht, B. A., 1989: *Aerosols, cloud microphysics, and fractional cloudiness*. *Science*, 245, 1227–1230. doi:10.1126/science.245.4923.1227.
- Andreae, M. O., D. Rosenfeld, P. Artaxo, A. A. Costa, G. P. Frank, K. M. Longo, and M.A.F. Silva-Dias, 2004: *Smoking rain clouds over the Amazon*. *Science*, 303, 1337–1342.
- Arakawa, A., and W. H. Shubert, 1974: *Interaction of a cumulus cloud ensemble with the large-scale environment. Part 1*. *J. Atmos. Sci.*, 31, 674–701.
- Bender, M. A., I. Ginis, R. Tuleya, B. Thomas, and T. Marchok, 2007: *The operational GFDL coupled hurricane-ocean prediction system and a summary of its performance*. *Mon. Wea. Rev.*, 135, 3965–3989.
- Black, R. A., and J. Hallett, 1999: *Electrification of the hurricane*. *J. Atmos. Sci.*, 56, 2004–2028.
- Bott, A., 1998: *A flux method for the numerical solution of the stochastic collection equation*. *J. Atmos. Sci.*, 55, 2284–2293.
- Cecil, D. J., E. J. Zipser, and S. W. NesBitt, 2002: *Reflectivity, ice scattering, and lightning characteristics of hurricane eyewalls and rainbands. Part 2, Intercomparison of observations*. *Mon. Wea. Rev.*, 130, 785–801.
- Chin, M., R. B. Rood, S. J. Lin, J. F. Muller, and A. M. Thompson, 2000: *Atmospheric sulfur cycle in the global model GOCART: Model description and global properties*. *J. Geophys. Res.*, 105, 24661–24687.
- Cotton, W. R., H. Zhang, G. M. McFarquhar, and S. M. Saleeby, 2007: *Should we consider polluting hurricanes to reduce their intensity?* *J. Wea. Mod.* 39, 70.
- Cotton, W. R., R. A. Pielke Sr., R. L. Walko, G. E. Liston, C. J. Treback, H. Jiang, R. L. McAnelly, J. Y. Harrington, M. E. Nicholls, G. G. Carrió, and J. P. McFadden, 2003: *RAMS 2001: Current status and future directions*. *Meteor. Atmos. Phys.*, 82, 5–29.
- DeMaria, M., M. Mainelli, L. K. Shay, J. A. Knaff, and J. Kaplan, 2005: *Further improvements to the statistical hurricane intensity prediction scheme (SHIPS)*. *Wea. Forecast.*, 20, 531–543.
- Dunion, J. P., and C. S. Velden, 2004: *The impact of the Saharan air layer on Atlantic tropical cyclone activity*. *Bull. Am. Meteorol. Soc.*, 85(3), 353–365.
- Fan J., M. Ovtchinnikov, J. Comstock, S. McFarlane, and A. Khain, 2009: *Modeling Arctic mixed-phase clouds and associated ice formation*. *J. Geophys. Res.*, 114, D04205. doi:10.1029/2008JD010782.
- Ferrier, B. S., 2005: *An efficient mixed-phase cloud and precipitation scheme for use in operational NWP models*. *Eos, Trans. Amer. Geophys. Union*, 86 (Spring Meeting Suppl.), abstract A42A-02.
- Fierro, A. O., L. Leslie, E. Mansell, J. Straka, D. MacGorman, and C. Ziegler, 2007: *A high-resolution simulation of microphysics and electrification in an idealized hurricane-like vortex*. *Meteorol. Atmos. Phys.* 98, 13–33. doi:10.1007/s00703-006-0237-0.
- Freud, E., D. Rosenfeld, M. O. Andreae, A. A. Costa, and P. Artaxo, 2008: *Robust relations between CCN and the vertical evolution of cloud drop size distribution in deep convective clouds*. *Atmos. Chem. Phys.*, 8, 1661–1675.
- Ginis, I., A. Khain, and E. Morosovsky, 2004: *Effects of large eddies on the structure of the marine boundary layer under strong wind conditions*. *J. Atmos. Sci.*, 61, 3049–3063.

- Gray, W. M., W. M. Frank, M. L. Corrin, and C. A. Stokes, 1976: *Weather modification through carbon dust absorption of solar energy*. J. Meteorol., 15, 355–386.
- Gunn, R., and B. B. Phillips, 1957: *An experimental investigation on the effect of air pollution on the initiation of rain*. J. Meteorol., 14, 272.
- Hallett, J., and S. C. Mossop, 1974: *Production of secondary ice crystals during the riming process*. Nature, 249, 26–28.
- Hong, Song-You, Kyo-Sun Sunny Lim, Yong-Hee Lee, Jong-Chul Ha, Hyung-Woo Kim, Sook-Jeong Ham, and J. Dudhia, 2010: *Evaluation of the WRF double-moment 6-class microphysics scheme for precipitating convection*. Advances in Meteorology, 2010, Article ID 707253, 10 pages. doi:10.1155/2010/707253.
- Houze, R. A., S. S. Chen, B. F. Smull, W. C. Lee, and M. M. Bell, 2007: *Hurricane intensity and eye-wall replacement*. Science, 315, 1235–1238.
- Iguchi, T., T. Nakajima, A. Khain, K. Saito, T. Takemura, and K. Suzuki, 2008: *A study of the cloud microphysical properties influenced by aerosols in an East Asia region using a meso-scale model coupled with a bin microphysics for clouds*. J. Geophys. Res., 113, D14215, 28 pp. doi:10.1029/2007JD009774.
- Jenkins, G. S., A. S. Pratt, and A. Heymsfield, 2008: *Possible linkages between Saharan dust and tropical cyclone rain band invigoration in the eastern Atlantic during NAMMA-06*. Geophys. Res. Lett., 35, L08815, 7 pp. doi:10.1029/2008GL034072.
- Jorgensen, D. P., E. J. Zipser, and M. A. LeMone, 1985: *Vertical motions in intense hurricanes*. J. Atmos. Sci., 42, 839–856.
- Khain, A. P., 2009: *Effects of aerosols on precipitation: A review*. Environ. Res. Lett., 4, 015004.
- Khain, A., and B. Lynn, 2009: *Simulation of a supercell storm in clean and dirty atmosphere using weather research and forecast model with spectral bin microphysics*. J. Geophys. Res., 114, D19209. doi:10.1029/2009JD011827.
- Khain A. P., N. BenMoshe, and A. Pokrovsky, 2008b: *Aerosol effects on microphysics and precipitation in convective clouds with a warm cloud base: An attempt of classification*. J. Atmos. Sci., 65, 1721–1748.
- Khain, A. P., D. Rosenfeld, and A. Pokrovsky, 2005: *Aerosol impact on the dynamics and microphysics of convective clouds*. Quart. J. Roy. Meteor. Soc., 131, 2639–2663.
- Khain, A., N. Cohen, B. Lynn, and A. Pokrovsky, 2008: *Possible aerosol effects on lightning activity and structure of hurricanes*. J. Atmos. Sci., 65, 3652–3677. doi:10.1175/2008JAS2678.1.
- Khain, A. P., L. R. Leung, B. Lynn, and S. Ghan, 2009: *Effects of aerosols on the dynamics and microphysics of squall lines simulated by spectral bin and bulk parameterization schemes*. J. Geophys. Res., 114, D22203. doi:10.1029/2009JD011902.
- Khain, A. P., M. B. Pinsky, M. Shapiro, and A. Pokrovsky, 2001: *Graupel-drop collision efficiencies*. J. Atmos. Sci., 58, 2571–2595.
- Khain, A. P., M. Ovtchinnikov, M. Pinsky, A. Pokrovsky, and H. Krugliak, 2000: *Notes on the state-of-the-art numerical modeling of cloud microphysics*. Atmos. Res., 55, 159–224.
- Khain A., A. Pokrovsky, M. Pinsky, A. Seifert, and V. Phillips, 2004: *Effects of atmospheric aerosols on deep convective clouds as seen from simulations using a spectral microphysics mixed-phase cumulus cloud model. Part 1, Model description*. J. Atmos. Sci., 61, 2963–2982.
- Koren I., Y. J. Kaufman, D. Rosenfeld, L. A. Remer, and Y. Rudich, 2005: *Aerosol invigoration and restructuring of Atlantic convective clouds*. Geophys. Res. Lett., 32, L14828. doi:10.1029/2005GL023187.
- Koren, I., L. A. Remer, O. Altaratz, J. V. Martins, and A. Davidi, 2010: *Aerosol-induced changes of convective cloud anvils produce strong climate warming*. Atmos. Chem. Phys., 10, 5001–5010.
- Kurihara, Y., 1973: *A scheme of moist convective adjustment*. Mon. Wea. Rev., 101, 547–553.
- Lensky, I. M., and R. Drori, 2007: *A satellite-based parameter to monitor the aerosol impact on convective clouds*. J. Appl. Meteor. Climatol., 46, 660–666. doi:10.1175/JAM2487.1.
- Lensky, I. M., and D. Rosenfeld, 2006: *The time-space exchangeability of satellite retrieved relations between cloud top temperature and particle effective radius*. Atmos. Chem. Phys., 6, 2887–2894.

Levin, Z., and W. R. Cotton (eds.), 2009: *Aerosol Pollution Impact on Precipitation: A Scientific Review*. WMO/IUGG report. Springer, 386 pp.

Li, X., W.-K. Tao, A. P. Khain, J. Simpson, and D. E. Johnson, 2009a: *Sensitivity of a cloud-resolving model to bulk and explicit bin microphysical schemes. Part I, Validation with a PRE-STORM case*. J. Atmos. Sci., 66, 3–21.

———, 2009b: *Sensitivity of a cloud-resolving model to bulk and explicit bin microphysical schemes. Part II, Cloud microphysics and storm dynamics interactions*. J. Atmos. Sci., 66, 22–40.

Lynn, B., A. Khain, J. Dudhia, D. Rosenfeld, A. Pokrovsky, and A. Seifert, 2005a: *Spectral (bin) microphysics coupled with a mesoscale model (MM5). Part 1, Model description and first results*. Mon. Wea. Rev., 133, 44–58.

———, 2005b: *Spectral (bin) microphysics coupled with a mesoscale model (MM5). Part 2: Simulation of a CaPe rain event with squall line*. Mon. Wea. Rev., 133, 59–71.

Magaritz, L., M. Pinsky, A. Khain, and O. Krasnov, 2009: *Investigation of droplet size distributions and drizzle formation using a new trajectory ensemble model. Part 2, Lucky parcels in non-mixing limit*. J. Atmos. Sci., 66, 781–805.

Meyers, M. P., P. J. DeMott, and W. R. Cotton, 1992: *New primary ice-nucleation parameterizations in an explicit cloud model*. J. Appl. Meteor., 31, 708–721.

O'Dowd, C. D., M. E. Smith, I. E. Consterdine, and J. A. Lowe, 1997: *Marine aerosol, sea-salt, and the marine sulphur cycle: A short review*. Atmos. Environ., 31, 73–80.

Pinsky, M., A. P. Khain, and M. Shapiro, 2001: *Collision efficiency of drops in a wide range of Reynolds numbers: Effects of pressure on spectrum evolution*. J. Atmos. Sci., 58, 742–764.

Pinsky, M., A. Khain, L. Magaritz, and A. Sterkin, 2008: *Simulation of droplet size distributions and drizzle formation using a new trajectory ensemble model of cloud topped boundary layer. Part 1, Model description and first results in non-mixing limit*. J. Atmos. Sci., 65, 2064–2086.

Pruppacher, H. R., 1995: *A new look at homogeneous ice nucleation in supercooled water drops*. J. Atmos. Sci., 52, 1924–1933.

Reimer, M., M. T. Montgomery, and M. E. Nichols, 2010: *A new paradigm for intensity modification of tropical cyclones: Thermodynamic impact of vertical wind shear on the inflow layer*. Atmos. Chem. Phys., 10, 3163–3168.

Rosenfeld, D., 1999: *TRMM observed first direct evidence of smoke from forest fires inhibiting rainfall*. Geophys. Res. Lett., 26 (20), 3105–3108.

———, 2000: *Suppression of rain and snow by urban and industrial air pollution*. Science, 287 (5459), 1793–1796.

Rosenfeld, D., and I. M. Lensky, 1998: *Satellite-based insights into precipitation formation processes in continental and maritime convective clouds*. Bull. Am. Meteorol. Soc., 79, 2457–2476.

Rosenfeld, D., and W. L. Woodley, 2003: *Closing the 50-year circle: From cloud seeding to space and back to climate change through precipitation physics. Cloud Systems, Hurricanes, and the Tropical Rainfall Measuring Mission (TRMM)*. 234 pp., Wei-Kuo Tao and Robert Adler, eds. Meteor. Monogr., 51, American Meteorological Society, 59–80.

Rosenfeld, D., Y. Kaufman, and I. Koren, 2006: *Switching cloud cover and dynamical regimes from open to closed Benard cells in response to aerosols suppressing precipitation*. Atmos. Chem. Phys., 6, 2503–2511.

Rosenfeld, D., Y. Rudich, and R. Lahav, 2001: *Desert dust suppressing precipitation—A possible desertification feedback loop*. Proc. Natl. Acad. Sciences, 98, 5975–5980.

Rosenfeld, D., A. Khain, B. Lynn, and W. L. Woodley, 2007: *Simulation of hurricane response to suppression of warm rain by sub-micron aerosols*. Atmos. Chem. Phys., 7, 3411–3424.

———, 2007: *Simulation of hurricane response to suppression of warm rain by sub-micron aerosols*. Atmos. Chem. Phys. Discuss., 7, 5647–5674.

Rosenfeld, D., W. L. Woodley, A. Lerner, G. Kelman, and D. T. Lindsey, 2008: *Satellite detection of severe convective storms by their retrieved vertical profiles of cloud particle effective radius and ther-*

- modynamic phase*. J. Geophys. Res., 113, D04208. doi:10.1029/2007JD008600.
- Rosenfeld, D., M. Fromm, J. Trentmann, G. Luderer, M. O. Andreae, and R. Servranckx, 2007: *The Chisholm firestorm: Observed microstructure, precipitation and lightning activity of a pyro-cumulonimbus*. Atmos. Chem. Phys., 7, 645–659.
- Rosenfeld, D., U. Lohmann, G. B. Raga, C. D. O’Dowd, M. Kulmala, S. Fuzzi, A. Reissell, and M. O. Andreae, 2008: *Flood or drought: How do aerosols affect precipitation?* Science, 321, 1309–1313.
- Rudich, Y., D. Rosenfeld, and O. Khersonsky, 2002: *Treating clouds with a grain of salt*. Geophys. Res. Lett., 29 (22), 4 pp. doi:10.1029/2002GL016055.
- Rudich, Y., A. Sagi, and D. Rosenfeld, 2003: *Influence of the Kuwait oil fires plume (1991) on the microphysical development of clouds*. J. Geophys. Res., 108, D15 4478. doi:10.1029/2003JD003472.
- Saunders, C.P.R., 1993: *A review of thunderstorm electrification processes*. J. Appl. Meteor., 32, 642–655.
- Seifert, A., and K. Beheng, 2006: *A two-moment cloud microphysics parameterization for mixed-phase clouds. Part 1, Model description*. Meteorol. Atmos. Phys., 92, 45–66.
- Shao, X. M., J. Harlin, M. Stock, M. Stanley, A. Regan, K. Wiens, T. Hamlin, M. Pongratz, D. Suszcynsky, and T. Light, 2005: *Katrina and Rita were lit up with lightning*. Eos, Trans. Amer. Geophys. Union, 86 (42), 398–399. doi:10.1029/2005EO420004.
- Sherwood, S. C., T.J.P. Vaughan, and J. S. Wettlaufer, 2006: *Small ice crystals and the climatology of lightning*. Geophys. Res. Lett., 33, L05804. doi:10.1029/2005GL.
- Skamarock, W. C., J. B. Klemp, J. Dudhia, D. O. Gill, D. M. Barker, W. Wang, and J. G. Powers, 2005: *A description of the Advanced Research WRF Version 2*. NCAR Tech. Note NCAR/TN-468+STR, 88 pp.
- Takahashi, T., 1978: *Riming electrification as a charge generation mechanism in thunderstorms*. J. Atmos. Sci., 35, 1536–1548.
- Thompson, G., R. R. Rasmussen, and K. Manning, 2004: *Explicit forecasts of winter precipitation using an improved bulk microphysics scheme. Part 1, Description and sensitivity analysis*. Mon. Wea. Rev., 132, 519–542.
- Vali, G., 1994: *Freezing rate due to heterogeneous nucleation*. J. Atmos. Sci., 51, 1843–1856.
- Wang, C., 2005: *A modeling study of the response of tropical deep convection to the increase of cloud condensational nuclei concentration. 1, Dynamics and microphysics*. J. Geophys. Res., 110, D21211. doi:10.1029/2004JD005720.
- Willoughby, H. E., D. P. Jorgensen, R. A. Black, and S. L. Rosenthal, 1985: *Project STORMFURY: A scientific chronicle 1962–1983*. Bull. Am. Meteorol. Soc., 66, 505–514.
- Wood, R., C. S. Bretherton, D. Leon, A. D. Clarke, P. Zuidema, G. Allen, and H. Coe, 2010: *An aircraft case study of the spatial transition from closed to open mesoscale cellular convection*. Atmos. Chem. Phys. Discuss., 10, 17911–17980.
- Zhang, H., G. M. McFarquhar, W. R. Cotton, and Y. Deng, 2009: *Direct and indirect impacts of Saharan dust acting as cloud condensation nuclei on tropical cyclone eyewall development*. Geophys. Res. Lett., 36, L06802. doi:10.1029/2009GL037276.
- Zhang, H., G. M. McFarquhar, S. M. Saleeby, and W. R. Cotton, 2007: *Impacts of Saharan dust as CCN on the evolution of an idealized tropical cyclone*. Geophys. Res. Lett., 34, L14812. doi:10.1029/2007GL029876.

Technical Editors

Patricia Weis-Taylor  
Michelle Dorsett  
Linda Bevard

Layout and Design

Rick Hinrichs

# Hurricane Aerosol and Microphysics Program (HAMP):

Improving Hurricane Forecasts by Evaluating the Effects of Aerosols on Hurricane Intensity

